Evolution and Stability of a Crack with a Process Zone. Experimental and Theoretical Studies

Final Report
(August, 1996)

Two Parameter Crack Layer Model: Equilibrium, Evolution, Stability

*

Aging Phenomena and the Intrinsic Material Geometry

by

A. Chudnovsky and Y. Shulkin
Department of Civil and Materials Engineering
2095 ERF, 842 W. Taylor Str.
University of Illinois at Chicago
Chicago, IL 60607

and

S. Preston
Department of Mathematical Sciences
Portland State University
Portland, OR 97207

Prepared for

Air Force Office for Scientific Research
Aerospace and Engineering Sciences
Building 410, Boiling AB
Washington DC. 20332
(Grant No. 92-J-0201)

REPORT DOCUMENTATION PAGE

Form Approved
OMB No. 0704-0188

1. AGENCY USE ONLY (Leave blank)	2. REPORT DATE	3. REPORT TYPE AND DATES COVERED
	09-30-96	FINAL 07/30/95 - 07/30/96

4. TITLE AND SUBTITLE

Evolution and Stabilities of a Crack and a Process Zone.
Experimental and Theoretical Studies

5. FUNDING REFERENCE

92-J-0201

6. AUTHOR(S)

A. Chudnovsky, Y. Shulkin and S. Preston

7. PERFORMING ORGANIZATION NAME(S) AND ADDRESS(ES)

Department of Civil and Materials Engineering
2095 ERF, 842 W. Taylor Street
The University of Illinois at Chicago
Chicago, IL 60607

8. PERFORMING ORGANIZATION REPORT NUMBER

9. SPONSORING / MONITORING AGENCY NAME(S) AND ADDRESS(ES)

Air Force Office for Scientific Research NA
Aerospace and Engineering Sciences
Building 410, Boiling AFB
Washington D.C. 20332

10. SPONSORING / MONITORING AGENCY REPORT NUMBER

~~N/A~~
92-J-0201

11. SUPPLEMENTARY NOTES

N/A

12a. DISTRIBUTION / AVAILABILITY STATEMENT

Approved for public release;
Distribution unlimited

12b. DISTRIBUTION CODE

N/A

13. ABSTRACT (Maximum 200 words)

The report contains two parts: (1) "Two parameter crack layer model" and (2) "Aging phenomena and the intrinsic material geometry". In the first part, the crack layer model is substantiated from the thermodynamic standpoint, the kinetic equations governing crack layer evolution are derived, and stability of the crack layer stationary state and propagation is analyzed. The proposed model is examined for the engineering thermoplastics studied in detail experimentally. In the second part, a variational approach to the derivation of constitutive equations of material aging is proposed. Elastic properties and irreversible deformations are represented by a 4D material metric tensor. Equations governing evolution of the tensor are obtained and studied. The theory is illustrated by examples.

14. SUBJECT TERMS

crack, process zone, crack layer, 2 parameter model, equilibrium, evolution, stability, lifetime, aging, metric tensor, intrinsic geometry

15. NUMBER OF PAGES

120

16. PRICE CODE

17. SECURITY CLASSIFICATION OF REPORT	18. SECURITY CLASSIFICATION OF THIS PAGE	19. SECURITY CLASSIFICATION OF ABSTRACT	20. LIMITATION OF ABSTRACT
UNCLASSIFIED	UNCLASSIFIED	UNCLASSIFIED	

Abstract

The present report summarizes the 4 year experimental and theoretical research program conducted by the Fracture Research Laboratory under AFOSR support and devoted to various aspects of materials brittle fracture and aging*). The report includes two parts - Part 1. "Two Parameter Crack Layer Model: Equilibrium, Evolution, Stability" and Part 2. "Aging Phenomena and the Intrinsic Material Geometry".

In the first part, a thermodynamic foundation of the crack layer (CL) kinetic model is given and various applications are discussed. Motion of the CL causes elastic energy release from the matrix and remote load as well as energy consumption due to formation of the process zone (PZ) and new crack surfaces. The thermodynamic force for crack or PZ advance is defined as the difference between the rate of the potential energy release and the rate of the energy dissipation; crack or PZ advance being possible only if the thermodynamic force is positive. The material degradation process taking place within the PZ is accounted for by a reduction of the specific fracture (Griffith) energy in time. The kinetic equations governing the process of CL growth are formulated in the form of relations between the rates of crack and PZ extensions and conjugated thermodynamic forces. Numerical solution of the non-linear equations reveals two modes of CL growth - continuous (the CL grows monotonously) and discontinuous (the process is a sequence of CL stationary states and transitions from one state to another). Stability analysis shows that processes of CL advance including crack growth (particularly, the transitions mentioned) are unstable. According to observations, in a realistic range of load and temperature, subcritical CL growth progresses in a discontinuous fashion. The modeling of this process leads to the lifetime-load-temperature relation which agrees well with that obtained experimentally.

In the second part, a new variational approach to the derivation of constitutive equations for material aging is presented. A 4D material metric tensor is introduced as an age parameter. This tensor represents an evolution of elastic properties as well as the irreversible deformations of the material. The equations governing evolution of the material metric tensor with the respective balance equations are derived and analyzed. The proposed equations are illustrated by examples.

*) These works have been reported previously:

1. A new method of lifetime prediction for brittle fracture of engineering thermoplastics, 1994.
2. A new experimental technique for modeling of crack and process zone propagation in engineering thermoplastics, 1995.
3. Crack and process zone behavior in a vicinity of inclusions, 1995.

Part 1

Two Parameter Crack Layer Model: Equilibrium, Evolution, Stability

Contents

1. Introduction

The crack layer concept [1, 2] to model subcritical crack growth is based on the assertion that the crack as a fracture object has to be considered jointly with a zone of damaged material that surrounds the crack and grows with it. The presence of such a zone is treated as a natural characteristic of any cracked body since the zone is observed in all engineering materials - metal, polymer, ceramic, composite. The crack and the zone further referred to as the process zone (PZ) form an entire system - the crack layer (CL). Propagation of the CL is a result of interaction between the crack and PZ within the CL and between the CL and the surrounding body called for brevity the matrix. Therefore the fracture process is affected by behavior of both the matrix and PZ materials. The given CL definition calls for a detailed information regarding properties of the matrix and PZ materials to model fracture evolution under particular loading and temperature conditions. The present report is concerned with development and application of the CL concept for the case when CL behavior is characterized by two parameters - crack and PZ lengths.

Subcritical crack growth leading to long-term brittle fracture is of considerable practical importance. The crack which causes the fracture is usually generated by a preexisting defect. At room temperature crack initiation and propagation occur at relatively low stresses and prove to be the major reason for failures of structural components under normal service conditions. The period of time required for the crack to be initiated and to propagate slowly up to a sudden onset of crack instability is called the lifetime, or the time to failure and denoted by t_f. Fundamental understanding and respective modeling of the mechanism governing crack initiation and growth creates a theoretical basis for reasonable prediction of the material lifetime.

The validity of CL model is examined in application to engineering thermoplastics because all the data required are readily available for both constant and cyclic loads [3-24]. The observations of slow crack growth reported allow a complete characterization of the CL model and comparison of its predictions with the results obtained experimentally.

According to [15], the PZ is formed ahead of the crack tip almost immediately upon loading and then extends together with the growing crack preceding its tip. Formation of the PZ can be treated as a material response to the state of high level stresses occurring in front of the crack tip and having the shape of nearly hydrostatic tension. The stress field produces microvoiding of the original material and subsequent stretching of the voided material. As a result, the PZ appears either as a region of craze fibrils, i.e. of the material strongly oriented towards the direction perpendicular to the crack plane and disconnected within the plane of crack extension, or in the

shape of a region subjected to large shear yielding. As stated above, the PZ material is conventionally considered similar to those of the drawn (necked) one. There are convincing evidences of a crucial influence of time-dependent properties of the PZ material, such as disentanglement and creep of the craze fibrils, on the rate of subcritical crack growth and the lifetime of polymers [10, 23, 24]. Modeling of the PZ from the continuum mechanics standpoint, particularly evaluation of the PZ length, is usually based on the Dugdale-Barenblatt (DB) model [25, 26]. However, as follows from more accurate analysis [22, 27], the length of the PZ observed turns out to be significantly smaller than that predicted by the DB model.

As experiments show, subcritical crack growth may evolve as a continuous (smooth) process or discontinuous (step-wise) one. Discontinuous crack growth in polymers under fatigue conditions has been reported rather long ago [4], but only recently [19] this process has been observed under constant load. In accordance with the latter, this manner of crack growth is explained by interaction of the two processes: degradation of the PZ material and crack extension into the PZ. The crack remains arrested while the PZ material is strong enough, and starts growing as soon as this material sufficiently weakens. Crack advance continuous up to the instant when it reaches the material that are too firm to be broken. Discontinuous crack growth is considered a general phenomenon which tends to become unobservable if the level of stresses decreases and/or the rate of degradation increases.

Description of the crack kinetics is usually based on the assumption that the stress-strains field in a small vicinity of the crack tip completely defines the conditions of crack initiation and growth. This means, in particular, that the rate of crack growth (in experiments [15] the rate of crack tip opening displacement is usually measured) only depends on such fracture parameters as stress intensity factor K or J-integral or others like that. Observations [6, 8, 13, 17-19] result in an approximate determination of the crack growth rate under constant load as a power function of the stress intensity factor K, i.e. the rate of the crack length or the notch tip opening displacement, $\dot{l}$ or $\dot{\delta}$, is defined to be proportional to K^n where n is a material constant. According to [28], n varies from 3 to 5 depending on the particular chemical structure of the polymer. The empirical relations mentioned has been established for the simplest conditions of crack propagation: the specimen material is homogeneous and the crack trajectory is straight line. Study of the case when the specimen contained an asymmetric inclusion and so, the crack trajectory was curved [29], has led to the conclusion that the crack kinetics could not be fully determined by the only parameters of the crack tip mentioned above and so, some additional characteristics of the process should be involved to reflect presence of the PZ and its effect on the direction and rate of crack growth.

From the viewpoint of lifetime prediction, the most important experimental result is the establishment of relations between the lifetime, applied load and temperature. Data about the lifetime of polymer structures at various levels of load and temperature have been reported for internally pressurized pipes [6] and for tensile single-edge notched (SEN) specimens [17, 18]. For definite sizes of specimen from a given material and for the particular load type (tension, three-point bending and so on), the lifetime under constant load and fixed temperature depends only on stress level σ, namely $t_f \propto \sigma^{-\alpha}$. In case [6] σ signifies the hoop stress in a pipe, and in case [17, 18] the applied stress; α is a material constant that slightly depends or none at all on temperature and varies approximately from 2.5 to 5.0 for different materials. It has been demonstrated that a certain treatment of the lifetime-stress relation obtained in short-term fracture tests at high temperatures allows a reasonable estimation of the lifetime-stress relation for long-term processes at room temperature [16-18, 21].

The three approaches to modeling of subcritical crack growth in polymers under constant load can be pointed out. The first assumes that kinetics of the process is uniquely defined by time-dependent properties of the matrix material. According to the most detailed theory of the kind [30], the crack propagates due to viscoelastic deformation of the matrix material. The second approach links crack growth with the time-dependent processes developing within the PZ material [9, 10, 19]. And, finally, the third approach is based on the CL concept [1, 2]. Based on the analysis of CL motion from the standpoint of irreversible thermodynamics, a complete specification for a solution of the general problem on the CL kinetics has been obtained. This approach applied for the case when the CL can be defined as a two-parameter system [22, 27, 31-34] leads to a modeling of various phenomena observed in thermoplastics, particularly discontinuous crack growth. In the framework of the third approach, it also should be mentioned the kinetic model [35] with a quasi-empirical condition of discontinuous crack propagation.

The present report is devoted to a thermodynamically consistent characterization of the simplified (two-parameter) CL kinetic model. The simplification of the model results from the observations that the PZ in thermoplastics occurs as a thin strip extending the crack, so that the CL can be geometrically determined by the crack and CL lengths only. Motion of the CL causes elastic energy release from the matrix and energy expenses due to formation of the PZ and new crack surfaces. Thermodynamic force for crack or PZ advance is defined as the difference between the rate of respective potential energy release and the rate of energy expenditure; crack or PZ advance being possible if the thermodynamic force is positive. Focusing only on modeling of CL growth and on lifetime assessment and taking account of the fact that the matrix releases only elastic energy, viscoelasticity of the matrix is admissible to be ignored. The degradation of the PZ

material is described as a reduction of the specific energy of crack extension in time. The kinetic equations governing the process of CL growth are formulated as relations linking the rates of crack and PZ extensions with conjugated thermodynamic forces. Numerical solution of the equations, non-linear because of the above constraints on crack and PZ advances, reveals two modes of CL growth under constant load: continuous (the CL grows all the time of the process) and discontinuous (the CL growth is a sequence of its stationary states and transitions from one state to another). Stability analysis shows that any process of CL advance including crack growth is unstable. Particularly, this means instability of the transitions from one CL stationary state to another in a discontinuous process. As examples of CL kinetic behavior, the two additional loading conditions are analyzed: first, the edges of a finite SEN plate are displaced with a prescribed rate (the ramp test if the rate is constant), and second, a dipole with a given rate of growth is applied to the crack boundaries in an infinite plate.

2. Process zone formation. Energy balance

Let a two-dimensional cracked body (Fig. 1a) be subjected to a remote load $p = \{p_x, p_y\}$ on bounding contour S_p inducing a stress-strain state of the opening mode (mode I) in a vicinity of the crack. The deformation caused by the remote load is assumed small and the material linearly elastic, so that the problem on the body in question is completely linear. As a response to the stress singularity at the crack tip predicted by the solution of the above linear problem, a region of the material ahead of the crack tip is transformed so that the stresses within it diminish. In case

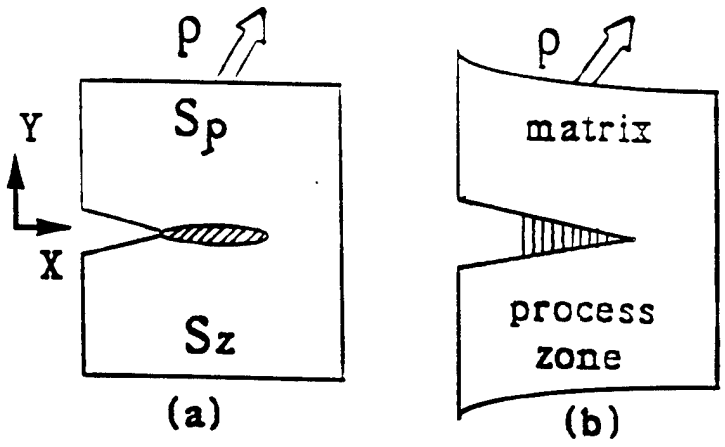

Figure 1. PZ formation: (a) before and (b) after the PZ occurs

of thermoplastics, this region called in previous section the process zone (PZ) usually appears in the shape of a thin strip as shown in Fig. 1a by contour S_z. Mechanism of PZ formation contains at least two stages: first cavitation within the original material, and second stretching or shearing of the cavitated material. As a result, the continuum under consideration is divided into two parts of different materials: the PZ (inside contour S_z) and the rest of the body (outside the contour) consisting of the original material and called previously the matrix (Fig. 1b). The additional matrix deformation produced by the PZ appearance is supposed small as before and so, the problem on the matrix stays linear.

Formation of the PZ can be described in terms of forces and displacements as follows. Because the region enveloped by contour S_z is narrow in the direction of y-axis, the values of

traction and displacement on the contour can be understood as stress component $\sigma = \sigma_{yy}$ and contour opening $\delta = 2u_y$. The state of the part inside S_z is treated as homogeneous in the y-axis direction and contour S_z is substituted with its projection L_z on x-axis. Let at the beginning of the process, i.e. at the instant of cavities nucleation, the traction on L_z and contour opening have values σ_m^0 and δ^0 respectively. At this point, the equality between the tractions acting on the external and internal parts of the body along L_z is violated: the traction applied to the external part (to the matrix) do not change and keeps value σ_m^0, but that for the internal part drops down to a certain value σ_z^0 ($< \sigma_m^0$). Nucleation of cavities leaves displacement compatibility between the two parts of the body valid, so that equalities $\delta_m^0 = \delta_z^0 = \delta^0$ take place for any point of L_z. The opening δ of S_z due to development of the cavities and subsequent stretching of the cavitated material with preservation of the mentioned compatibility gives rise to changes in the contour tractions. The value of the traction acting on the matrix, σ_m, decreases obeying the elasticity law of the matrix, whereas that for the traction exerted on the cavitated region, σ_z, varies in accordance with the stress-strain relation of the material subjected to cavitation and stretching. This non-balanced process comes to an equilibrium when the tractions on the both sides of S_z get equal to each other, i.e. $\sigma_m = \sigma_z = \sigma^*$ at all points within L_z. The respective equilibrium value of opening displacement δ is denoted by δ^*.

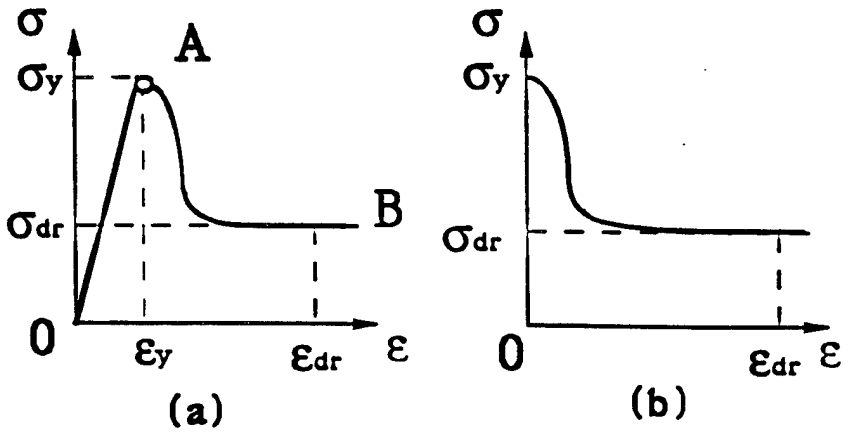

Figure 2. Diagram $\sigma - \varepsilon$ of cold drawing: (a) observed, (b) simplified

For complete specification of the problem on PZ formation, a stress-strain relation governing PZ behavior during this process has to be known. For polymers, it is widely accepted that the PZ material is identical with that obtained as a result of cold drawing of the original

material. This allows the characterization of the PZ at any point in terms of the diagram connecting engineering stress σ and strain ε (Fig. 2a). By σ_y and σ_{dr} one implies the yield and drawing stresses, and by ε_y and ε_{dr} the strains before and after drawing respectively. Segment OA describes elastic deformation and AB drawing, the transition from undrawn state to drawn one, since it results in a fall of stress σ, being unstable. Further, for simplicity, the elastic part of diagram σ vs. ε is neglected, $\varepsilon_y = 0$ (Fig. 2b), and the strain after drawing can be determined as $\varepsilon_{dr} = \lambda_n - 1$ where λ_n is the natural draw ratio. Moreover, it is assumed that during PZ formation each point of the region within L_z goes through the complete transformation from the undrawn state to the drawn one, i.e. any PZ fibril is subjected to the drawing stress and experiences deformation with the natural draw ratio, i.e. $\sigma = \sigma_{dr}$ and $\varepsilon = \lambda_n - 1$.

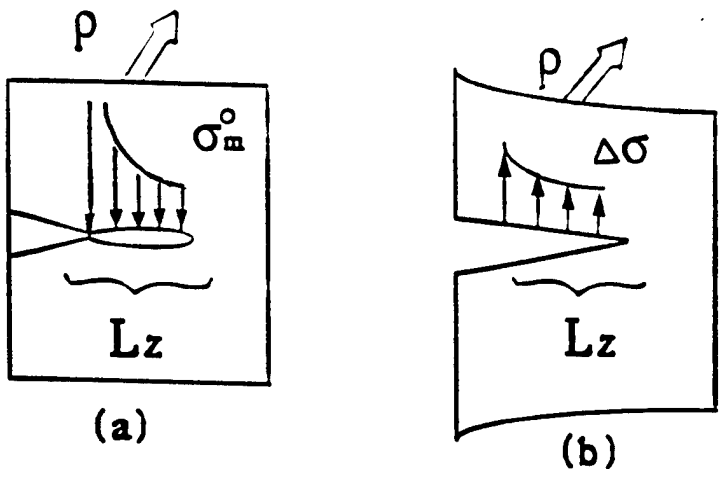

Figure 3. Matrix unloading: (a) initial and (b) additional tractions on L_z

According to the above, the opening of L_z at the instant of cavities nucleation has to be taken to equal zero, i.e. $\delta^0 = 0$. Let, for definiteness, opening δ due to PZ formation and matrix unloading change as $\delta = \alpha\delta^*$ where α grows from 0 to 1. This process, because of matrix linear elasticity, can be decomposed into the two stages: first removal of the part of the body within (Fig. 3a) and second application of traction $\Delta\sigma = \alpha(-\sigma_m^0 + \sigma_{dr})$ to the cut boundaries (Fig. 3b), so that the total traction changes as $\sigma_m = (1-\alpha)\sigma_m^0 + \alpha\sigma_{dr}$. The matrix behavior can be displayed by straight line $\sigma_m(\delta)$ in Fig. 4a. The figure also illustrates the PZ behavior during its formation by curve $\sigma_z(\delta)$ which is analogous to curve $\sigma(\varepsilon)$ in Fig. 2b. As a result of PZ formation, the stresses in a vicinity of the crack tip are released as shown in Fig. 4b.

Consider the energy balance of PZ formation, admitting the process to be isothermal and the remote load prescribed. Under conditions indicated, the relevant thermodynamic potential is the Gibbs energy G.

Since the elastic deformation of the material within L_z is disregarded, all energy changes associated with cavitation fall out from consideration. Stretching or shearing of the cavitated material results in the following change of G:

$$\Delta G = \Delta F_m + F_z - W_p \tag{1}$$

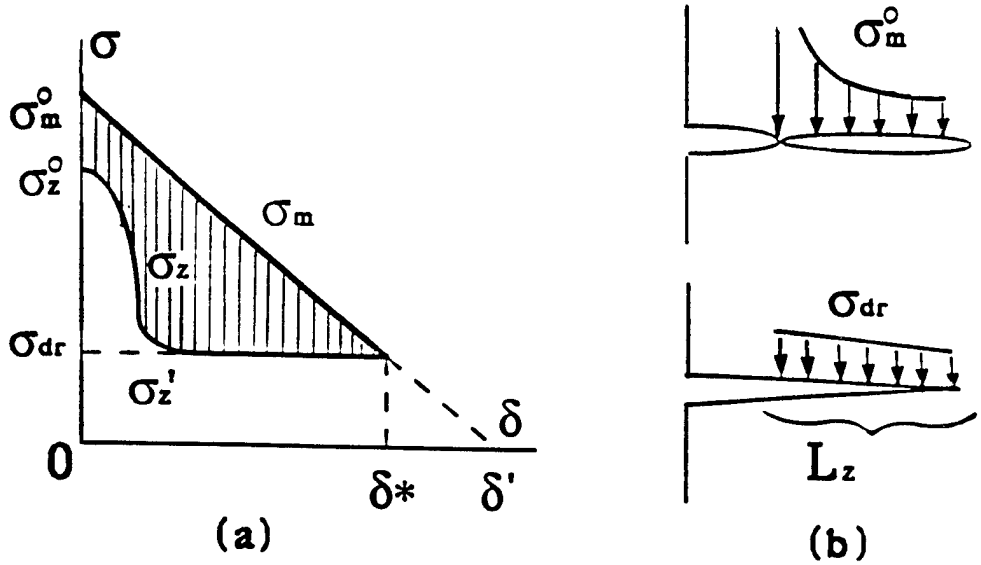

Figure 4. Stress evolution ahead of crack tip: (a) diagrams σ_m and σ_z vs. δ, (b) stress release

where ΔF_m and F_z are change in strain energy of the matrix and the "deformation potential" of the cavitated region, and W_p is the work done by the remote load on the displacement of contour S_p due to the processes considered. The deformation potential is equal to the work of traction σ_z on opening δ and is written in the form

$$F_z = W_z = \int_{l_z} h \left(\int_0^{\lambda_n - 1} \sigma \, d\varepsilon\right) dx. \tag{2}$$

Here by l_z one implies the length of L_z and by h the width of the original material region transformed into the PZ; the opening displacement within L_z and PZ strain are linked by $\delta = h\varepsilon$.

In the right side of (1), the first and third terms taken together signify the change in the total potential energy of the matrix and the apparatus maintaining the remote load,

$$\Delta \Pi_m = \Delta F_m - W_p, \tag{3}$$

and $-\Delta \Pi_m\ (>0)$ is the energy release from the matrix and remote load. Now, equation (1) can be rewritten as

$$\Delta G = \Delta \Pi_m + F_z. \tag{4}$$

One more expression for (1) results from the fact that the process in question is in equilibrium and so, the change of the strain energy of the matrix equals the work done by all external forces. This means that

$$\Delta F_m = W_p - W_m \tag{5}$$

where $-W_m$ is the work done by traction σ_m on opening δ of L_z:

$$W_m = -\int_{l_z} \left(\int_0^{\delta} \sigma_m \, d\delta \right) dx; \tag{6}$$

minus indicates the fact that traction σ_m and opening displacement δ have the opposite directions. Equations (3) and (5) yield $\Delta \Pi_m = -W_m$ and with the first of (2) leads to a new representation of equation (1):

$$\Delta G = -W_m + W_z. \tag{7}$$

This allows a graphical interpretation of energy balance as shown in Fig. 4a. Namely, the areas of the rectilinear and curvilinear trapezoids under lines $\sigma_m(\delta)$ and $\sigma_z(\delta)$ represent the energy release from the matrix and remote load, $-\Delta \Pi_m$, and the change in the PZ deformation potential, ΔF_z, respectively, so that the shaded area in Fig. 4a corresponds to the negative of (1). If a PZ size is fixed, then ΔG as a functional of δ gains a minimum value for the equilibrium opening δ^*, i.e.

$$\Delta G^* = \Delta G[\delta^*] \leq \Delta G[\delta]. \tag{8}$$

Further, the value ΔG^* of ΔG only is used and superscript $*$ therefore omitted.

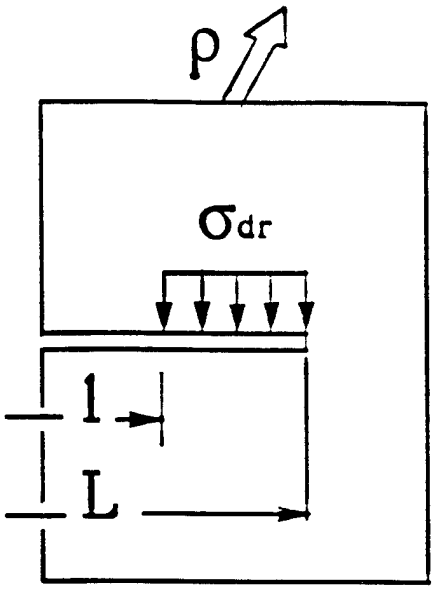

Figure 5. Approximation of matrix state

According to the second law of thermodynamics, the PZ may occur only if $-\Delta G > 0$, i.e. the energy release from the matrix and remote load due to PZ formation is greater than the respective energy expenditure within the PZ (the area hatched in Fig. 4a is "positive"). It should be emphasized that the energy balance is indifferent to "contents" of change (2) in the deformation potential of the PZ during its formation, i.e. the balance would be the same no matter whether the PZ completely accumulates the energy received from the matrix, or it dissipates this energy as heat in the surroundings, or both processes take place. For its meaning, ΔG is a functional of the domain of the original material transformed into the PZ.

Since the PZ has the shape of a thin strip, its opening displacement as well as the opening displacement of the crack can be approximated by the opening displacement of the slit extending the crack over the PZ length l_z. This allows the geometrical characterization of the CL by the two parameters - the crack and CL lengths, l and $L = l + l_z$ (Fig. 5).

The change in the total energy of the matrix and remote load, $\Delta \Pi_m$, does not depend on the path of matrix unloading and under the way chosen above is evaluated as

$$\Delta \Pi_m = -\int_{l_0}^{L}\{\int_0^{\delta^*}[(1-\alpha)\sigma_m^0 + \alpha\sigma_{dr}]\delta^* d\alpha\}dx = -\frac{1}{2}\int_{l_0}^{L}\sigma_m^0\,\delta^* dx - \frac{1}{2}\int_{l_0}^{L}\sigma_{dr}\,\delta^* dx, \qquad (9)$$

where l_0 is the crack length at the instant under consideration. Quantity $-\Delta \Pi_m$ corresponds to the trapezoid area under line $\sigma_m(\delta)$ in Fig. 4a. It can be shown that (Appendix A)

$$\int_{l_0}^{L}\sigma_m^0\,\delta^* dx = \int_0^{L}\sigma_p\,\delta^* dx + 2\Pi_0 \qquad (10)$$

where σ_p stands for the negative of stress component σ_{yy} produced by the remote load in the uncracked body along x-axis, δ^* within $[0, l_0]$ is understood the crack opening displacement after PZ formation, and by Π_0 one implies the change in the total energy of the matrix and remote load due to transition from the uncracked body to the cracked one. Substituting (10) into (9), the change in the total energy as a result of PZ formation gains the resultant expression:

$$\Delta\Pi_m = -\Pi_0 - \frac{1}{2}\int_0^L \sigma_p \delta^* dx - \frac{1}{2}\int_{l_0}^L \sigma_{dr} \delta^* dx, \tag{11}$$

the energy release from the matrix and remote load due to PZ formation being equal to the negative of (11). It makes sense to notice that the presence of the PZ reduces the energy release. It is seen from the comparison of $\Delta\Pi_m$ and $\Delta\Pi'_m$ for the cases with and without a PZ, respectively. The latter is determined by the expression

$$\Delta\Pi'_m = -\Pi_0 - \frac{1}{2}\int_{l_0}^L \sigma_p \delta' dx \tag{12}$$

in which δ' is the opening displacement due to crack extension from $x = l_0$ to $x = L$. Quantity $-\Delta\Pi'_m$ is illustrated by the area of the triangle under line $\sigma_m(\delta)$ in Fig. 4a.

If behavior of the PZ material had been "perfectly plastic" with stress σ_{dr} (see Fig. 4a, dashed line $\sigma'_z(\delta) \equiv \sigma_{dr}$), then the deformation potential would have been determined by

$$\hat{F}_z = \int_{l_0}^L \sigma_{dr} \delta^* dx. \tag{13}$$

Hence with (4) and (11) there follows for the respective change in the Gibbs potential:

$$\Delta\hat{G} = -\Pi_0 - \frac{1}{2}\int_0^L \sigma_p \delta^* dx + \frac{1}{2}\int_{l_0}^L \sigma_{dr} \delta^* dx. \tag{14}$$

Quantities $\hat{F}_z$ and $-\Delta\hat{G}$ are presented by the areas respectively of the rectangle under line $\sigma'_z(\delta)$ and the triangle between lines $\sigma_m(\delta)$ and $\sigma'_z(\delta)$ in Fig. 4a. Since the real PZ material is formed as a result of drawing, according to Fig. 2b

$$\int_0^{\varepsilon_{dr}} \sigma \, d\varepsilon = (1+\eta)\sigma_{dr}\,\varepsilon_{dr} \tag{15}$$

where by definition

$$\eta = \frac{\int_0^{\varepsilon_{dr}} \sigma \, d\varepsilon - \sigma_{dr}\,\varepsilon_{dr}}{\sigma_{dr}\,\varepsilon_{dr}} \tag{16}$$

and $\eta > 0$. As accepted above, coefficient η characterizing the "shape" of the stress-strain relation for the PZ material, has the same value for all points of the PZ, so that

$$F_z = (1+\eta)\int_{l_0}^{L} h\sigma_{dr}\,\varepsilon_{dr} dx. \tag{17}$$

Curve $\sigma_z(\delta)$ in Fig. 4a depicts PZ behavior, and the area of the trapezoid under this curve gives quantity F_z. According to the assumption accepted above, the width increment of the original material strip due to PZ formation is equal to the opening displacement of contour S_z, i.e. $h\varepsilon_{dr} = \delta^*$, and equation (17) becomes

$$F_z = (1+\eta)\int_{l_0}^{L} \sigma_{dr}\delta^* dx. \tag{18}$$

Equations (4), (11) and (18) lead to the following expression for the change in the Gibbs potential due to PZ formation:

$$\Delta G = -\Pi_0 - \frac{1}{2}\int_0^L \sigma_p\,\delta^* dx - \frac{1}{2}\int_{l_0}^L \sigma_{dr}\,\delta^* dx + (1+\eta)\int_{l_0}^L \sigma_{dr}\,\delta^* dx. \tag{19}$$

Equation (19) can be rewritten as

$$\Delta G = \Delta\hat{G} + Z \tag{20}$$

where $\Delta\hat{G}$ is the change of the Gibbs potential in case of the perfectly plastic PZ material previously determined by (14), and

$$Z = \eta\int_{l_0}^{L} \sigma_{dr}\,\delta^* dx \tag{21}$$

is the energy consumed within the PZ due to its overloading during formation (see Figs. 2b and 4a).

There exists a simple link between the bodies with the PZ and with the Dugdale-Barenblatt cohesive zone (CZ). The CZ is a crack extension, boundaries of which interact between each other with the traction uniformly distributed and equal, say, to σ_{dr} (the real and extended cracks sometimes are called the physical and effective cracks respectively). In case of the CZ, the negative of energy release from the matrix is given by (11) like that for the PZ, and the traction potential is determined by (13) like that for the perfectly plastic PZ material. Thus, the change in the Gibbs potential due to CZ formation is written as (14). However, the meaning of quantity $\hat{F}_z$ involved in the energy balance for the CZ essentially differs from that for the perfectly plastic PZ. Namely, quantity (13) for the PZ is the deformation potential of the material filled the space between the matrix boundary within L_z, whereas for the CZ it means the potential of external forces acting on the matrix boundaries along L_z. It is also obvious that energy balance (20) for the PZ can formally be reduced to that for the CZ by setting $\eta = 0$.

3. Degradation of PZ material

Experimental studies on the materials obtained by cold drawing of polymers show that such materials under the loading equivalent to that in a tensile specimen at drawing experience creep and/or long-term rupture. For example, there are data regarding drawn material degradation for some engineering thermoplastics [9-11, 23, 24]. Similar processes can be reasonably assumed to occur within the PZ material. The present paper is only dealing with long-term rupture of the PZ material that is most likely a thermally activated process and can be described by the fluctuation theory of fracture [36]. The approach employed further is based on an analogy between the processes of phase transition [37, 38] and fracture and can be described as follows.

Fracture of the PZ material is associated with the entropy production within the process zone under tensile stress $\lambda_n \sigma_{dr}$. Let s^i be the specific (per unit area of the crack surface) entropy production in the act of rupture at a given PZ point x and time t, and s_0 be a critical value of specific entropy, i.e. the value at which material failure takes place, all indicated values being counted from a certain reference level. The critical increment of entropy density then can be written in the form

$$\Delta s(x,t) = s_0 - s^i(x,t) \tag{22}$$

where Δs signifies the entropy barrier for the material failure at point x and time t. In (22), s^i increases from zero to s_0 and Δs diminishes from s_0 to zero with time. In parallel, introduce the specific (per unit area of the crack surface) fracture energy γ absorbed on new crack surfaces due to PZ rupture. The irreversible entropy and fracture energy are postulated to be connected by

$$s^i(x,t) = \frac{2}{T}\gamma(x,t). \tag{23}$$

where T is temperature in degrees Kelvin. From (22) and (23), the balance for the fracture energy follows:

$$\Delta\gamma(x,t) = \gamma_0 - \gamma(x,t). \tag{24}$$

During the process of long-term rupture, γ increases from zero to γ_0 and $\Delta\gamma$ decreases from γ_0 to zero. Now, γ_0 can be treated as the energy needed for the process zone to rupture at the initial moment, and $\Delta\gamma$ as the energy required for that at a current moment. Thus, the long-term rupture is characterized by descent of the material fracture energy and is, in essence, a process of material degradation.

Decrease of the energy reserve $\Delta\gamma$ with time is described by the simplest linear equation

$$\frac{d}{dt}\Delta\gamma = -r\Delta\gamma \tag{25}$$

where r is a phenomenological coefficient equal to the reverse value of the relaxation time t_r for the rupture process, $r = 1/t_r$. Integrating (25) with the initial condition $\Delta\gamma = \gamma_0$ at $t = t_x$, where t_x is the time of the process zone formation at point t_x, the quantity $\Delta\gamma$ is obtained as the function of time

$$\Delta\gamma(x,t) = \gamma_0 \exp[-r(t-t_x)]. \tag{26}$$

Correspondingly, the energy absorbed due to fracture of the process zone material is

$$\gamma(x,t) = \gamma_0\{1-\exp[-r(t-t_x)]\}. \tag{27}$$

The above coefficient r, or relaxation time t_r is nothing but a time scale for the process of material degradation and is a certain function of temperature. For example, the time scale can be defined in the form [36]

$$t_r = \frac{1}{r} = t_0 \exp\frac{Q_0 - \chi\sigma_{dr}}{RT} \tag{28}$$

where t_0, Q_0 and χ signify parameters of a given material: a characteristic time, an activation energy for time-temperature dependent processes and the coefficient that reflects the material microstructure respectively, R stands for the universal gas constant and T the temperature in degrees Kelvin. The quantity γ_0 is also temperature dependent and, for general reasons, should be considered as a decreasing function of temperature.

4. Energy balance for CL propagation

Propagation of the CL implies two events occurring in parallel - PZ advancement and crack lengthening. The first means that the PZ captures a new region of the matrix located ahead of its tip, and the second, the crack cuts off the PZ from its root. So, energy balance of CL growth should include the energy expenses not only due to PZ formation, but also due to formation of new boundaries of the crack. Let at a current instant the lengths of the crack and CL be equal to l and L respectively. For its meaning the total potential energy of the matrix and remote load is determined as a function of current values of these lengths. This energy, when counted from that for the uncracked body, is evaluated according to (11) by

$$\Pi = \Pi_0 + \Delta\Pi_m = -\frac{1}{2}\int_0^L \sigma_p \delta\, dx - \frac{1}{2}\int_l^L \sigma_{dr}\delta\, dx. \tag{29}$$

Here Π_0 and $\Delta\Pi_m$ stand for the changes in the total potential energy due to formation of the current crack and PZ respectively, and δ the CL opening in the state considered. The PZ deformation potential is determined in the form following from (17):

$$F_z = (1+\eta)\int_l^L \sigma_{dr}\,\delta\, dx. \tag{30}$$

Energy balance expressed by (4), (13), (14), (20) and (29) should be added by the term reflecting the change in energy due to formation of new crack surfaces:

$$G = \Pi + F_z + \Gamma = P + Z + \Gamma. \tag{31}$$

Here the Gibbs potential is counted from that for the uncracked body, and $P = \Pi + \hat{F}_z$ and Z are the Gibbs potential due to formation of a current CL with perfectly plastic PZ and the energy of PZ overloading respectively . The new quantity Γ is the energy accumulated on the boundaries of the crack due to its advance and determined as follows. Let t_x be the time of PZ formation at a point x $(l < x < L)$, i.e. the instant when the CL tip goes through this point, $L(t_x) = x$. At a current time $t(>t_x)$, the energy γ accumulated within the PZ due to its rupture is postulated to be distributed along x axis such that

$$\gamma = \begin{cases} \gamma_0, & l_0 \le x \le l(t); \\ \gamma(x,t), & l(t) < x < L(t); \\ 0, & L(t) \le x \end{cases} \tag{32}$$

where $\gamma(x, t)$ is given by (27). Proceeding from (32), the energy Γ accumulated on the crack boundaries is determined as

$$\Gamma = 2\,[\,\gamma_0(l-l_0)+\int_l^L \gamma(x,t)\,dx\,]. \tag{33}$$

By virtue of (32)

$$\Gamma(l,\ L+\Delta L,\ t)\ -\ \Gamma(l,\ L,\ t)\ \equiv\ 0, \tag{34}$$

that is, the partial derivative of function (32) with respect to L is identically equal to zero.

The balance of the entropy production due to CL growth is given by the expression

$$T\frac{dS^i}{dt} = -\frac{\partial G}{\partial l}\dot{l} - \frac{\partial G}{\partial L}\dot{L} - \frac{\partial G}{\partial t} \tag{35}$$

in which the dote signifies a derivative with respect to time. The couples $\dot{l}$, $\dot{L}$ and

$$X_l = -\frac{\partial G}{\partial l},\quad X_l = -\frac{\partial G}{\partial l} \tag{36}$$

play respectively the roles of the thermodynamic fluxes and forces [39] for crack lengthening and CL advancement. The last term in the right side of (35) which is, according to (27) and (33), determined as

$$-\frac{\partial G}{\partial t} = 2\int_l^L \dot{\gamma}(x,t)dt \tag{37}$$

signifies the contribution in the entropy production of PZ material degradation.

5. CL as a two parameter system with unilateral constraints

According to the assumption of section 2, the region of the original material that is transformed into the PZ (enclosed by contour S_z in Fig. 1a) has the shape of a thin strip, and the matrix state is approximated by the state of the cracked body with appropriate sizes of the slit and traction distribution along the slit boundary (see Fig. 5). This approximation, if no special limitations are introduced, leads to a CL tip singularity, that, however, is not treated as a real characteristic of the stress-strain field and only used for evaluation of the energy sinks at crack and PZ extensions.

It is convenient to divide the thermodynamic forces defined by (36) into the parts corresponding to the second of (31):

$$X_l = P_l + Z_l - \Gamma_l, \quad X_L = P_L + Z_L \tag{38}$$

where

$$P_l = -\frac{\partial P}{\partial l}, \quad Z_l = -\frac{\partial Z}{\partial l}, \quad \Gamma_l = \frac{\partial \Gamma}{\partial l} \tag{39}$$

and

$$P_L = -\frac{\partial P}{\partial L}, \quad Z_L = -\frac{\partial Z}{\partial L}; \tag{40}$$

for the second of (38) the identity $\partial \Gamma / \partial L \equiv 0$ resulting from (34) is used. The first parts of (39) and (40) are evaluated as (Appendix B)

$$P_l = \sigma_{dr}(\delta_p + \delta_z), \quad P_L = \frac{1}{E}(K_p + K_z)^2 \tag{41}$$

where δ_p and δ_z are the crack tip opening displacements (CTODs) and K_p and K_z the stress intensity factors (SIFs) due to, respectively, the remote load p and traction σ_{dr} on the boundary of the matrix with the PZ (see Fig. 5 from which it is seen that δ_z and K_z are negative). All these characteristics of the stress-strain field are functions of both lengths, l and L. Proceeding from (21), the second parts of (39) and (40) can be shown to take in the form (see Appendix B)

$$Z_l = \eta \sigma_{dr} \delta_z, \quad Z_L = \frac{2\eta}{E} K_z (K_p + K_z). \tag{42}$$

And finally, as it follows from (26), (27) and (33),

$$\Gamma_l = 2\Delta\gamma \tag{43}$$

where $\Delta\gamma$ stands for the energy reserve to PZ fracture ahead of the crack tip. It should be noted that quantity (43) and the first of (38) depends not only on the crack and CL lengths, but also explicitly on time because, as follows from (26), $\Delta\gamma$ is a function of time,

$$\Delta\gamma(l,t) = \gamma_0 \exp[-r(t-t_l)]. \tag{44}$$

The second law of thermodynamics, $T(dS^i/dt) \geq 0$, written separately for advance of the CL and degradation of the PZ material yields the inequalities

$$X_l \dot{l} + X_L \dot{L} \geq 0, \quad -\frac{\partial G}{\partial t} \geq 0 \tag{45}$$

the second of which, in view of (27) and (37), is apparently satisfied. In the first of (43) the equality takes place only for a stationary state of the CL, i.e. only if $\dot{l} = 0$ and $\dot{L} = 0$.

The crack and PZ are not healed so that

$$\dot{l} \geq 0, \quad \dot{L} \geq 0. \tag{46}$$

These inequalities, in turn, impose certain limitations on relations between the thermodynamic fluxes and forces. Let, for simplicity, these relations be formulated by

$$\dot{l} = \varphi[X_l(l,L,t)], \quad \dot{L} = \psi[X_L(l,L)], \tag{47}$$

that is, each of the fluxes is connected only with its conjugated force. As seen from (47), the indicated separation of the fluxes and forces does not lead to a separation of the constitutive variables l and L. By virtue of (45) and for the physical meaning of the fluxes and forces the functions φ and ψ in (47) should possess the following properties: if $X_l \leq 0$ and $X_L \leq 0$, then $\varphi \equiv 0$ and $\psi \equiv 0$ so that $\dot{l} = 0$ and $\dot{L} = 0$ (the CL is arrested); for $X_l > 0$ and $X_L > 0$, φ and ψ are increasing functions of X_l and X_L respectively (the CL grows).

The next condition to be satisfied,

$$l \leq L, \tag{48}$$

is obvious because the difference $L - l$ is the PZ length. One more limitation imposed on the CL length is given in the next section.

Thus, the process in question is characterized by kinetic equations with respect to two constitutive variables which, at the beginning of the process, are satisfied certain initial conditions and, during the entire process, obey limitations in the shape of inequalities. Thus, the CL growing through the matrix is a system with two degrees of freedom with unilateral constraints.

6. Uniform tension. CL equilibrium and stability

The remote load to be mainly regarded in this paper (exept section 14) is such that the stress-strain state of the uncracked body is a uniform uniaxial tension towards y-axis, so that the stress σ_p is constant along x-axis.

If material characteristics of the matrix and PZ and sizes of the matrix and crack are prescribed, then themodynamic force X_L is a function of CL length L only. This length is called equilibrium if it satisfies the equation

$$X_L(l, L) = 0 \tag{49}$$

in which l is considered fixed. From (49) with the second of (41) and (42) it follows

$$K_p + (1 + 2\eta)K_z = 0, \quad K_p + K_z = 0. \tag{50}$$

For the uniformly tensile remote load, the left sides of the first and second of (50), K_1 and K_2, vary with L at constant l as shown in Fig. 6a. Equation (49) then has two roots L_1 and L_2, and the second, greater of them coincides with the length of the effective crack in the DB model [25, 26].

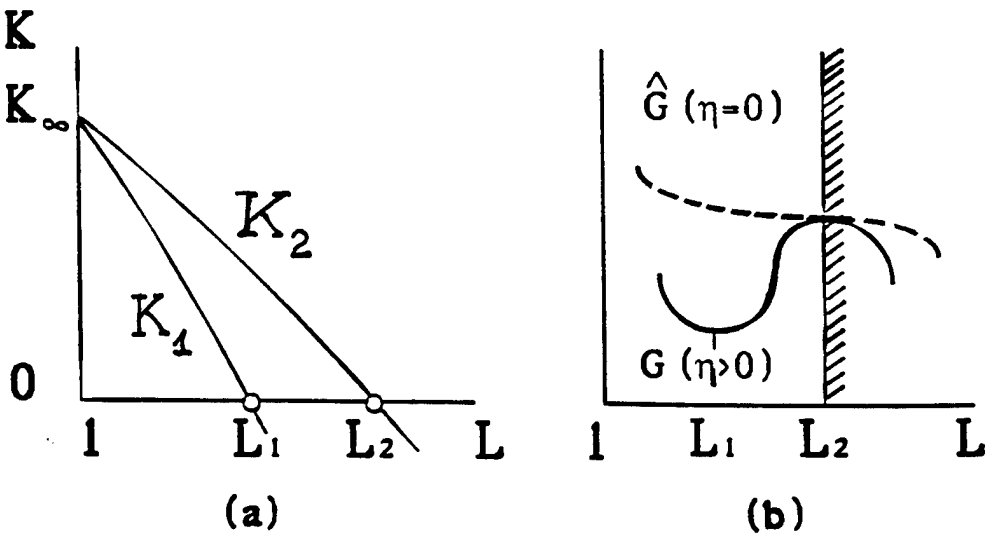

Figure 6. Stability of CL equilibrium: (a) SIFs vs. CL length, (b) profile of Gibbs' potential

It is easy to prove that the first equilibrium state, at $L = L_1$, is stable, whereas the second one, at $L = L_2$, unstable. Indeed, the second equations of (36), (41) and (42) yield

$$\frac{\partial^2 G}{\partial L^2} = -\frac{1}{E}\left(\frac{\partial K_1}{\partial L} K_2 + K_1 \frac{\partial K_2}{\partial L}\right). \tag{51}$$

If $L = L_1$, then $K_1 = 0$, $\partial K_1 / \partial L < 0$, and $K_2 > 0$ (see Fig. 6a), and the stability condition $\partial^2 G / \partial L^2 > 0$ is met. In the case of $L = L_2$, analogous consideration results in the inequality $\partial^2 G / \partial L^2 < 0$ which signifies instability.

The profile of the Gibbs potential as a function of the CL length is depicted by the solid curve in Fig. 6b. When η becomes zero, the Gibbs potential $G(L)$ for the general case of PZ material turns into the Gibbs potential $\hat{G}(L)$ for the perfectly plastic PZ, root L_1 merges with root L_2, and the shape of the energy profile is transformed into that indicated by the dashed curve. In view of the second parts of (36), (41) and (50), function $\hat{G}(L)$ at $L = L_1 = L_2$ has a stationary (inflection) point, not a minimum one. On the other hand, as Fig. 6a shows, at $L > L_2$ the total SIF K_2 becomes negative. From the physical standpoint, the inequality $K_2 < 0$ is unacceptable because it means an overlapping of the PZ boundaries. With limitation $L \le L_2$ (see the shaded line in Fig. 6b) function $\hat{G}(L)$ at $L = L_1 = L_2$ has a unilateral degenerate minimum. Hence there follows that the DB model possesses a (weak) stability with respect to advance of the effective crack tip.

Thus, for each given crack length l, two equilibrium states of the CL with sizes L_1 and L_2 ($L_1 < L_2$) can be pointed out, but only the first of them is stable. Further only L_1 will be called the CL equilibrium length for the given crack length l. The CL equilibrium length will be denoted by $L_{eq}(l)$, or briefly L_{eq} if this cannot cause a misunderstanding. A growth of the PZ beyond the range $l \le L \le L_{eq}$ is impossible because it would produce an increase in the Gibbs potential (see Fig. 6b). So, at every moment of CL growth

$$L \le L_{eq}(l), \tag{52}$$

that is, the CL length cannot exeed the equilibrium value for the current crack length.

7. Crack initiation. Stability of crack advance

Let the remote load be uniform tensile and prescribed and CL have sizes l_0 and $L \le L_{eq}(l_0)$. If at a given instant t_0 the thermodynamic force for crack advance is negative, $X_l(l_0, L, t_0) < 0$, the crack does not grow, $\dot{l} = 0$. No limitations regarding behavior of the CL length L are imposed so that this length might either stay constant or increase. i.e. $X_L(l_0, L) \le 0$, $\dot{L} = 0$ or $X_L(l_0, L) > 0$, $\dot{L} > 0$. If the CL is arrested, then the function formed by omitting $-\Gamma_l$ in the first of (38),

$$Y_l = P_l + Z_l, \tag{53}$$

does not change, and if the CL grows, the function increases (Fig. 7a where Y_l as a function of L varies like graph $p_l(L)$ in Fig. Cb, Appendix C).

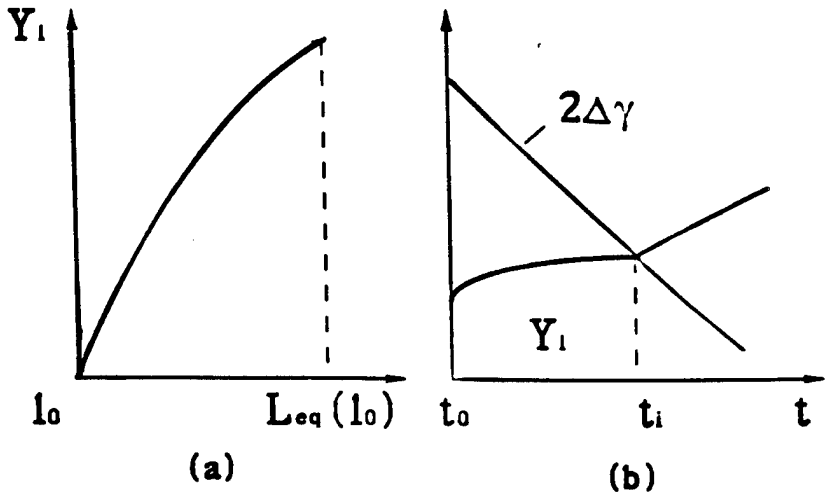

Figure 7. Crack advance at fixed CL tip: (a) Y_l as a function of L, (b) determinaion of initiation time

At the same time, as a result of PZ material degradation the energy $\Delta\gamma$ required for the crack to advance and defined by (26) diminishes, and in both cases, $\dot{L} = 0$ and $\dot{L} > 0$, the thermodynamic force for crack advance,

$$X_l = Y_l - 2\Delta\gamma\ (< 0), \tag{54}$$

approaches zero (Fig. 7b which assumes that $\dot{L} > 0$ and Y_l grows with time).

The time of crack initiation, $t = t_i$, is determined by

$$X_l [l_0, L(t_i), t_i] = Y_l [l_0, L(t_i)] - 2\Delta\gamma (l_0, t_i) = 0 , \tag{55}$$

where in view of (52) $L(t_i) \le L_{eq}(l_0)$. From this instant, the force X_l becomes positive and the crack grows. At the "frozen" time, $t = t_i$, or which is the same at the fixed CL length, $L = L(t_i)$, the onset of crack growth is stable or unstable depending on whether the value of derivative

$$\frac{\partial^2 G}{\partial l^2} = -\frac{\partial X_l}{\partial l} = -\frac{\partial Y_l}{\partial l} + 2\frac{\partial \Delta\gamma}{\partial l} \tag{56}$$

taken at $l = l_0$ and $L = L(t_i)$ is positive or negative respectively. Behavior of Y_l as a function of l is shown in Fig. 8a (see graph $\overline{P}_l(l)$ in Fig. Ca, Appendix C). For its meaning derivative $\partial\Delta\gamma/\partial l$ might be different from zero (but cannot be negative), however, further it is disregarded for simplicity.

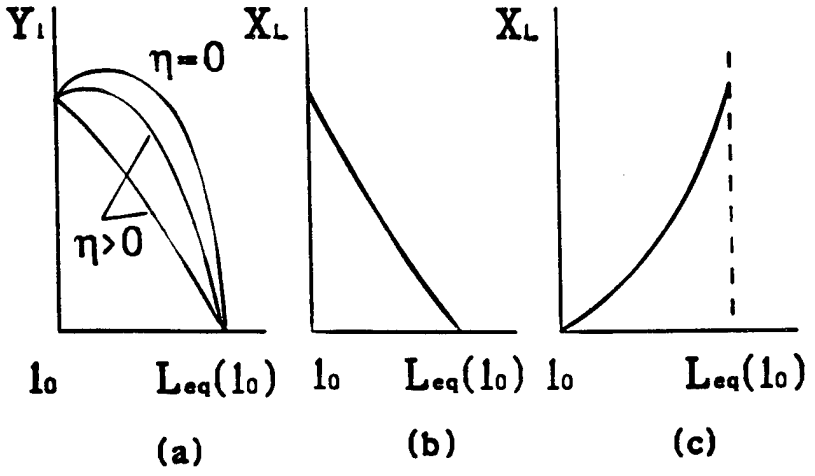

Figure 8. Thermodynamic forces: (a) Y_l as a function of l, (b) X_L as a function of L, (c) X_L as a function of l

At first, let the CL length at the initiation time be equilibrium, i.e. $L(t_i) = L_{eq}(l_0)$. Stability analysis then is reduced to examination of function Y_l in a vicinity of point $l = l_0$. If

$\eta = 0$, $\partial Y_l / \partial l > 0$ and crack tip advance is unstable. Particularly, it means the DB model is unstable with respect to advance of the physical crack even under the condition that the effective crack is arrested. If $\eta > 0$, the sign of $\partial Y_l / \partial l$ is not defined, the probability of that $\partial Y_l / \partial l$ is negative and crack advance is stable growing with η.

In case when the length of the CL at the initiation time is smaller than the equilibrium one, $L(t_i) < L_{eq}(l_0)$, all reasoning can also be based on Fig. 8a with the only difference that the point of function Y_l examination should be shifted to the right. As seen, the less the PZ is developed by the initiation time, the higher the probability of stable onset of crack growth.

8. CL stability relative to crack and PZ advances

In the two previous sectionsis, the stability analysis concerned with the cases when either the crack is arrested and the PZ freely grows (section 6), or conversely, when the PZ is in a stationary position and the crack is released (section 7). In the present considerations, the CL is assumed unrestricted with respect to both crack and PZ extensions.

The remote load is supposed to be uniformly tensile and prescribed, and the CL attained sizes l_0 and L_0 by a given instant t_0. At first, let $X_l(l_0, L_0, t_0) > 0$ and $X_L(l_0, L_0) > 0$, and there are no constraints regarding changes in both sizes of the crack and PZ, except the requirement for these changes to be positive. If $\delta l \geq 0$ and $\delta L \geq 0$ are various admissible deviations from the CL sizes, the second differential of the Gibbs potential is presented by

$$\delta^2 G = \frac{\partial^2 G}{\partial l^2}\delta l^2 + 2\frac{\partial^2 G}{\partial l\,\partial L}\delta l\,\delta L + \frac{\partial^2 G}{\partial L^2}\delta L^2 \tag{57}$$

where all derivatives are calculated at $l = l_0$ and $L = L_0$ under time fixed. The CL state in question is regarded to be stable if $\delta^2 G > 0$ at any admissible deviation δl and δL, and unstable if there exists at least one deviation for which $\delta^2 G < 0$.

Let the PZ length L_0 be as far from the equilibrium size $L_{eq}(l_0)$ that inequality

$$\frac{\partial^2 G}{\partial l^2} = -\frac{\partial X_l}{\partial l} = -\frac{\partial Y_l}{\partial l} > 0 \tag{58}$$

is met (see Fig. 8a). It means that lengths l_0 and L_0 are such that the portion of Fig. 8a bounded by points l_0 and L_0 contains only a descending segment of curve $Y_l(l)$. Everywhere within $[l_0, L_0]$

$$\frac{\partial^2 G}{\partial L^2} = -\frac{\partial X_L}{\partial L} > 0 \tag{59}$$

(Fig. 8b where graph has the same shape like that for graph $\overline{P}_L(L)$ in Fig. Cb, see Appendix C). The mixed derivatives of the Gibbs potential G satisfy the conditions

$$\frac{\partial^2 G}{\partial l\,\partial L} = -\frac{\partial X_L}{\partial l} = -\frac{\partial Y_l}{\partial L} = \frac{\partial^2 G}{\partial L\,\partial l} < 0 \qquad (60)$$

(Figs. 7a and 8c: behavior of X_L as a function of l is the same like that for $\overline{P}_L(l)$ in Fig. Ca, see Appendix C). Proceeding from (56)-(58), stability analysis is reduced to a searching of real (positive) roots of the quadratic equation

$$\frac{\partial^2 G}{\partial L^2}\mu^2 + 2\frac{\partial^2 G}{\partial l\,\partial L}\mu + \frac{\partial^2 G}{\partial l^2} = 0 \qquad (61)$$

where $\mu = \delta L/\delta l$. In the case when

$$\frac{\partial^2 G}{\partial L^2}\frac{\partial^2 G}{\partial l^2} - \left(\frac{\partial^2 G}{\partial l\,\partial L}\right)^2 \le 0 \qquad (62)$$

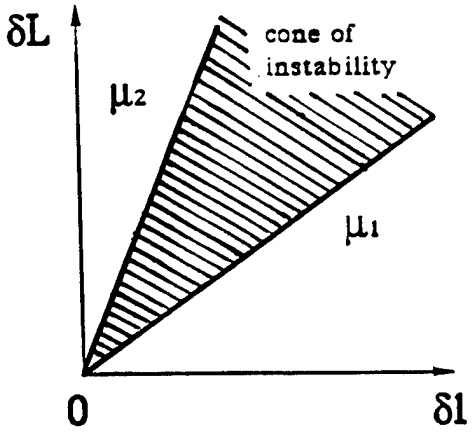

Figure 9. Positive quadrant of {δl,δL}-plane and cone of instability

equation (59) does have two real roots that merge to one if relation (60) is an equality. Let inequality (60) be satisfied, and μ_1 and μ_2 ($\mu_1 < \mu_2$) be the roots of (59). Then, there has to exist a region in the positive quadrant of $\{\delta l, \delta L\}$ plane, namely cone $\mu_1 < \mu < \mu_2$ (Fig. 9), such that for any its internal point $\delta^2 G < 0$. Existence of such a cone signifies that the CL state is unstable. If

$$\frac{\partial^2 G}{\partial L^2}\frac{\partial^2 G}{\partial l^2} - \left(\frac{\partial^2 G}{\partial l\,\partial L}\right)^2 > 0, \qquad (63)$$

then equation (59) does not have real roots, $\delta^2 G > 0$ everywhere within the positive quadrant of $\{\delta l, \delta L\}$-plane, and the CL state is stable.

The condition $X_L = 0$ accepted above means that the CL length is smaller than the equilibrium one, $L_0 < L_{eq}(l_0)$. In the case when $L_0 = L_{eq}(l_0)$, variations δl and δL are bounded by the additional condition resulting from (50):

$$\delta L - \frac{d L_{eq}}{d l} \delta l \leq 0 \tag{64}$$

where the derivative is taken at $l = l_0$. This means the region of admissible deviations is contracted from the positive quadrant to the cone defined by inequalities $\delta l \geq 0$ and (62). Now either inequality (56) remains valid, or it is substituted by

$$\frac{\partial^2 G}{\partial l^2} \leq 0 \tag{65}$$

(see the left portion of Fig. 8a where graph $Y_l(l)$ might have ascending segment). If (56) takes place, then the CL state is stable or unstable depending on whether the intersection of the cone of instability and the cone of admissible deviations is zero or not, respectively. If (65) is true, then the CL state is unstable because $\delta^2 G < 0$ at $\delta l > 0$ and $\delta L = 0$ (see the previous section).

As an example of stability analysis, an infinite matrix under uniform tensile remote load is considered. The PZ length is supposed to be essentially smaller than that for the equilibrium CL, or more precisely,

$$L - l << L_{eq}(l) - l, \tag{66}$$

This case is chosen to be examined proceeding from the two following reasons: first, if the CL with certain sizes is unstable in an infinite plate, it definitely will be unstable also in a finite plate, and second, if the CL with sizes l and L_1 is unstable in some matrix, then in the same matrix the CL with sizes l and L_2, where $L_2 > L_1$, certainly will be unstable; in the compared cases, otherwise (material characteristics, load, etc.) is understood to be identical.

For simplicity, it is accepted that $\eta = 0$. With notations

$$\frac{l}{L} = cos\theta, \quad \theta << 1, \tag{67}$$

the derivatives of the Gibbs potential can be shown to equal (Appendix D)

$$\frac{\partial^2 G}{\partial l^2} = \frac{\partial^2 G}{\partial L^2} = -\frac{\partial^2 G}{\partial l \partial L} = \frac{4\sigma_{dr}\sigma_p}{E\theta}. \tag{66}$$

This means that equation (59) has the two coinciding solution $\mu_1 = \mu_2 = 1$, that is, the cone of instability degenerates to a single ray dividing the positive quadrant $\delta l \geq 0$, $\delta L \geq 0$ in halves. The CL state is neutral with respect to deviation $\delta l = \delta L$, i.e. $\delta^2 G = 0$ at $\mu = 1$, and stable with respect to all other deviations, i.e. $\delta^2 G > 0$ at $\mu \neq 1$ ($\mu > 0$). Presence of one deviation at which the CL state is neutral is the indication that in any different case (a finite matrix and/or a bigger PZ) the cone of instability will be non-degenerate and a CL state unstable.

The above example leads to the conclusion valid for the case of $\eta = 0$: if the crack is not arrested, the CL state is unstable, whatever it is. Thus, the CL can be in one of the two states: either the crack is arrested and the CL on the whole is stable, or the crack is released and the CL is unstable. This situation is similar to that taking place for the Griffith model in which the crack either does not grow at all, or grows in an unstable mode, i.e. dynamically.

The case of $\eta > 0$ can also be analyzed based on behavior of quantities Y_l and X_L as functions of l and L (see Figs. 7a and 8). A state of the CL with $\eta > 0$ may be stable while it is unstable for $\eta = 0$ and the same otherwise. Moreover, even if a state of the CL is unstable, CL propagation is thinkable to develop in a quasi-static mode. This stems from the fact that PZ extension controlled by the respective kinetic equation (see the next section) goes on with a finite speed and in virtue of that, the mentioned instability cannot appear in the shape of catastrophe.

9. Kinetic equations, their numerical solution and dimensionless form

The process of CL propagation like any non-equilibrium process allows the interpretation as a transition of the system from a non-equilibrium state into its equilibrium. Assuming that the deviation of each CL current state from the corresponding equilibrium one is not too large, relations (45) for CL growth can be taken in the form of linear approximation of the functions φ and ψ connecting the thermodynamic fluxes and forces. As a result, the kinetic equations governing CL growth are written as follows

$$\begin{aligned} \dot{l} &= k_l X_l(l, L), \quad \text{if } X_l > 0, \\ \dot{L} &= k_L X_L(l, L), \quad \text{if } X_L > 0, \end{aligned} \tag{69}$$

and

$$\begin{aligned} \dot{l} &= 0, \quad \text{if } X_l \le 0, \\ \dot{L} &= 0, \quad \text{if } X_L \le 0. \end{aligned} \tag{70}$$

In (69) the phenomenological coefficients k_l and k_L that, from their physical meaning, have to be positive are functions of temperature and material characteristics, but in the framework of linear approach are considered independent of the thermodynamic fluxes and forces. Equations (69) and (70) should be supplemented by the initial conditions

$$l(0) = l_0, \quad L(0) = L_0. \tag{71}$$

Evolution of the CL includes also the PZ material degradation that is described by (26):

$$\Delta\gamma(x, t) = \gamma_0 \exp[-r(t - t_x)]. \tag{72}$$

The thermodynamic fluxes obeys limitations (46),

$$\dot{l} \ge 0, \quad \dot{L} \ge 0, \tag{73}$$

and the thermodynamic forces X_l and X_L are determine by (38), (41) and (42). Besides, two more limitations have to be satisfied, namely (48) and (52):

$$l \le L \le L_{eq}(l). \tag{74}$$

Equations (69)-(72) and inequalities (73) and (74) give complete specification for a description of the CL kinetics.

The formulated problem is non-linear and can be solved only numerically. The procedure of its numerical solution is implemented in the form of the following step-by-step process.

The matrix with CL is considered under a prescribed remote load, and all necessary material and geometrical characteristics of the system is assumed to be known. Let after n-th step of the process, at time $t = t_n$, the CL have sizes l_n and L_n satisfying (74).

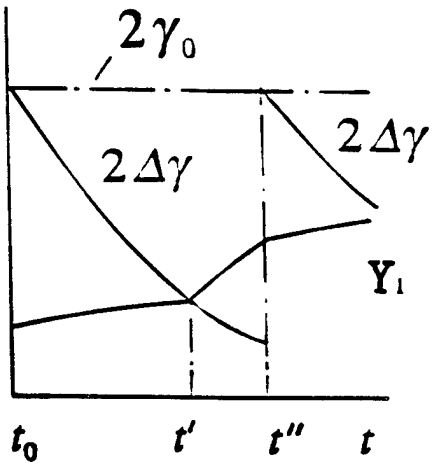

Figure 10. Force $X_1 = Y_1 - 2\Delta\gamma$

At first, a linear singular boundary value problem on the matrix is solved and as a result, the values of the SIFs, $K_{p,n}$ and $K_{z,n}$, and CTODs, $\delta_{p,n}$ and $\delta_{z,n}$ for the present CL state are found (see Fig. 5). In addition, for the current time and crack tip position, the value of the energy reserve $\Delta\gamma_n = \Delta\gamma(l_n, t_n)$ is computed employing (70). Then, the thermodynamic forces, $X_{l,n}$ and $X_{L,n}$ are determined by means of (38), (41) and (42), and the rates of crack and CL extensions, $\dot{l}_n$ and $\dot{L}_n$, are obtained by (69) or (70) depending on whether the forces are positive or not.

The transition from time t_n to time t_{n+1} is based on the second order Runge-Kutta method. The $(n+1)$-th time step $\Delta t_{n+1} = t_{n+1} - t_n$ is selected so that conditions (74) are met for the new CL sizes l_{n+1} and L_{n+1} as well, and the error for the step does not exceed a prescribed allowable value.

Since the quantity $\Delta\gamma$ might behave like a jump function, the same manner of behavior might be exhibited by the force X_l. This is schematically illustrated by Fig. 10 according to which the crack starts grow at instant t_i (time of crack initiation) when X_l becomes positive and comes to a halt at instant t_a (time of crack arrest) when X_l jumps down from a positive value to a negative one (in Fig. 10, t_0 is the time of the previous crack stop). To "catch" the instant of discontinuity appearance, a special numerical procedure is used the description of which exceeds the limits of the paper. The process of calculations stops when the rates of crack and CL advances

turn into infinite, or somewhat more specifically, a small time step causes big increments of the crack and CL lengths (another approach to halting of the numerical process will be given in section 11). This signals the end of slow CL growth due to either global fracture of the body (division of the body into two parts), or change in the process mode (switching from subcritical mode to supercritical one, see the next section). The elapsed time including the time of crack initiation and the time of CL propagation previously was called the lifetime, or the time to failure and denoted by t_f (see section 1).

Analysis of crack layer behavior could be simplified by transferring to dimensionless variables. For that, it is convenient to introduce a new quantity,

$$l_* = \frac{2E\gamma_0}{\sigma_{dr}^2} \tag{75}$$

(E is the matrix Young modulus), which has dimension of length and is called the characteristic length of the matrix-CL system. The CL and matrix dimensionless sizes, dimensionless remote load and dimensionless time are given by

$$\bar{l} = \frac{l}{l_*}, \ \bar{L} = \frac{L}{l_*}; \ \ \bar{W} = \frac{W}{l_*}, \ \bar{H} = \frac{H}{l_*}; \ \ \sigma = \frac{\sigma_\infty}{\sigma_{dr}}; \ \ \tau = rt = \frac{t}{t_r} \tag{76}$$

where W and H are the matrix sizes respectively along the CL direction and perpendicular to it. The thermodinamic forces (38)-(40) with (53) can be presented as

$$\begin{aligned} X_l &= \frac{\sigma_{dr}^2 l_*}{E}[y_l(\bar{l}, \bar{L}, \bar{W}, \bar{H}, \eta, \sigma) - \exp(\tau_x - \tau)], \\ X_L &= \frac{\sigma_{dr}^2 l_*}{E} x_L(\bar{l}, \bar{L}, \bar{W}, \bar{H}, \eta, \sigma). \end{aligned} \tag{77}$$

Here according to (38), (41) and (42)

$$y_l = \bar{\delta}_p + (1+\eta)\bar{\delta}_z, \quad x_L = [\bar{K}_p + (1+2\eta)\bar{K}_z](\bar{K}_p + \bar{K}_z) \tag{78}$$

and the dimensionless SIFs and CTODs, $\bar{\delta}_p$, $\bar{\delta}_z$ and $\bar{K}_p$, $\bar{K}_z$, are calculated under $E = 1, \sigma_{dr} = 1$ and dimensionless sizes of the CL and matrix. Introducing the dimensionless phenomenological coefficients

$$\bar{k}_l = \frac{\sigma_{dr}^2}{rE} k_l, \quad \bar{k}_L = \frac{\sigma_{dr}^2}{rE} k_L, \tag{79}$$

the equations (67)-(70) and limitations (71) and (72) now can be rewritten in the completely dimensionless form. Two processes of CL growth are similar if and only if all dimensionless parameters $\bar{l}_0, \bar{L}_0, \bar{W}, \bar{H}, \eta$ and σ in these processes are identical. For similar processes, particularly, dimensionless lifetimes τ_f coincide.

10. Two types of CL growth

The above numerical solution displays two types of CL behavior depending on particular values of process characteristics (characteristic length, dimensionless sizes, shape and level of remote load). The first type, a smooth (continuous) CL propagation (Fig. 11a), occurs when the thermodynamic force X_l is positive during all the process. The second type is a step-wise (discontinuous) propagation (Fig. 11b) which consists of a succession of alternating initiations and arrests of the crack and PZ. In such a process, the crack stays immovable for a part of the lifetime (see Fig. 10), and this delays advancement of the PZ. Therefore, of two "comparable" processes, smooth and step-wise, the former proves to be faster. Processes are defined to be comparable if all parameters are identical except for remote load or temperature. For example, crack layer growth can be switched from the step-wise mode to the smooth one and significantly accelerated by raising load level or temperature. This follows from that, according to (41) and (42), the thermodynamic force (53) grows with load and the fracture energy γ_0 for the PZ material diminishes with temperature (see section 3). An increase of the CL length also can be the reason for the transformation of the step-wise growth into smooth one, so that a process might be step-wise from the beginning and smooth in the end.

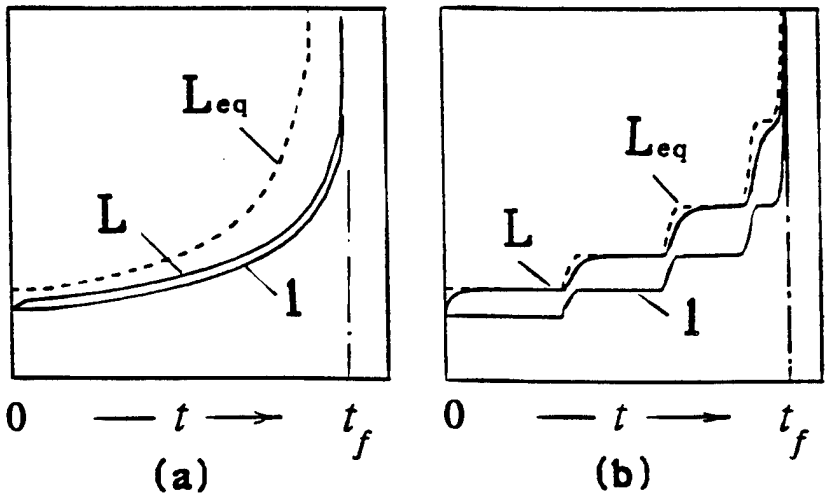

Figure 11. CL growth: (a) smooth, (b) step-wise

During the entire lifetime of the CL propagation shown in Fig. 11a, the CL length lags behind the equilibrium one, whereas almost all the time of the growth depicted in Fig. 11b, the CL

maintains the equilibrium size. The relationship between a current CL length and the equilibrium one depends on the ratio of the rates of crack and CL advances. Proceeding from (41) and (42), the forces for these advances are roughly estimated as quantities of the same order of magnitude, and then, in accordance with (69), the completeness of PZ development is mainly determined by the relation between values of the phenomenological coefficients k_l and k_L. The numerical simulation presented in Fig. 11a is performed at k_l and k_L of the same order of magnitude and in Fig. 11b for k_l ten times greater than k_L. So in case of the smooth mode, the CL can be in equilibrium only when k_L has a greater order of magnitude compared with the one for k_l. On the other hand, it is natural to presuppose that the PZ develops slower than the crack. From this, it can be concluded that the "underdevelopment" of the PZ is a typical feature of the smooth mode. On the contrary, for the step-wise mode, because of delay in crack growth, the CL has time to reach the equilibrium even if k_L is significantly smaller than k_l.

Analysis of the numerical solution shows that in case of the smooth mode, the lifetime strongly depends on the phenomenological coefficients, namely, at the coefficients of the same order of magnitude, the lifetime is approximately inversely proportional to them. On the contrary, in the step-wise mode the lifetime depends only weakly on these coefficients. Increase of the coefficients leads to reduction of the time required for the CL to change the state. If this time is already noticeably smaller than the duration of CL stay in a stationary state (like in the process shown in Fig. 11b), then further increase of the coefficients practically does not affect the lifetime at all. For such processes, the rate of CL growth is mostly determined by how much time precedes an initiation of CL advance which, in turn, depends on the two characteristics of the PZ - on initial value γ_0 of the energy reserve to material fracture and on relaxation time t_r of material degradation (see sections 3). So, properties of the PZ material strongly influence the lifetime of a step-wise CL propagation. In case of the smooth mode, under the natural assumption that degradation goes not faster than CL extention, the lifetime is almost independent of γ_0 and t_r, or more precisely, increase in the former causes a slight deceleration of the process (see section 14), and the latter does not play any role because all the time the energy reserve $\Delta\gamma$ practically keeps a constant value which is close to the initial one, γ_0.

From the standpoint of the analysis given in section 8, a smooth process is unstable since it is accompanied by crack growth. The instability, in particular, manifests itself in that the rates $\dot{l}$ and $\dot{L}$ of crack and CL advancements monotonically increase with time (see Fig. 11a). Indeed, if the process is accelerated, then, according to (67), the thermodynamic forces X_l and X_L, monotonically increase, too, and this and relations (36) yield

$$\frac{dX_l}{dt} = \frac{\partial X_l}{\partial l}\dot{l} + \frac{\partial X_l}{\partial L}\dot{L} + \frac{\partial X_l}{\partial t} = -\frac{\partial^2 G}{\partial l^2}\dot{l} - \frac{\partial^2 G}{\partial L \partial l}\dot{L} - \frac{\partial^2 G}{\partial t \partial l} > 0,$$
$$\frac{dX_L}{dt} = \frac{\partial X_L}{\partial l}\dot{l} + \frac{\partial X_L}{\partial L}\dot{L} = -\frac{\partial^2 G}{\partial l \partial L}\dot{l} - \frac{\partial^2 G}{\partial L^2}\dot{L} > 0. \qquad (80)$$

Hence, because $\dot{l} > 0$ and $\dot{L} > 0$,

$$\frac{\partial^2 G}{\partial l^2}\dot{l}^2 + 2\frac{\partial^2 G}{\partial L \partial l}\dot{l}\dot{L} + \frac{\partial^2 G}{\partial L^2}\dot{L}^2 + \frac{\partial^2 G}{\partial t \partial l}\dot{l} < 0 \qquad (81)$$

that is the indication of CL growth instability. However, development of this process is controlled by kinetic equations (69) and by virtue of this, the CL growth retains a quasi-static character. As to a step-wise process, alternation of CL rest and motion corresponds to alternation of stability and instability respectively, but globally, the process remains stable until the current value of force Y_l determined by (53) reaches value $2\Delta\gamma_0$ (this matter will be more extensively discussed in the next section). At this point the process of slow CL growth is switched from the step-wise mode to the smooth one, or in other words, from the stable (subcritical) stage to the unstable (supercritical) one.

As numerous observations on thermoplastics, first of all on polyethylene, show, the step-wise (discontinuous) manner of growth is usual for the quasi-brittle crack under both constant and cyclic loadings (such a phenomenon for polyethylene is described, for example, in [4, 19]). For this reason, further slow crack growth is largely associated with the CL behavior in the step-wise mode. There is one more reason for this preference. One of the practical purposes of this modeling is a prediction of the relationship between the lifetime and applied load for the long-term brittle fracture. The model simulating a step-wise CL growth predicts a relationship of this kind which is in reasonable agreement with that obtained experimentally (see section 14). At the same time, no plausible lifetime-load dependence can be inferred by employing the model of smooth CL growth.

11. Step-wise growth. Simplified model

A step-wise CL propagation can be treated as a sequence of transitions from one CL equilibrium to another like that shown in Fig. 11b. Such kind of CL growth occurs as a result of that the thermodynamic forces governing crack and PZ advances act discontinuously over short intervals of time.

Let the remote load be prescribed uniformly tensile. It is supposed that at present instant t the CL is in equilibrium, $X_L(l, L) = 0$ and $L = L_{eq}(l)$, and the energy reserve $2\Delta\gamma$ for the PZ material to rupture is as small as the value of force (53) for the given CL sizes,

$$Y_l(l, L) - 2\Delta\gamma(l, t) = 0. \tag{82}$$

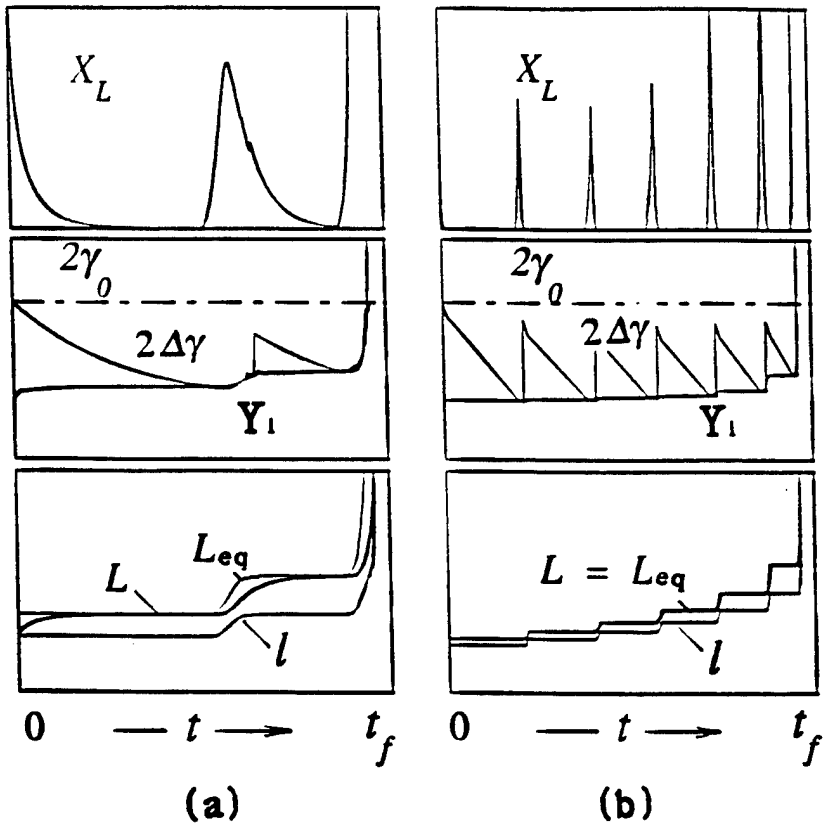

Figure 12. Step-wise CL growth: (a) high σ and small $\bar{k}_L$, (b) low σ and big $\bar{k}_L$

It means that at the instant in question the crack starts growing. Increase of l violates the CL equilibrium, and force X_L becomes positive (see Fig. 8c). So, the crack initiation causes a PZ advance. In turn, this advance generates increase in Y_l and decrease in X_L (see Fig. 7 and 8b respectively). In parallel, the energy reserve ahead of the crack tip, $2\Delta\gamma(l,t)$, changes in accordance with degradation law (72). This "competition" of the thermodynamic forces goes on until the crack tip reaches the original undegraded material or the material transformed into the PZ not long ago and therefore having yet a relatively high level of the energy reserve $2\Delta\gamma$. At this point, the energy reserve jumps up and correspondingly thermodynamic force X_l drops down to a negative value, so that the crack proves to be arrested (see Fig. 10). Meanwhile, the PZ continues to grow approaching the new equilibrium length. This relatively short process is followed by a waiting for a next crack initiation after which a new step of CL propagation begins. The above description is illustrated by Fig. 12 for two step-wise processes the first of which refers to a high remote load σ and slow PZ advance, i.e. a small coefficient $\bar{k}_L$, and the second one, conversly, to a low remote load and fast PZ advance. As seen, the higher level of the remote load, the smaller number of steps during the lifetime and the bigger each step of the process. Increase in the rate of PZ advance leads to a decrease of the time necessary for a CL stationary state to be changed and, as a result, of the time to failure. Dependence of the lifetime on kinetic coefficient $\bar{k}_L$ is illusrated by the curve in Fig. 13. If the value of $2\gamma_0$ increases, then the "waiting" time (from establishing a stationary state to a next crack initiation) becomes longer, but otherwise (the shape of transition from one stationary state to another and number of steps within the process) remains the same.

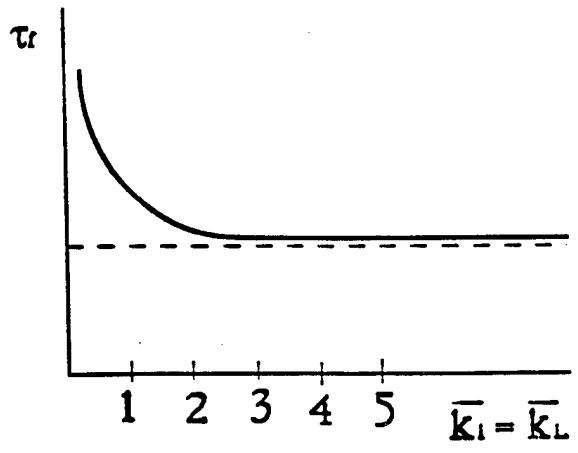

Figure 13. Dependence of lifetime on kinetic coefficients

The above allows a simplification of the model for CL step-wise growth based on the two following assumptions. The first of them says that the CL is always in equilibrium, $L = L_{eq}(l)$. According to the second assumption, the time required for the CL to change the state is small in comparison with the waiting time for crack initiation. It means that the intervals of transitions from one equilibrium to another contribute only small portion of the lifetime, that therefore can be determined as a sum of all waiting intervals. The above assumptions result in the conclusion that the crack lengths in two

sequential equilibrium states of the CL are linked by

$$l_{m+1} = L_{eq}(l_m), \tag{83}$$

i.e. the crack grows making jumps through the PZ up to its tip (Fig. 14). It is obvious that this way of process modeling leads to that the phenomenological cefficients k_l and k_L entirely fall down from considerations. Numerical analysis shows that this approach is justified if k_l and k_L are large enough, or more specific, if the dimensionless coefficients (79) are met conditions $\bar{k}_l \approx \bar{k}_L \geq 5$ (see Fig. 13). For such values of k_l and k_L, the lifetime becomes insensitive to them and in practice coincides with the lifetime of the simplified process. The lifetime for the simplified process is given by the horizontal line in Fig. 13; if $\bar{k}_l = \bar{k}_L \geq 5$, the mistake in lifetime computation resulted from the above simplification does not exceed 5%.

To simplify writings, the PZ material is considered perfectly plastic, i.e. $\eta = 0$. For the simplified model, the second of (69) is substituted by the condition

$$X_L(l, L) = 0 \tag{84}$$

which governs CL growth due to crack growth. Since $L = L_{eq}(l)$ for any l, potential $P = \Pi + \hat{F}_z$ (see section 4) becomes a function of the crack length only and, based on (36), (38), (39) and (53), is presented by expression

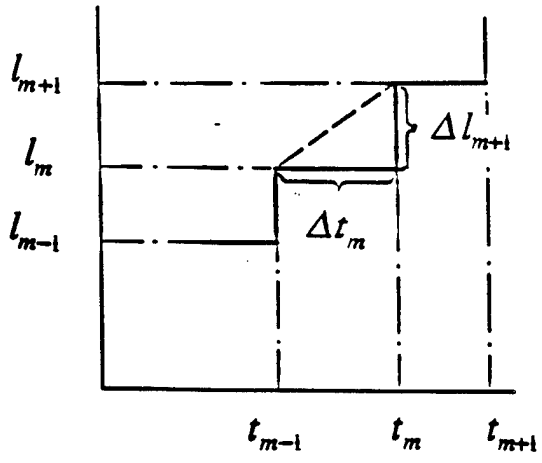

Figure 14. Simplified model of step-wise growth

$$\tilde{P}(l) = P[l, L_{eq}(l)] = P[l_0, L_{eq}(l_0)] - \int_{l_0}^{l} \frac{\partial \tilde{P}}{\partial l} dl. \tag{85}$$

In turn, (85) can be reduced to

$$\tilde{P}(l) = -a(l)l^2 \tag{86}$$

where $a(l)\,(>0)$ is a known increasing function or constant for a finite or infinite matrix respectively. In the simplified model, the PZ is formed simultaneously at all its points, and according to (33) while the crack keeps a constant length, say, $l = l_{m+1}$, the energy accumulated within the PZ due to material degradation changes as

$$\tilde{\Gamma}(l_m, t) = 2\gamma_0(l_m - l_0) + 2\gamma_0[L_{eq}(l_m) - l_m]\{1 - \exp[-r(t - t_{m-1})]\} \tag{87}$$

where $t_{m-1} \le t < t_m$ (see Fig. 14). Using (53), thermodynamic force X_l during the waiting interval from t_m to t_{m+1} becomes

$$\tilde{X}_l(l_m, t) = \tilde{P}_l(l_{m+1}) - 2\Delta\gamma(l_m, t) < 0 \tag{88}$$

where with (26)

$$\Delta\gamma(l_m, t) = \gamma_0 \exp[-r(t - t_{m-1})]. \tag{89}$$

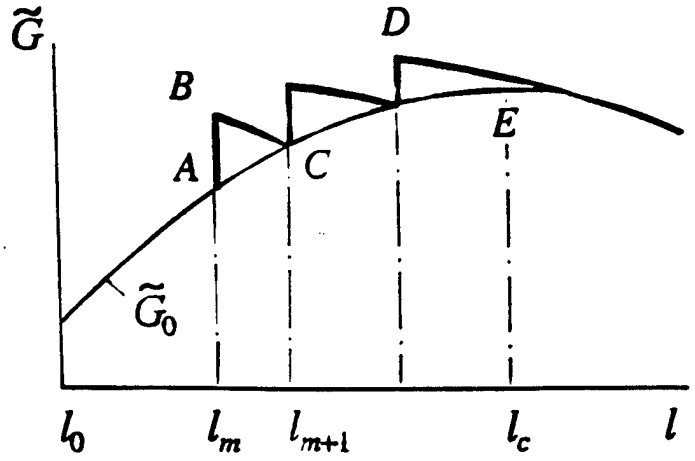

Figure 15. Gibbs' potential as a function of crack length

The next crack advance and change in CL state occur when the right side of (88) reaches zero, and so on.

Equations (86)-(89) allow the representation of the Gibbs potential $\tilde{G}(l) = G[l, L_{eq}(l)]$ in the shape of the saw-tooth curve shown in Fig. 15 where the smooth curve depicts function

$$\tilde{G}_0 = - a(l)l^2 + 2\gamma_0(l - l_0). \tag{90}$$

One segment of the saw-tooth curve corresponds to one step of the process, for example segment ABC to the m-th step. The step begins from formation of the CL with crack length $l = l_m$ (point A). Then the CL stays stationary during the interval from t_{m-1} to t_m (see Fig. 14). Over this interval, as seen from (85) and (87), $\tilde{P}$ remains constant and $\tilde{\Gamma}$ increases so that the Gibbs potential $\tilde{G} = \tilde{P} + \tilde{\Gamma}$ increases, too (the vertical line AB). Crack jump $l_m \to l_{m+1}$ and the respective change in the CL length appear instantaneously (segment BC). The tangent to this segment at point B is horizontal which signifies condition $X_l = 0$. Since $\eta = 0$, $\tilde{P} \equiv \tilde{Y}_l$ and according to Fig. 7a,

$$\frac{d^2\tilde{G}}{dl^2}_{|l=l_m} = -\frac{d\tilde{Y}_l}{dl}_{|l=l_m} < 0 \tag{91}$$

where the equality is exact because now $\partial\Delta\gamma/\partial l \equiv 0$. Inequality (91) indicates that point B is a maximum of $\tilde{G}$, and so transition $B \to C$ from the m-th state to the $(m+1)$-th one is unstable. Such kind of instability should be called local because the CL state B is followed by a crack arrest at state C. By contrast, the instability of the CL equilibrium at point D is global because the next equilibrium at point F "lies" outside the domain of CL subcritical growth, i.e. ahead of point E which corresponds to a maximum of function $\tilde{G}(l)$ and signifies the transition to CL supercritical (smooth) growth.

The above remains valid for the general case of the PZ, $\eta > 0$, if function $\tilde{Y}_l(l)$ satisfies inequality (91).

12. Critical crack length. Lifetime-load relation

In this section, as in the previous one, the CL simplified step-wise growth is considered under uniform tensile remote load constant in time. A crack length is called critical and denoted by l_c if the CL state with sizes l_c and $L_{eq}(l_c)$ corresponds to the transformation from a step-wise (stable) mode of the process into a smooth (unstable) one. The critical crack length is determined by condition

$$\partial \tilde{Y}_l(l_c) - 2\gamma_0 = 0 \tag{92}$$

so that l_c supplies a maximum of function $\hat{G}_0(l)$ determined by (90) (see Fig. 15, point E). Using the dimensionless representation for $\tilde{Y}_l$ given by the first of (77), equation (92) is written as

$$\tilde{y}_l(\bar{l}, \overline{W}, \overline{H}, \eta, \sigma) - 1 = 0. \tag{93}$$

The solution of (93) with respect to $\bar{l}$ yields

$$\bar{l}_c = \bar{l}_c(\overline{W}, \overline{H}, \eta, \sigma) \tag{94}$$

Here, as follows from (75) and (76), the dimensionless sizes $\overline{W}$ and $\overline{H}$ are not only a geometrical characteristics, but also material ones. Critical length $\bar{l}_c$ increases with $\overline{W}$, $\overline{H}$ and η and decreases with σ. For the case when $\overline{H}$ does not affect the stress-strain field in a vicinity of the CL tip and $\eta = 0$, expression (94) becomes

$$\bar{l}_c = \bar{l}_c(\overline{W}, \sigma). \tag{95}$$

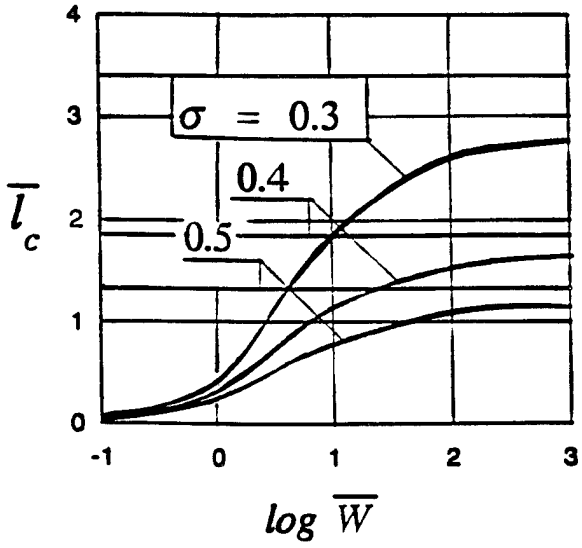

Figure 16. Critical crack length vs. specimen width

For a finite matrix with a single edged CL, critical length $\bar{l}_c$ depends on matrix width $\overline{W}$ at fixed σ as shown in Fig. 16 where the horizontal lines indicate the values of $\bar{l}_c$ for an infinite matrix.

As defined in section 1, the lifetime is the time period during which the CL is initiated and propagates from initial sizes l_0 and L_0 to the critical ones l_c and $L_{eq}(l_c)$. In the general case, the lifetime can be presented as

$$t_f = t_f(l_0, W, H, \eta, \sigma) \tag{96}$$

or in the dimensionless variables

$$\tau_f = \tau_f(\bar{l}_0, \overline{W}, \overline{H}, \eta, \sigma) \tag{97}$$

Let the matrix be infinite and PZ material perfectly plastic, $\eta = 0$. In this case the "shape" of the CL stays constant over all process:

$$\frac{l}{L_{eq}} = cos\theta \tag{98}$$

where $\theta = \pi\sigma/2$. Because of (83) and (98) an increment of the crack length at the m-th step of the process is determined by

$$\Delta l_{m+1} = l_{m+1} - l_m = \frac{1-cos\theta}{cos\theta} l_m \tag{99}$$

From (82) with $\tilde{Y}_l = \tilde{P}_l$,

$$\tilde{P}_l(l_m) - 2\gamma_0 e^{-r\Delta t_m} = 0, \tag{100}$$

waiting time Δt_m at the m-th step is found as

$$\Delta t_m = \frac{1}{r} \ln \frac{2\gamma_0}{\tilde{P}_l(l_m)}. \tag{101}$$

Smoothing of the process, $\dot{l} \equiv \Delta l_{m+1}/\Delta t_m$ (see Fig. 14), and use (99) and (101) yield

$$\frac{dl}{dt} = r \frac{1-\cos\theta}{\cos\theta} \frac{l}{\ln[2\gamma_0/\tilde{P}_l(l)]}. \tag{102}$$

As seen, when $\tilde{P}_l(l)$ approaches $2\gamma_0$, or which is the same, crack length l approaches critical value l_c, the rate of crack growth indefinitely increases, $\dot{l} \to \infty$.

Equation (102) in the dimensionless variables can be presented as (Appendix E)

$$\frac{d\bar{l}}{d\tau} = \frac{1-\cos\theta}{\cos\theta} \frac{\bar{l}}{\ln(\bar{l}_c/\bar{l})} \tag{103}$$

where

$$\bar{l}_c = \frac{\pi}{8|\ln\cos\theta|}. \tag{104}$$

Integration of (103) with the conditions for the beginning and termination of the process

$$\bar{l} = \bar{l}_0 \ (\tau = 0), \quad \bar{l} = \bar{l}_c \ (\tau = \tau_f) \tag{105}$$

results in

$$\tau_f = \frac{\cos\theta}{2(1-\cos\theta)} (\ln\frac{\bar{l}_c}{\bar{l}_0})^2. \tag{106}$$

In the dimensional variables

$$t_f = t_r \frac{\cos\theta}{2(1-\cos\theta)} (\ln\frac{l_c}{l_0})^2 \tag{107}$$

where

$$l_c = \frac{\pi E\gamma_0}{4\sigma_{dr}^2} (\ln\theta)^{-1}, \quad \theta = \frac{\pi\sigma_\infty}{2\sigma_{dr}} \tag{108}$$

Relation (106) between lifetime τ_f and load parameter θ in logarithmic axes for a fixed value of $\bar{l}_0$,

$$\log\tau_f = f(\log\theta), \tag{109}$$

has the shape indicated in Fig. 17 (the solid curve). The smaller $\bar{l}_0$, the closer the curve given by (109) to the straight line

$$\log \tau_f = B - \beta \log \theta \qquad (110)$$

obtained by the least squares method (the dashed line).

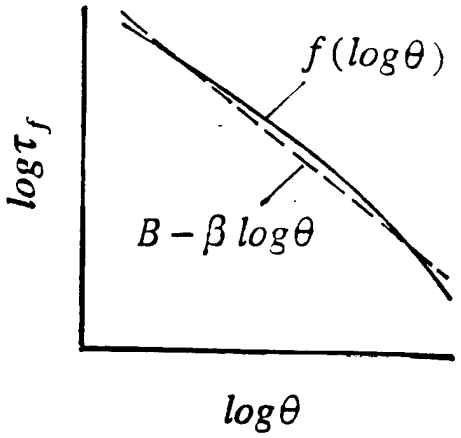

Figure 17. Lifetime vs. load

Let parameter θ not exceed $\pi/4$, i.e. dimensionless load σ be not greater than 0.5. This upper limit of load corresponds to the transition from brittle failure to ductile [17,18]. For a reasonable range of θ, say, for $\pi/16 \le \theta \le \pi/4$, at small values of $\bar{l}_0$ coefficient β in (110) approximately equals 2.2. In the opposite case when $\bar{l}_0$ is large, for example $\bar{l}_0$ is the critical length $\bar{l}_c = 1.133$ for $\theta = \pi/4$, coefficient β becomes about 6. The second coefficient in (110), B, also changes with $\bar{l}_0$, namely an increase of $\bar{l}_0$ causes a decrease of B.

What has been said regarding perfectly plastic PZ, $\eta = 0$, holds for $\eta > 0$, the only difference is in that parameter θ here is determined as (see Appendix E)

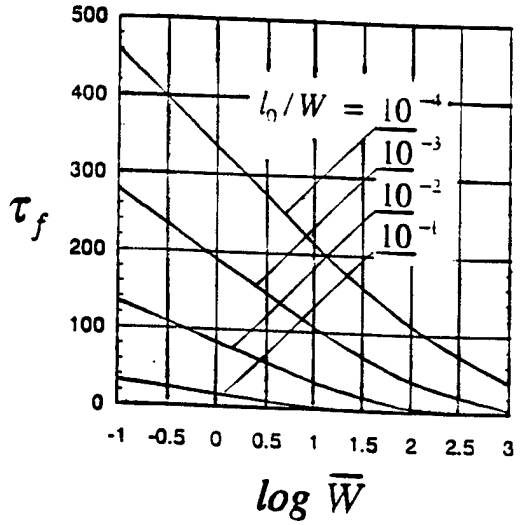

Figure 18. Lifetime vs. specimen width ($\eta = 0, \sigma = 0.3$)

$$\theta = \frac{\pi\sigma}{2(1+2\eta)}. \qquad (111)$$

This also can be extended to the case when the matrix is finite and $\eta > 0$ since matrix width W and coefficient η only slightly affect the "shape" of lifetime-load relation (110), although their influence on the lifetime itself might by very significant. In other words, variations in W and η may lead to a noticeable change of B in (110), but leave β almost invariable. Particularly, dependence of lifetime τ_f on matrix width

$\overline{W}$ at varies constant ratios l_0 / W is illusrated by the curves in Fig. 18 constructed for $\eta = 0$ and $\sigma = 0.3$. This plot can be treated, for example, as follows. Let the matrix-CL system with given sizes $\overline{W}$ and l_0 be considered for various materials and let a change of material characteristics E, σ_{dr} and γ_0 cause a change of critical length l_*. Then, an increase of l_* results in a decrease of $\overline{W}$ and l_0 so that ratio l_0 / W remains invariable and dimentionless lifetime τ_f increases. Such behavior of τ_f depending on $\overline{W}$ at fixed l_0 / W also holds for the smooth mode of CL growth.

The above lifetime-load relation at fixed temperature is examined by comparison with that obtained experimentally for thermoplastics. Particularly, equation (110) with the indicated range of β is in a good agreement with numerous experimental data about brittle fracture of polyethylenes according to which

$$log t_f = A - \alpha \, log \sigma_\infty \tag{112}$$

where α varies from 3 to 5 [28]. Thus, the present model correctly describes the process of subcritical crack growth in terms of lifetime-load relation at a given temperature. To establish connection between these relations for different temperatures, equation (28) expressing dependence of time scale t_r on temperature is employed. Based on the model and on experimental data [17, 18], a time-load-temperature relation for one type of thermoplastics has been constructed in [40].

13. Tension under prescribed displacement

Here, the simplified step-wise process is employed to describe CL propagation through a finite matrix edges of which are displaced with a prescribed rate (Fig. 19). Load σ_p is assumed uniformly distributed along the transverse edges of the matrix, and the edge displacement v_p is understood as the generalized displacement conjugated to the edge load:

$$v_p = \frac{1}{W}\int_0^W v(x,H)dx. \tag{113}$$

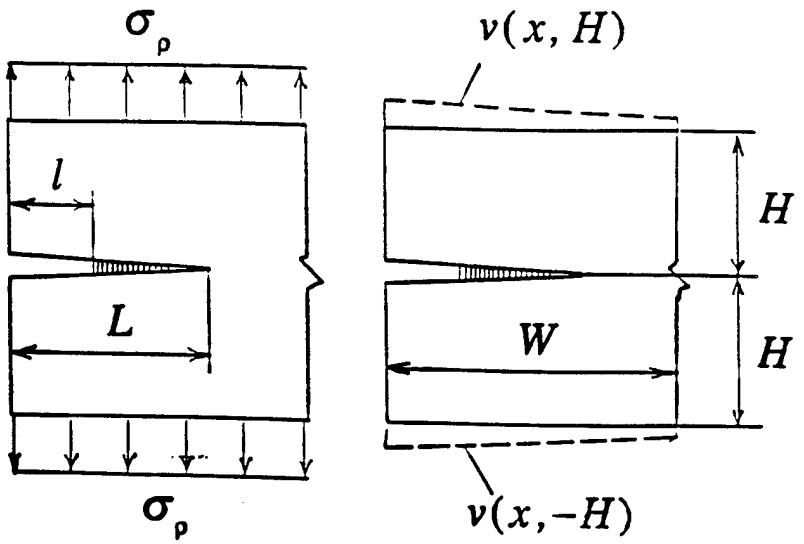

Figure 19. Illustration of boundary conditions

Displacement v_p can be shown to be connected with the edge load σ_p by (Appendix F)

$$v_p = \frac{\sigma_p H}{E} + \frac{\sigma_p}{W}\int_0^L \overline{v}(x,0)dx + \frac{\sigma_{dr}}{W}\int_l^L \overline{v}(x,0)dx. \tag{114}$$

In the right side of (114) the first term signifies the displacement of the body without the CL and the sum of two other terms is the additional displacement arising from CL presence; $\overline{v}(x,0)$ stands for the CL opening due to unit edge load, $\sigma_p = 1$. Let, for definiteness, the edge displacement change with time as $v_p = \dot{v}_p t$ where rate $\dot{v}_p$ is given. Quantities σ_p, l and L being

unknown functions of time are subject to determination. For the simplified model, the crack and CL lengths, l and L, are linked by equation $X_L = 0$, or

$$K_p(L, \sigma_p) + (1+\eta) K_z(l, L) = 0 \tag{115}$$

which means that the CL always has the equilibrium length for a current crack length and edge load,

$$L = L_{eq}(l, \sigma_p). \tag{116}$$

The criterion of crack initiation is formulated as

$$Y_l(l, L, \sigma_p) - 2\Delta\gamma(l, t) = 0. \tag{117}$$

The system of equations (114)-(117) establishes a complete specification of a solution.

The CL growth is divided into separate stages. During each of them a crack length l stays invariable. Increase of edge displacement v_p leads to increase of edge load σ_p and of the CL length L. These changes are described by non-linear equations (114) and (115) which are solved numerically by means of an iterative procedure. An increase of σ_p and L causes a respective increase of Y_l. On the other hand, as a result of PZ material degradation, the energy reserve $\Delta\gamma$ decreases. A current stage of the process comes to an end at that instant when condition (117) of CL local instability is reached (see section 11), and the CL jumps to the new state in which, according to (83), the crack length equals to the previous CL length.

A character of relation between the edge load and displacement depends on relation between the rate of edge displacement growth which is controlled and the rate of PZ material degradation which is a material property. The latter mostly determines the rate of CL advance: the faster degradation, the faster CL growth. So, the process under consideration can be treated as a result of two processes evolving simultaneously: displacement increase and CL propagation. These processes are competitive because growth of the edge displacement leads to increase of the edge load, whereas extension of the CL results in load decrease.

For a given material, i.e. for a given rate of degradation, relation between the edge load and displacement at two rates of displacement are shown in Fig. 20. If the rate of displacement is low (Fig. 20a), then the CL grows until its tip reaches the opposite edge of the matrix. During this process, force Y_l always remains smaller then $2\gamma_0$, i.e. the condition of global instability,

$$Y_l(l, L, \sigma_p) - 2\gamma_0 = 0, \tag{118}$$

never takes place. In the case when the displacement (cross head) rate is high (Fig. 20b)

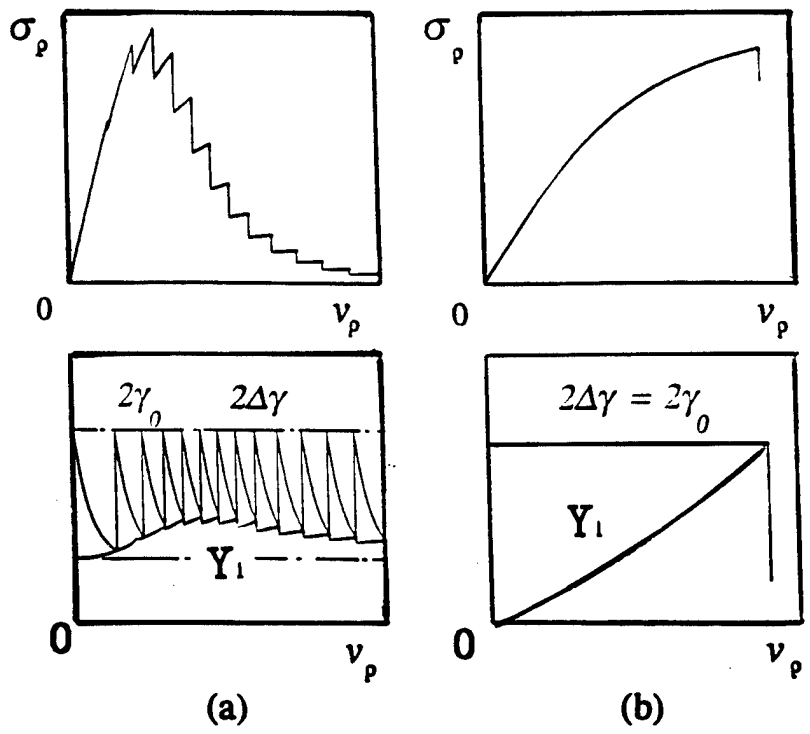

Figure 20. Load and thermodynamic forces vs. displacement at:
(a) low and (b) high cross head rates

the duration of a process stage proves to be so short that degradation of the PZ material has little time to occur. Then condition (117) can be written in the form

$$Y_l(l, L, \sigma_p) - 2\gamma_0(1 - rt_i) = 0 \tag{119}$$

where time t_i of crack initiation is such that $rt_i << 1$. As seen from comparison of (118) with (117), the condition of local instability actually does not differ from that for global instability. As a result, the crack initiation time is inversely proportional to the displacement rate $t_i \propto 1/\dot{v}$, and the curves σ_p vs. v_p for various $\dot{v}$ coincide, or in other words, if $\dot{v} \to \infty$, relation $\sigma_p - v_p$ approaches a certain limiting one.

14. Dipole on crack boundaries

Let an infinite matrix be loaded by the two forces (dipole) applied on the crack boundaries as shown in Fig. 21. Step-wise propagation of the CL induced by the dipole is studied on the basis of the simplified model of the process. In this case, the SIF and CTOD due to the dipole are expressed in the form (see [41, 42] and Appendix F)

$$K_p = \frac{P}{\sqrt{\pi L}}, \quad \delta_p = \frac{4P}{\pi E} \frac{1}{ln[(L + \sqrt{L^2 - l^2})/l]} \tag{120}$$

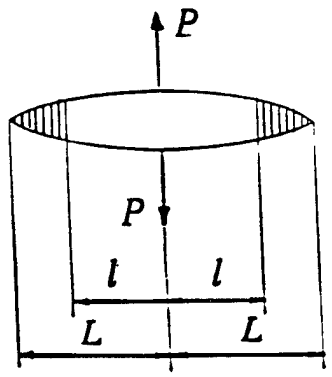

Figure 21. Infinite matrix. Dipole on crack boundaries

and those for traction σ_{dr}, K_z and δ_z, remain the same (see Appendix D). Proceeding from the simplified model of CL growth, equation $X_L = 0$ is written as

$$K_p(L, P) + (1 + 2\eta)K_z(l, L) = 0. \tag{121}$$

Hence (see Appendix F)

$$\frac{l}{L_{eq}} = cos\theta, \quad \theta = \frac{P}{2(1 + 2\eta)\sigma_{dr} L}, \tag{122}$$

and the thermodynamic force (53) is determined by

$$Y_l(l, \theta) = \frac{8\sigma_{dr}^2 l}{\pi E}\{\frac{\theta}{\cos\theta}[\frac{1}{\ln\frac{1 + \sin\theta}{\cos\theta}} - (1 + \eta)\sin\theta] - (1 + \eta)\ln\cos\theta\}. \tag{123}$$

The dipole is assumed to increase as $P = \dot{P}t$ where rate $\dot{P}$ is a given constant. Like in the previous section, the CL growth is a sequence of crack stationary positions. As it follows from (122) and (123), increase of P at fixed l leads to growth of L and Y_l, whereas $\Delta\gamma$ diminishes due to PZ material degradation. The crack stays arrested until condition

$$Y_l(l, \theta) - 2\Delta\gamma(l, t) = 0 \tag{124}$$

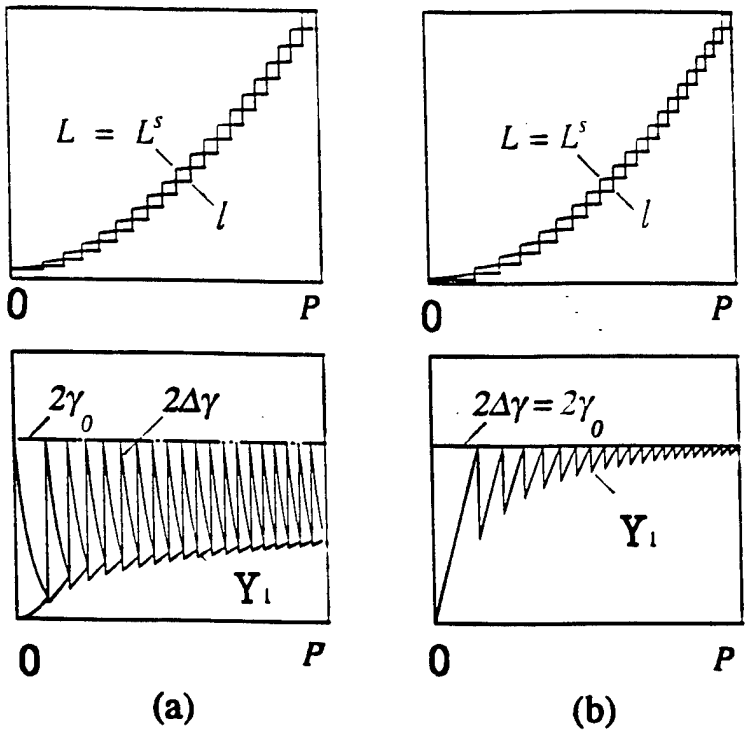

Figure 22. Crack and CL lengths and thermodynamic forces vs. dipole at: (a) low and (b) high rates of dipole increase

is satisfied, and upon achievement of (124) the crack instantly sprouts through the PZ. This causes a drop down of Y_l and jump up of $\Delta\gamma$, and as a result the crack is found to be arrested again. The typical behavior of the CL is shown in Fig. 22a. As the process is evolving, the value of Y_l at the instant of crack initiation approaches $2\gamma_0$. However, even attainment of condition $Y_l = 2\gamma_0$ may not terminate the process. An example of such CL behavior is given by Fig. 22b in which the process is related to a high rate $\dot{P}$. Here the condition of local instability in fact does not differ from that for global instability (see the previous section). In case of a finite matrix, the process comes to an end when the CL tip reaches the matrix edge.

15. Concluding remarks

The crack layer model - if material parameters are determined appropriately - allows a prediction of the lifetime for brittle fracture that is in a good agreement with that obtained from observations. This is the most important result from the standpoint of applications.

The experimental procedure to determine material parameters has to include studies of a particular thermoplastic itself, as well as of the material occurring as a result of cold drawing of the original polymer. This procedure requires development in conformity with nature of the material.

Fracture behavior of a polymer material is connected with its chemical properties and also essentially depends on the process of structural element manufacturing that produces anisotropy, residual stresses, etc. The combination of these two factors - what a material is in terms of chemistry and how a structure from this material is manufactured - creates an initial condition of the material within the structure.

The material condition changes with time, i.e. the material ages. An approach to describe the phenomenon of material aging is proposed in Part 2.

Appendix A. On evaluation of energy release due to PZ formation

The purpose of this section is to check equality (10),

$$\int_{l_0}^{L} \sigma_m^0 \, \delta^* dx = \int_0^L \sigma_p \, \delta^* dx + 2\Pi_0, \tag{A1}$$

where notations are given in section 2. The two states of the cracked body shown in Fig. Aa and b are considered.

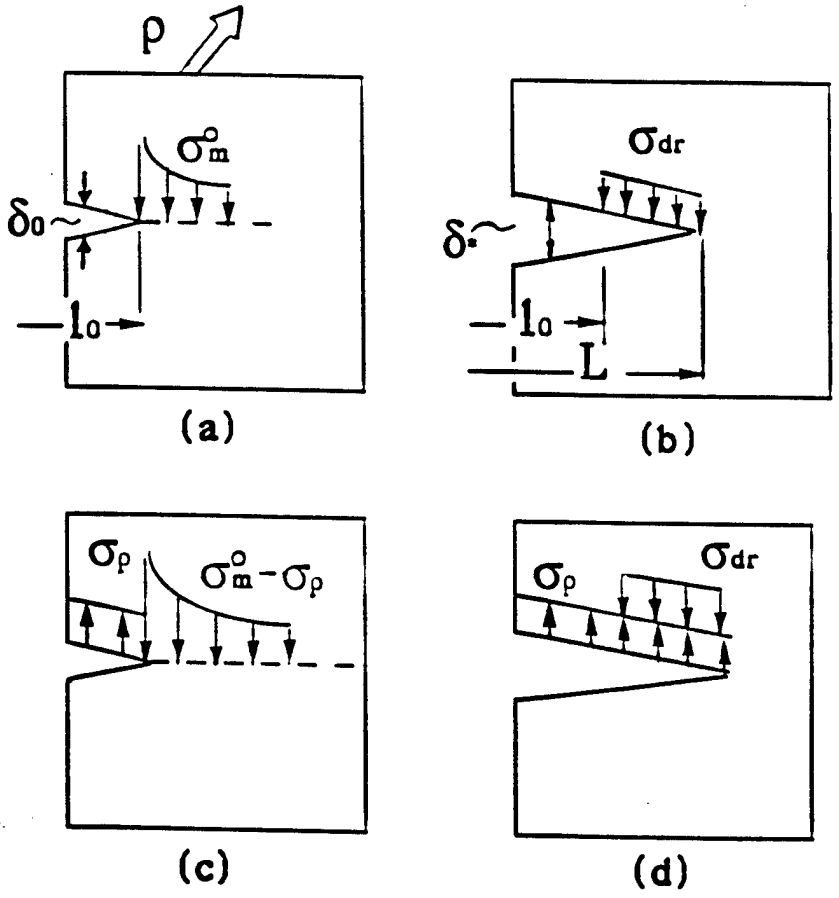

Figure A. On energy balance of PZ formation

In terms of the CL opening displacement, states in Fig. Aa and b are equivalent to those depicted in Fig. Ac and d. The work-reciprocal theorem applied to the two last states yields

$$\int_0^{l_0} \sigma_p \, \delta^* dx - \int_{l_0}^{L} (\sigma_m^0 - \sigma_p) \, \delta^* dx = \int_0^{l} \sigma_p \, \delta_0 \, dx, \tag{A2}$$

or

$$\int_{l_0}^{L} \sigma_m^0 \, \delta^* dx = \int_0^{l_0} \sigma_p \, \delta^* dx - \int_{l_0}^{L} \sigma_p \, \delta_0 \, dx. \tag{A3}$$

Here the last term in the right side is the double work done by the traction acting on the crack boundary on the crack opening displacement δ_0 due to the transition of the body from the uncracked state to the cracked one. The change in the elastic strain energy, F_0, and the work done by all external forces due to this transition are linked as

$$F_0 = -\frac{1}{2} \int_0^{l_0} \sigma_p \, \delta_0 \, dx + W_{p,0} \tag{A4}$$

where $W_{p,0}$ is the work of the remote load. Hence, with notation Π_0 for the change in the total energy due to cracking, there follows

$$-\int_0^{l} \sigma_0 \, \delta_0 \, dx = 2(F_0 - W_{p,0}) = 2\Pi_0. \tag{A5}$$

Upon substituting (A5) into (A3) the latter becomes identical to (A1).

Appendix B. Thermodynamic forces as functions of SIFs and CODs

According to (29),

$$-\frac{\partial \Pi}{\partial l} = \frac{\partial}{2\partial l}(\int_0^L \sigma_p \delta\, dx + \int_l^L \sigma_{dr} \delta\, dx) = \frac{1}{2}[\int_0^L \sigma_p \frac{\partial \delta}{\partial l} dx - \sigma_{dr}\delta(l) + \int_l^L \sigma_{dr} \frac{\partial \delta}{\partial l} dx] \qquad \text{(B1)}$$

where $\delta(l) = \delta_p + \delta_z$ (see notations in section 5) and $\partial\delta/\partial l$ is the CL opening caused by the forces shown in Fig. B1a. Application of of the work-reciprocal theorem to the two states depicted in Fig. B1a and b results in

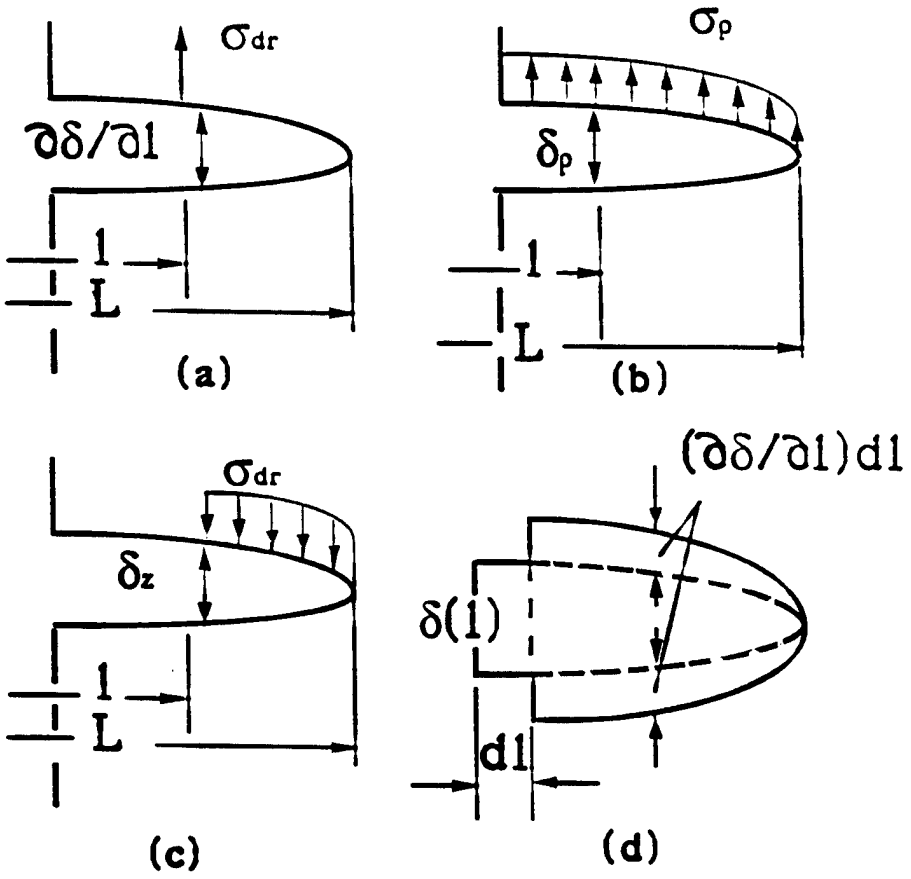

Figure B1. On evaluation of thermodynamic force for crack advance

$$\int_0^L \sigma_p \frac{\partial \delta}{\partial l} dx = \sigma_{dr} \delta_p. \tag{B2}$$

Similarly for the two states shown in Fig. B1a and c

$$-\int_l^L \sigma_{dr} \frac{\partial \delta}{\partial l} dx = \sigma_{dr} \delta_z. \tag{B3}$$

Substitution of (B2) and (B3) into (B1) yields

$$\frac{\partial \Pi}{\partial l} = \sigma_{dr} \delta_z. \tag{B4}$$

The derivative of (30) with respect to l is postulated to equal

$$\frac{\partial F_z}{\partial l} = -\sigma_{dr} \delta(l) + (1+\eta) \int_l^L \sigma_{dr} \frac{\partial \delta}{\partial l} dx. \tag{B5}$$

Here in the right side the first term describes PZ unloading as a result of crack advance, and the second term expresses PZ widening due to an additional transformation of the matrix material to the PZ one (Fig. B1d). Division of the PZ deformation potential as indicated by (13), (18) and (21) with (B5) leads to

$$-\frac{\partial \hat{F}_z}{\partial l} = \sigma_{dr}(\delta_p + 2\delta_z), \quad Z_l = -\frac{\partial Z}{\partial l} = \eta \sigma_{dr} \delta_z. \tag{B6}$$

Using (B3) and combining (B4) and the first of (B6), the part of the thermodynamic force determined by the first of (39) becomes identical to the first of (41):

$$P_l = -\frac{\partial \Pi}{\partial l} - \frac{\partial \hat{F}_z}{\partial l} = \sigma_{dr}(\delta_p + \delta_z). \tag{B7}$$

Equation (29) with $\delta(L) = 0$ gives

$$-\frac{\partial \Pi}{\partial L} = \frac{\partial}{2\partial L}(\int_0^L \sigma_p \delta\, dx + \int_l^L \sigma_{dr} \delta\, dx) = \frac{1}{2}(\int_0^L \sigma_p \frac{\partial \delta}{\partial L} dx + \int_l^L \sigma_{dr} \frac{\partial \delta}{\partial L} dx). \qquad \text{(B8)}$$

The first integral here can be evaluated based on an analysis of the two states shown in Fig. B2a and b where $s = s_p + s_z$ and s_p and s_z stand for stress component σ_{yy} ahead of the CL tip induced by tractions σ_p and σ_{dr} respectively (see Fig. Ad).

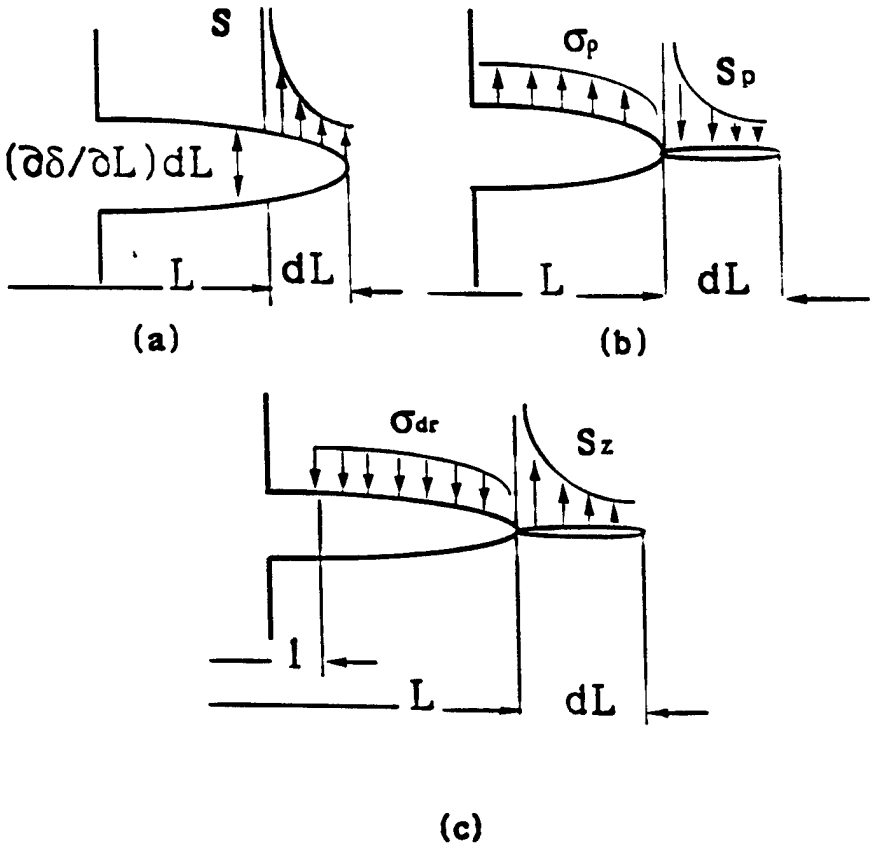

Figure B2. On evaluation of thermodynamic forces for CL advance

Use of the known formulas,

$$s_p = \frac{K_p}{\sqrt{2\pi r}}, \quad \frac{\partial \delta}{\partial L} dL = \frac{8(K_p + K_z)}{E\sqrt{2\pi}} \sqrt{dL - r} \quad (0 \le r \le dL), \qquad \text{(B9)}$$

and the work-reciprocal theorem,

$$\int_0^L \sigma_p \frac{\partial \delta}{\partial L} dx - \int_0^{dL} \frac{2K_p(K_p + K_z)}{\pi E} \sqrt{\frac{dL - r}{r}} dr = 0, \tag{B10}$$

give

$$\int_0^L \sigma_p \frac{\partial \delta}{\partial L} dx = \frac{2K_p(K_p + K_z)}{E}. \tag{B11}$$

The work-reciprocal theorem for the two states shown in Fig. B2a and c allows an evaluation of the second integral in (B8) as

$$\int_0^L \sigma_{dr} \frac{\partial \delta}{\partial L} dx = -\frac{2K_z(K_p + K_z)}{E}. \tag{B12}$$

As follows from (B10) and (B12),

$$\frac{\partial \Pi}{\partial L} = -\frac{(K_p + K_z)(K_p - K_z)}{E}, \tag{B13}$$

and according to (B12),

$$\frac{\partial \hat{F}_z}{\partial L} = -\frac{2K_z(K_p + K_z)}{E}, \quad Z_l = -\frac{\partial Z}{\partial L} = \frac{2\eta K_z(K_p + K_z)}{E}. \tag{B14}$$

Combination of (B13) and the first of (B14) yields

$$P_L = -\frac{\partial \Pi}{\partial L} - \frac{\partial \hat{F}_z}{\partial L} = \frac{(K_p + K_z)^2}{E}. \tag{B15}$$

Appendix C. Thermodynamic forces as functions of crack and CL lengths

The remote load is considered uniformly (relative to x-axis) tensile, so the uncracked body is subject to an uniaxial tension (towards y-axis). For the case $\eta = 0$ and for given matrix sizes, forces (41) are functions of two variables - the crack and CL lengths, l and L. Let the crack length be fixed, $l = l_0$, and the CL length, $L = L_0$, be determined as the solution of the equation

$$P_L(l_0, L) = 0. \tag{C1}$$

As seen from the second of (41), the total SIF for this CL length is equal to zero,

$$K_p(L_0) + K_z(l_0, L_0) = 0, \tag{C2}$$

and so the above-determined CL length coincides with one of the effective crack in the DB model.

It is convenient to introduce the following dimensionless functions

$$\bar{P}_l(l) = \frac{P_l(l, L_0)}{P_l(l_0, L_0)}, \quad \bar{P}_l(L) = \frac{P_l(l_0, L)}{P_l(l_0, L_0)} \tag{C3}$$

of the crack length l with the range of the variable from l_0 to L_0. The graphs of functions (C3) are shown in Fig. Ca, where the tangent to the curve $p_L(l)$ at point $l = l_0$ is horizontal, i.e.

$$\frac{\partial^2 P}{\partial l \, \partial L}_{|l=l_0,\, L=L_0} = 0. \tag{C4}$$

Another pair of dimensionless functions

$$\bar{P}_L(l) = \frac{P_L(l, L_0)}{P_L(l_0, L_0)}, \quad \bar{P}_L(L) = \frac{P_L(l_0, L)}{P_L(l_0, L_0)} \tag{C5}$$

of the CL length L with the same range of the variable have the graphs depicted in Fig. Cb; the dashed line displays the second function for the case when the crack layer length is large enough in

comparison with the matrix width. Here the tangent to the curve $p_L(L)$ at point $L = L_0$ is horizontal, and so

$$\left.\frac{\partial^2 P}{\partial L\,\partial l}\right|_{l=l_0,\,L=L_0} = 0 \qquad \text{(C6)}$$

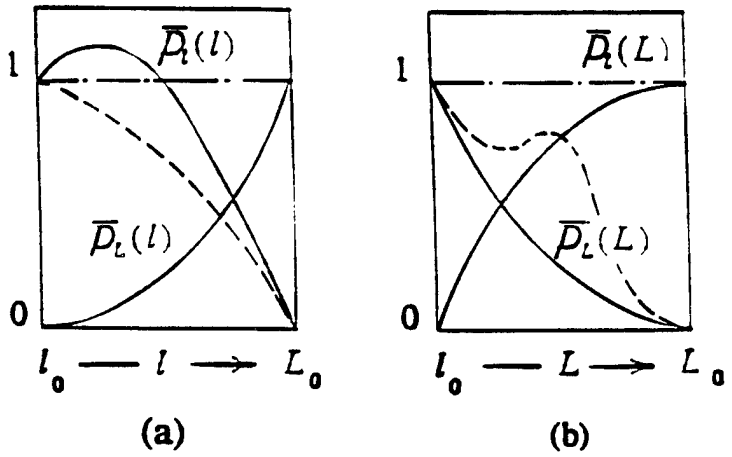

Figure C. Thermodynamic forces as functions of crack and CL lengths

which accords with (C4). Besides, the tangent to the curve $p_L(L)$ at point $L = L_0$ is horizontal, too,

$$\left.\frac{\partial^2 P}{\partial L^2}\right|_{l=l_0,\,L=L_0} = 0, \qquad \text{(C7)}$$

as it immediately follows from definition (C1) of L_0.

The graphs in Fig. C and equations (C4), (C6) and (C7) give an idea about shapes not only of the first partial derivatives of P, but also of the second ones, and will be essentially employed at the further analysis of CL stability and kinetics.

For the case $\eta > 0$, length L_0 of the CL is determined as the solution of the equation

$$K_p(L) + (1 + 2\eta)K_z(l_0, L) = 0 \qquad \text{(C8)}$$

with l_0 fixed. By analogy with (C3) and (C5) the dimensionless functions

$$\overline{Y}_l(l) = \frac{Y_l(l, L_0)}{Y_l(l_0, L_0)}, \quad \overline{Y}_L(L) = \frac{Y_L(l_0, L)}{Y_L(l_0, L_0)};$$

$$\overline{X}_L(l) = \frac{X_L(l, L_0)}{X_L(l_0, L_0)}, \quad \overline{X}_L(L) = \frac{X_L(l_0, L)}{X_L(l_0, L_0)} \tag{C9}$$

are introduced. Their graphs have the shapes mostly similar to ones shown in Fig. C, but there are two differences: first, function $\overline{Y}_l(l)$ might (but not necessarily) behave in a rather different way (see the dashed curve in Fig. Ca), and second, instead of equalities (C4), (C6) and (C7) the inequalities

$$\frac{\partial^2(P+Z)}{\partial l \partial L}_{|l=l_0, L=L_0} = \frac{\partial^2(P+Z)}{\partial L \partial l}_{|l=l_0, L=L_0} < 0, \quad \frac{\partial^2(P+Z)}{\partial L^2}_{|l=l_0, L=L_0} < 0 \tag{C10}$$

take place.

Appendix D. Infinite matrix. Second derivatives of Gibbs' potential

Let an infinite matrix with a crack of length $2L$ be subject to an uniform tensile remote load so that σ_p is constant. Then,

$$K_p = \sigma_p \sqrt{\pi L}, \quad K_z = -2\sigma_{dr}\sqrt{\frac{L}{\pi}}\cos^{-1}\frac{l}{L},$$

$$\delta_p = \frac{4\sigma_p}{E}\sqrt{L^2 - l^2}, \; \delta_z = -\frac{8\sigma_{dr}}{\pi E}[\sqrt{L^2 - l^2}\cos^{-1}\frac{l}{L} + l\ln\frac{l}{L}]. \tag{D1}$$

If a PZ length is essentially smaller than a crack layer length,

$$\frac{l}{L} = \cos\theta, \quad \theta << 1, \tag{D2}$$

the derivatives of (D1) relative to l and L are determined as

$$\frac{\partial K_p}{\partial l} = 0, \quad \frac{\partial K_p}{\partial L} = \frac{\sigma_p}{2}\sqrt{\frac{\pi}{L}}, \quad \frac{\partial K_z}{\partial l} = -\frac{\partial K_z}{\partial L} = \frac{2\sigma_{dr}}{\sqrt{\pi L}\theta},$$

$$\frac{\partial \delta_p}{\partial l} = -\frac{\partial \delta_p}{\partial L} = -\frac{4\sigma_p}{E\theta}, \quad \frac{\partial \delta_z}{\partial l} = -\frac{\partial \delta_z}{\partial L} = -\frac{8\sigma_{dr}}{\pi E}. \tag{D3}$$

For the case $\eta = 0$, expressions (D3) with (41) yield

$$\frac{\partial^2 G}{\partial l^2} = \frac{\partial^2 G}{\partial L^2} = -\frac{\partial^2 G}{\partial l \partial L} = \frac{4\sigma_{dr}\sigma_p}{E\theta}. \tag{D4}$$

Appendix E. Infinite matrix. Kinetic equation and critical crack length

For the case in question, SIFs and CODs are determined by (D1). The equation of CL equilibrium, i.e. the first of (50), yields

$$\frac{l}{L_{eq}} = \cos\theta, \quad \theta = \frac{\pi\sigma_p}{2(1+\eta)\sigma_{dr}} \quad (< 1). \tag{E1}$$

Then, thermodynmic force $\tilde{Y}_l$ determined as

$$\tilde{Y}_l(l) = \sigma_{dr}[\delta_p(l, L_{eq}) + (1+\eta)\delta_z(l, L_{eq})] \tag{E2}$$

is written in the form

$$\tilde{Y}_l = \frac{8\sigma_{dr}^2 l}{\pi E}[\eta\theta\tan\theta - (1+\eta)\ln\theta]. \tag{E3}$$

At $\eta = 0$, (E3) gives $\tilde{P}_l$, and with (75) it results in

$$\frac{2\gamma_0}{\tilde{P}_l(l)} = -\frac{\pi l_*}{8l\ln\cos\theta}. \tag{E4}$$

The critical crack length is found as a solution of (92), or in the considered case, from equation $\tilde{P}_l(l) = 2\gamma_0$. With notations $\bar{l} = l/l_*$ and $\bar{l}_c = l_c/l_*$ (E4) allows the representation of kinetic equation (102) in the form of (103) and the dimensionless critical crack length in the form of (104).

Appendix F. Edge displacement of a cracked body

The edge displacement of the matrix with the CL (Fig. 19) comes out as a sum of two terms. The first is the displacement produced by the edge load σ_p in the solid body, i.e. without the CL, $v_p^{(1)} = \sigma_p H / E$. The second is the displacement due to presence of the CL. To evaluate it, the two states shown in Fig. F are considered. On the basis of the work-reciprocal theorem

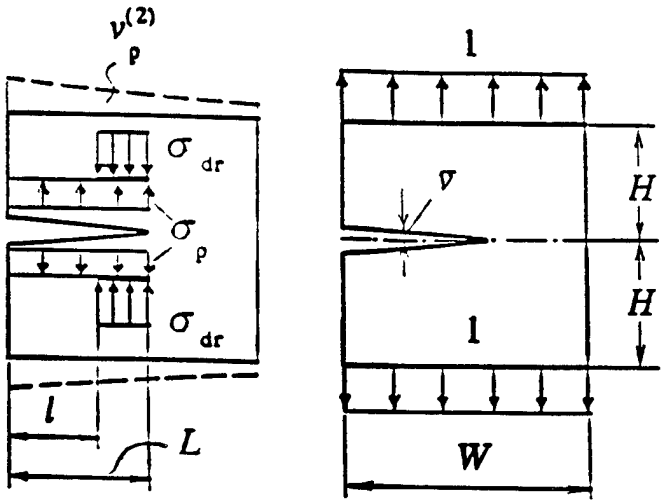

Figure F. On evaluation of edge displacement

$$\int_0^W v_p^{(2)} dx = \sigma_p \int_0^L \bar{v}(x) dx - \sigma_{dr} \int_l^L \bar{v}(x) dx. \qquad \text{(F1)}$$

Hence

$$v_p = \frac{\sigma_p H}{E} + \frac{\sigma_p}{W} \int_0^L \bar{v}(x) dx - \frac{\sigma_{dr}}{W} \int_l^L \bar{v}(x) dx. \qquad \text{(F2)}$$

Appendix G. Infinite matrix. COD and thermodynamic force due to dipole

The state shown in Fig. G is considered. The displacement conjugated to dipole Q is the crack opening δ. According to the Castigliano theorem,

$$\delta = \frac{\partial F}{\partial Q} \tag{G1}$$

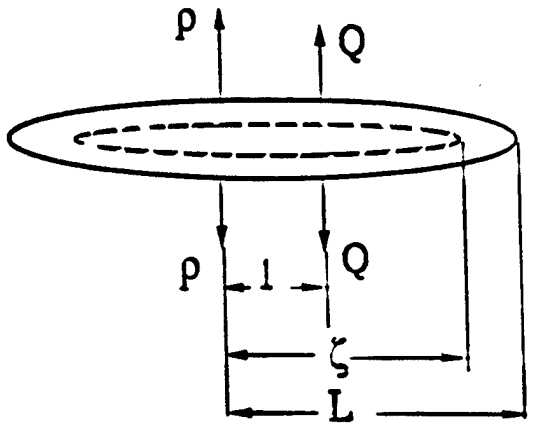

Figure G. On evolution of COD due to dipole

where F is the elastic energy that can be evaluated by

$$F = \int_0^L \frac{\partial F}{\partial \varsigma} d\varsigma. \tag{G2}$$

By $\partial F / \partial \varsigma$ one implies the rate of change in the elastic energy due to symmetrical (in both directions) crack growth. Then,

$$\frac{\partial F}{\partial \varsigma} = \frac{1}{E}(K_l^2 + K_r^2) \tag{G3}$$

where ς stands for the crack current length, and K_l and K_r are SIFs for the left and right crack tips respectively. Substituting first (G3) and into (G2) and then the result obtained into (G1), the expression for δ becomes

$$\delta = \frac{2}{\pi E}\int_l^L (K_l \frac{\partial K_l}{\partial Q} + K_r \frac{\partial K_r}{\partial Q}) d\varsigma. \tag{G4}$$

In the case in question

$$K_l = \frac{1}{\sqrt{\pi\varsigma}}(P + \sqrt{\frac{\varsigma - l}{\varsigma + l}} Q) \quad K_r = \frac{1}{\sqrt{\pi\varsigma}}(P + \sqrt{\frac{\varsigma + l}{\varsigma - l}} Q) \quad (\varsigma > l); \tag{G5}$$

if $\varsigma \le l$, the second terms in the right sides of (G4) have to be dropped. Now, (G5) is put into (G4) which with $Q = 0$ gives the value of crack opening δ due to dipole P alone:

$$\delta_p = \frac{2P}{\pi E}\int_l^L \frac{1}{\varsigma}\left(\sqrt{\frac{\varsigma - l}{\varsigma + l}} + \sqrt{\frac{\varsigma + l}{\varsigma - l}}\right) d\varsigma = \frac{4P}{\pi E}\ln\left\{\frac{L}{l}\left[1 + \sqrt{1 - \left(\frac{L}{l}\right)^2}\right]\right\}. \tag{G6}$$

The equation of CL equilibrium defined by the first of (50) is written as

$$\frac{P}{\sqrt{\pi L}} - 2(1+\eta)\sigma_{dr}\sqrt{\frac{L}{\pi}}\cos^{-1}\frac{l}{L} = 0 \tag{G7}$$

where the seconds of (D1) and (G5) are used. Equation (G7) results in

$$\frac{l}{L_{eq}} = \cos\theta, \quad \theta = \frac{P}{2\sigma_{dr}(1+2\eta)L}. \tag{G8}$$

And finally, by means of the firsts of (41) and (42) as well as the fourth of (D1), (G6) and (G8) the expression for thermodynamic force Y_l defined by (53) is evaluated in the form (123).

Bibliography

1. A. Chudnovsky, V. Dunaevsky and V. Khandogin, *Archives of Mechanics* 30 (1978) 165-174.
2. A. Chudnovsky, *Crack Layer Theory*, NASA CR-174634 (1984).
3. E. H. Andrews, *Fracture in Polymers*, Aberdeen University Press (1968).
4. R. W. Herzberg and J. Manson, *Fracture of Engineering Plastics*, Academic Press (1980).
5. A. J. Kinloch and R. J. Young, *Fracture Behavior of Polymers*, Elsevier Applied Science (1983).
6. J. G. Williams, *Fracture Mechanics of Polymers*, Ellis Horwood Lim. (1984).
7. H.-H. Kausch, *Polymer Fracture*, Springer Verlag (1987).
8. M. K. Chan and J. G. Williams, *Polymer* 24 (1983) 234-244.
9. P. Trassaert and R. Schirrer, *Journal of Materials Science* 8 (1983) 3004-3010.
10. R. Schirrer, J. Le Masson, B. Tomatis and R. Lang, *Polymer Engineering and Science* 24 (1984) 820-824.
11. I. M. Ward and M. A. Wilding, *Journal of Polymer Science: Polymer Physics Ed.* 22 (1984) 561-575.
12. N. Brown and S. K. Bhattacharya, *Journal of Materials Science* 20 (1985) 4553-4560.
13. X. Lu and N. Brown, *Journal of Materials Science* 21 (1986) 4081-4088.
14 D. Barry and O. Delatycki, *Journal of Polymer Science: Part B: Polymer Physics* 25 (1987) 883-899.
15. Y. L. Huang and N. Brown, *Journal of Polymer Science: Part B: Polymer Physics* 28(1990) 2007-2021.
16. C. F. Popelar, C. H. Popelar and V. H. Kenner, *Polymer Engineering and Science* 30 (1990) 578-586.
17. X. Lu and N. Brown, *Journal of Materials Science* 25 (1990) 29-34.
18. X. Lu and N. Brown, *Journal of Materials Science* 26 (1991) 612-620.
19. X. Lu, R. Qian and N. Brown, *ibid* 917-924.
20. D. Barry and O. Delatycki, *Polymer* 33 (1992) 1261-1265.
21. C. H. Popelar, V. H. Kenner and J. P. Wooster, *Polymer Engineering and Science* 31 (1991) 1693-1700.
22. K. Kadota, *Ph. D. Thesis*, The University of Illinois at Chicago, Chicago (1992).

23. L. J. Rose, A. D. Channell, C. J. Frye and G. Capaccio, *Journal of Applied Polymer Science* 54 (1994) 2119-2124.
24. S. H. Beech, A. D. Channell and L. J. Rose, *14th Plastics Fuel Gas Pipe Symposium* (1995) 216-228.
25. D. S. Dugdale, *Journal of the Mechanics and Physics of Solids* 8 (1960) 100-104.
26. G. I. Barenblatt, *Advances in Applied Mech*anics 7 (1962) 55-129.
27. A. Stojimirovic, K. Kadota and A. Chudnovsky, *Journal of Applied Polymer Science* 46 (1992) 1051- 1054.
28. N. Brown and X. Lu, *International Journal of Fracture* 69 (1995) 371-377.
29. W. L. Huang, *Ph.D. Thesis*, The University of Illinois at Chicago, Chicago (1992).
30 R. A. Schapery, *International Journal of Fracture* 11 (1975) 141-158, 369-387, 549-562.
31. A. Stojimirovich and A. Chudnovsky, *International Journal of Fracture* 57 (1992) 281-289.
32. K. Kadota and A. Chudnovsky, in *Recent Advances in Damage Mechanics and Plasticity*, AMD-Vol. 132/Md-Vol. 30, J. W. Ju (ed.), ASME (1992) 115-130.
33. K. Kadota and A Chudnovsky, *Proceedings of ASME Winter Annual Meeting* (1991) 101-114.
34. A. Chudnovsky and K. Kadota, *Proceedings of PACAM III* (1993) 419-422.
35. F. Costanzo and D. H. Allen, *International Journal of Fracture* 63 (1993) 27-57.
36. S. N. Zhurkov, *International Journal of Fracture Mechanics* 1 (1965) 311-323.
37. M. Born and R. Furth, *Proceedings of Cambridge Philosophical Society* 36 (1940) 454-470.
38. R. Furth, *Proceedings of Royal Society* 177A (1941) 217-230.
39. R. Haase, *Thermodynamics of Irreversible Processes*, Addison-Wesley Publishing Company (1969).
40. A. Chudnovsky, Y. Shulkin, D. Baron and K.P. Lin, *Journal of Applied Polymer Science* 56 (1995) 1465-1478.
41. H. Tada, *The Stress Analysis of Cracks*, Del Research Corporation, Heelertown, Pennsylvania (1973).
42. Y. Murakami, *Stress Intensity Factors Handbook*, Vol. 1, Pergamon Press (1987).

Part 2

Aging Phenomena and the Intrinsic Material Geometry

Contents.

I. Introduction.

Material aging is understood as changes of material properties with time. The aging is usually observed as an improvement of some properties and a deterioration of others. For example an increase of rigidity and strength and reduction in toughness with time are commonly observed in engineering materials. In an attempt to model aging phenomena on a continuum (macroscopical) level one faces three major tasks. The first is to identify an adequate **age parameter** that represents, on a macroscopic scale, the micro and submicroscopical features, underlying the aging phenomena such as nucleation, growth and coalescence of microdefects, physico-chemical transformations etc. The age parameter should be considered as a parameter of state, in addition to the conventional parameters such as stress tensor and temperature.

The second task consists of formulation of a constitutive equation of aging, i.e., equations of age parameter evolution expressed in terms of controlling factors, e.g., load and temperature. It is expected that at common circumstenses a small variation of controlling factors results in a small variation of age parameter. However, at certain conditions, a sudden large variation of age parameter may result from a small perturbation of controlling factors. Experimental examination, classification and analysis of the condition that lead to such a catastrophic behavior, constitute the third task of the modeling. Formulation of local failure criteria within the scope of continuum mechanics is an example of this task.

In many engeneering materials the aging is manifested in variations of mass density as well as in the spectrum of relaxation time. Thus in a macroscopic test the aging can be detected in variations of **intrinsic** (material) **length** and **time scales**. Following this notion, in the present paper we employ the **material metric tensor G** as an **age parameter**. An evolution of G in **4D -material space-time** determines in our approach an inelastic behaviour and time dependent material properties recorded by an **external** observer.

The objective of the present work is to derive the constitutive equations of aging based on Extremal Action Principle. The variational approach seems to be most promissing in view of complexity of the problem and lack of experimental data. It provides with a guide line for the experimental examination of the basic assumptions and modifications, if necessery.

The major task in implementation of extremal action principle is the construction of an appropriate Lagrangian. In variational formulations of Elasticity theory the Lagrangian

is usually constructed in terms of invariants of the gradient of deformation. In Classical Field Theories invariants of metric, connection and the corresponding curvatures together with the gradients of "material fields" are emploied in the Lagrangian ([2],[16],[18]). In the present paper we combine the above approaches and revisit the classical continuum mechanics from the point of view of an intrinsic (material) geometry that includes an inner time.

A brief exposition of various works in Gravity, Elasticity and Geometrical Field Theories most pertenent to the present studies is given in Appendix A.

In Section 2 we discuss the kinematics of an aging media emploing a 4-dimentional material space-time $P = R \times B$ endowed with the 4D-metric G of Lorentz type (intrinsic metric) embedded into 4-dimentional Absolute (Newton's) space-time M^4. We define the mass form and formulate the mass conservation law that, in the context, gives a non-trivial relation between the "reference density" ρ_0 and the time evolution of the material metric G. A strain tensor E and a "ground state" are introduced as a measure of deformation and a natural analog of the "unstrained state" respectively. The central part of the work is the Section 3 where we propose a variational formulation of aging theory. The equation of Elasticity together with the generalized Hooke's equation are conventionaly derived considering the variation of the action integral with respect to the deformations ϕ^i. Similarly, new equations of evolution of the age parameter (and, therefore, of elastic moduli, mass density and inelastic deformation) result from the variation of the action integral with respect to the material metric tensor. The balance equations (conservation laws) resulting from the symmetries of the Absolute (Newton's) space-time and material (intrinsic) space-time respectively and the relations between them are discussed in the Section 4. Considerations of the paper are illustrated in section 5 by the example - linearized model of aging of a rod whose time dependent elastic properties and irreversible deformation are associated with an evolving metric in 2D material space-time. In Section 6 we discuss the nonlinear aging of a rod under the constant load (creep).

2. Kinematics of aging media.

Material body is considered here, in a conventional way, as a 3D manifold B, i.e. a set of "idealized" material points (with the coordinates $X^I, I = 1,2,3$). Cylinder $P = R \times B$ (with the coordinates $(X^0 = T, X^I, I = 1,2,3)$) equiped with the Lorentz type "intrinsic" ("material") metric tensor G with components G_{IJ} is refered to a material "space-time" (P, G). We require that all the sections $B_T = \{T = const\}$ are space-like, while the material "world lines" $\{R \times (X^I, I = 1,2,3)\}$ are time-like with respect to the metric G.

Metric G defines the 4D volume elment

$$dV = \sqrt{-|G|}d^4X,$$

here $|G|$ is the determinant of the matrix (G_{IJ}).

History of deformation of the body B is represented by a diffeomorphic embedding $\phi : P \longrightarrow M$ of the material space-time P into the Minkowski space $M = R^4$ (with the coordinates $(t = x^0, x^i, i = 1,2,3)$), equiped with the 3D Eucledian space metric h with components δ_{ij}. In examples below we restrict ϕ by requiring $t = \phi^0(X) = T$. Such deformations are called "sinchronized".

Using the deformation ϕ, we define the slicing of P by the level surfaces of the zeroth component of ϕ

$$B_{\phi,t} = \phi^{0\ -1}(t) = \{(T, X) \in P | \phi^0(T, X) = t\}. \tag{1}$$

For the sinchronized deformation $B_{\phi,t} = B_{T=t}$, therefore these surfaces are **spacelike** (see above). We assume the same to be true in the general case.

There is a "flow vector field" u_ϕ in P associated with the slicing $B_{\phi,t}$ of the space-time P. It is the only time directed vector field orthogonal to the slices $B_{\phi,t}$ for all values of t and $< u_\phi, u_\phi >= -1$ (see [2],[16]). For sinchronized deformation ϕ and the block-diagonal metric G in coordinates $T, X^I, I = 1,2,3$ we have

$$u_\phi = [-G_{00}]^{-\frac{1}{2}} \frac{\partial}{\partial T}.$$

In addition to the volume element, the **mass form**

$$dM = \rho_0 dV$$

is defined in P. The reference mass density ρ_0, defined by this representation satisfies the **mass conservation law**

$$\mathcal{L}_{u_\phi} dM = 0,$$

where $\mathcal{L}_{u_\phi}$ is the substantial (Lie) derivative in the direction of the field u. In the sinchronized case the mass conservation law is equivalent to the following representation of the reference density:

$$\rho_0(T, X^I) = \rho_0(0, X)\sqrt{\frac{G_{00}}{|G|}}, \tag{2}$$

where $\rho_0(0, X)$ is the initial value of ρ_0 (we assume that $G(0, X)$ is the Minkowski metric). Space density ρ is defined, as usual, by the condition

$$\phi^*(\rho dv) = \rho_0 dV,$$

that gives

$$\rho \circ \phi = \frac{\rho_0\sqrt{-G}}{J(\phi)},$$

where $J(\phi)$ is the Jacobian of the deformation ϕ.

Slicing $B_{\phi\ ,t}$ defines the covariant tensor

$$\gamma = G + u_\phi \otimes u_\phi,$$

(see [24],[2]). Denote by Π the orthonormal projector $\Pi = G^{-1}\gamma$ to the planes tangent to the slices $B_{\phi t}$. Tensor γ induces the time dependent 3D-metric g_t on the slices $B_{\phi\ ,t}$ (see [10]). In the sinchronized case and the block-diagonal metric G, g_t is just the restriction of 4D-metric G to the slices B_T. We do not put any futher condition on the metric g_t. In particular, it may have non-zero curvature (i.e incompatibility of deformation). Apparently there are residue stresses associated with this curvature.

We also introduce the 4D tensor

$$K_4 = G^{-1}C_4(\phi) - \dot{u_\phi} \otimes u_{.\ \phi},$$

where $C_4(\phi) = \phi^* h$, and define 3D-elastic covariant strain tensor E^{el} as follows

$$E(\phi)^{el} = \frac{1}{2}\Pi ln(K)\Pi = \frac{1}{2}\Pi ln(G^{-1}\phi^* h - \dot{u_\phi} \otimes u_{.\ \phi})\Pi. \tag{3}$$

Then, 3D elastic strain tensor $E(\phi)^{el}$ results from the restrictions of tensors G^{-1} and $\phi^* h$ to the slices $B_{\phi t}$ (see Appendix B). It is a natural measure of a deviation of the actual

state from the "ground state". For the sinchronized deformation ϕ and the block-diagonal metric G,

$$E^{el} = \frac{1}{2} ln(g_t^{-1} C(\phi))$$

i.e conventional logarithmic measure of deformation.

The total deformation E^{tot} of the body at each given moment T that measures the deviation of the deformed Eucledian metric $\phi^* h|_{B_{\phi,t}}$ from the initial (Eucledian) 3D-metric h on B_T translated there from B,

$$E^{tot} = \frac{1}{2} ln(h^{-1} C(\phi)),$$

in important practical cases can be represented as the sum of the elastic deformation

$$E^{el} = \frac{1}{2} ln(g_t^{-1} C(\phi)),$$

and an irreversible deformation

$$E^{ir} = \frac{1}{2} ln(h^{-1} g_t)$$

(the logarithm of (1,1)-tensors is taken on the slices $B_{\phi\ ,t}$):

$$E^{tot} = E^{el} + E^{ir}. \tag{4}$$

The diagram below presents the above decomposition.

The actual state under the load at any given moment T results from both elastic (with the variable elastic moduli) and inelastic (irreversible) deformations. The "ground state" of the body is characterized by the 3D-metric g_t. This state is the background to which the elastic deformation is added to reach the actual state (compare [29]).

Transition from the reference state to the "ground state" that manifests in the evolution of the (initial) Eucledian metric h to the metric g_t can not be described, in general, by any point transformation. Transition from the "ground state" to the actual state at the moment t also is not compatible in this sense. Yet the transition from the reference state to the actual state is represented by the diffeomorphism ϕ_t.

Here we consider the **material 4D-metric** G and the **deformation** ϕ (or elastic strain tensor $E^{el}(\phi)$ plus the zeroth component ϕ^0 of the deformation) to be the dynamical variables of the theory. Reference density ρ_0 is found by the formula given above if its initial value $\rho_0(T=0)$ is known. In this study we restrict ourselves to the (quasi)-static version of the theory. Dynamical case is discussed elsewhere.

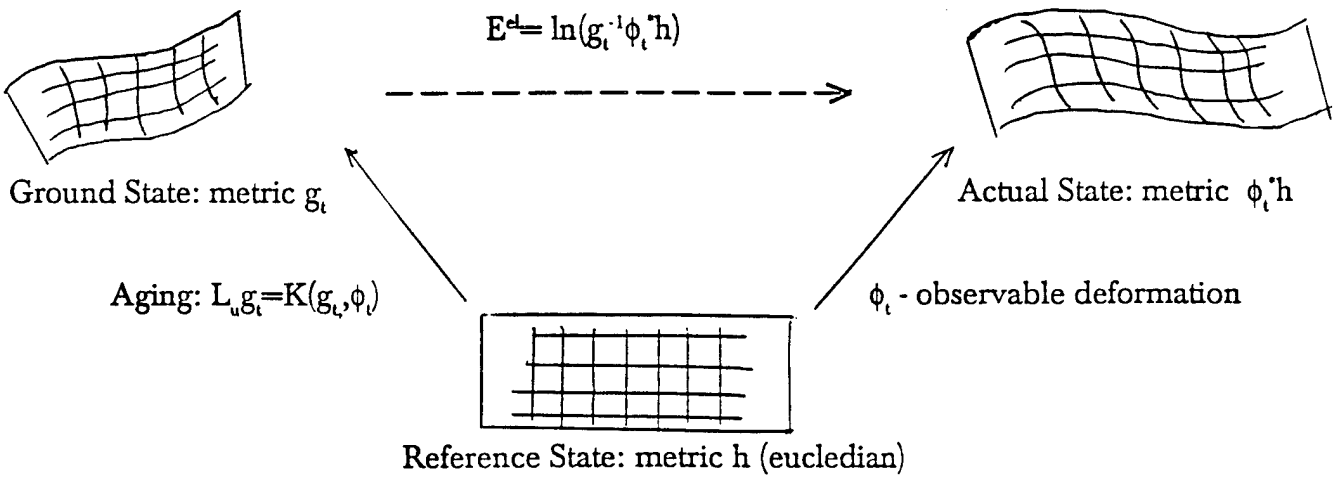

Figure 1. Decomposition of kinematics of aging media

3. Variational formulation of equations of aging.

Variational principle

Following the framework of the classical field theory we take Lagrangian density $\mathcal{L}(G, E, \phi^0)$ refered to the **volume form** $dV = \sqrt{-|G|}d^4X$ as a density that depends on the dynamic variables of our model i.e. 4D-material metric G and the deformation history ϕ: $\mathcal{L}(G, E^{el}, \phi^0) = L(G, E^{el}, \phi^0)dV$, with $L(G, E^{el}, \phi^0)$ being the Lagrangian.

Deformation ϕ is essentially 3-dimensional in the sense that it deformes only the spacial Eucledian metric h in M and, the 4D-tensor

$$C_4(\phi) = \phi^* h$$

is the degenerate metric in P. We compare it with the tensor $\gamma = G + u_\phi \otimes u_\phi$. Elastic deformation E^{el} measures the deviation of $C(\phi)$ from γ on the slices $B_{\phi,t}$.

Coincidence of $\gamma|_{B_T}$ and $C(\phi)$ is possible if there is no elastic deformation and if deformation ϕ describes just an evolution of the metric g_t.

Zeroth component ϕ^0 of the deformation plays the special role in our considerations. Relation between the laboratoy time t and the proper intrinsic time τ in P is given (in a homogeneous case where $t = \phi^0(T)$) by the relation

$$d\tau = \sqrt{-G_{00}}dT = \frac{\sqrt{-G_{00}}}{\phi^0_{,0}}dt,$$

and, therefore, ϕ^0 (or rather, its derivatives) characterise the rate of proper intrinsic time flow - "rate of aging" of the material.

Based on these arguments we present the Lagrangian $L(G, E)$ as the sum of the "ground state" Lagrangian $L_m(G)$ that depends on the metric G only, of the elastic part $L_e(G, E)$ that is a perturbation of the metric part due to the elastic deformation and of the intrinsic time evolution part $L_t(\phi^0, G)$:

$$L = L_m(G) + L_e(E^{el}) + L_t(\phi^0, G). \tag{5}$$

In a quasistatic theory we ignore the kinetic energy and the second term is simply related to the elastic strain energy f that is assumed to be a function of two first invariants of the (1,1)-strain tensor E^{el} : $Tr(E^{el})$ and $Tr((E^{el})^2)$.

$$L_e(E^{el}) = \bar{\rho}_0(f(E^{el}) + \rho_0(0)F), \tag{6}$$

where

$$\bar{\rho}_0 = \rho_0/\rho_0(0) = \sqrt{\frac{G_{00}}{|G|}}$$

is the reference density normalized to its initial value and the strain energy has the form

$$f(E^{el}) = \frac{\mu}{2}Tr(E^{el\ 2}) + \frac{\lambda}{2}(Tr(E^{el}))^2,$$

μ and λ are initial values of elastic constants. F is the potential of the body forces.

In more general consideration, one can take the strain energy L_e as a function of joint invariants of tensor E^{el} with the tensor $\mathcal{K}$ and the Ricci tensor $Ric(g_t)$ of the metric g_t.

Notice that when the intrinsic metric G coincides with the Minkowski metric (with c=1), tensor E^{el} is the usual strain tensor of the classical elasticity theory ([19],[21]) and the expression (6) is the conventional quadratic form of the strain energy of linear elsticity.

The term $L_m(G)$ in (5) can be interpreted as the "cohesive energy" of the solid. We assume that the ground state Lagrangian $L_m(G)$ depends on G, on the invariants of the tensor of extrinistic curvature

$$\mathcal{K} = \mathcal{L}_{u_\phi}\gamma$$

of slices $B_{\phi\ ,t}$ in the material space-time P (see [10],[24],[30]) and on the Ricci tensor $Ric(g_t)$ of the metric g_t. In the case of a block-diagonal metric G,

$$\gamma = \begin{pmatrix} 0 & 0 \\ 0 & g \end{pmatrix}$$

and, therefore, $\mathcal{K}$ is, essentially, the time derivative of the 3D projection g of material metric G:

$$\mathcal{K}^I_J = \frac{1}{\sqrt{-G_{00}}}G^{IA}G_{AJ,0}.$$

Tensor $\mathcal{K}$ is interpreted as the rate of change of effective intrinsic spacial scales in the media due to different inelastic processes together with the influence of elastic deformatin on these processes.

The ground state Lagrangian L_m is constructed as a linear combination of quadratic invariants of tensors $Ric(g_t)$ and $\mathcal{K}$:

$$L_m(G) = F(G) + Q(G)Tr(\mathcal{K}) + \alpha Tr(\mathcal{K}^2) + \beta Tr(\mathcal{K})^2 + \tau R(g_t). \qquad (7)$$

Here $F(G)$ is the initial energy density (per unit mass) that is considered (as well as the coefficient $Q(G)$) as a function of the 3D volume $|g_t = \Pi G \Pi|$ and $G_{00} + (1-\Pi)G(1-\Pi)$, $R(g_t)$ is the scalar curvature of the 3D metric g. Coefficients $\alpha\tau$ are numerical parameters to be choosen later.

In simpliest cases (homogeneous case, 1D case) scalar curvature R of the metric g_t is zero and the last term in (7) vanishes. More general case where g has nonzero curvature localized on some surfaces or lines (situation studied in gravity by A.Taub [31]) will be considered elsewhere.

Notice that the 4D-scalar curvature $R(G)$ of the metric G can be expressed as $-(tr(\mathcal{K}^2) - (tr\mathcal{K})^2) + R(g_t)$, up to a divergence term (see [24], Sec.21.6 or [10]). As a result, Hilbert-Einstein action $R(G)\sqrt{-|G|}$ is the special case of (7).

Role of the third term as the "intrinsic time evolution part" was mentioned above.

Following the standard procedure for the Lagrangian formulations of the Elasticity (see, for example, [21]) we add the surface term $\int \dot{W}(\phi, G)d^3\Sigma$ with $\dot{W}$ representing the power of surface truction; to formulate the action integral on a tube domain $U = [0,t] \times V$, with $(V, \partial V)$ being an arbitrary subdomain of B with the boundary ∂V:

$$A_U(G,\phi) = \int_V (L_m(\mathcal{K}) + L_e(E))dV + \int_{\partial V} \dot{W}(\phi, G)d^3\Sigma. \qquad (8)$$

Euler-Lagrange Equations.

Variation principle of extremal action $\delta A = 0$ taken with respect to the dynamic variables ϕ and G gives a system of Euler-Lagrange equations that can be interpreted as the coupled elasticity and aging equations

$$\begin{cases} \dfrac{\partial \mathcal{L}_e}{\partial \phi^m} - \dfrac{\partial}{\partial X^I}\left(\dfrac{\partial \mathcal{L}_e}{\partial \phi^m_{,I}}\right) + \rho_0\sqrt{-|G|}(\nabla F)_m = 0, \quad I = 0,1,2,3. & (9) \\ \dfrac{\delta \mathcal{L}_m}{\delta G^{IJ}} = -\dfrac{\sqrt{-|G|}}{2} T_{IJ}, \quad I = 0,1,2,3. & (10) \end{cases}$$

Elasticity Equations (9) are obtained by taking the variation δA with respect to the components ϕ^i inside the domain U. These equations (excepr of one with I=0) coincide with the conventional equations of equilibrium of the Nonlinear Elasticity. However their special features are associated with the different definition of the elastic strain tensor E^{el} and with the dependence of the elastic Lagrangian $\mathcal{L}_e$ on time through the metric G and in general through the Ricci tensor and the extrinsic curvature tensor. As a result, tensor of elastic constants is a function of these parameters and, therefore, of time. Evolution of these parameters is defined by the equations (10) (refered as Aging Equations).

Zeroth equation describes the evolution of the intrinsic time parameter τ and reflects the change in the rate of the processes going in the media (in terms of relaxation times) - aging of the material. Its more detailed study and the relation with the thermodynamical propweries of the media will be subject of the other paper. This equation is trivially fulfiled for sinchronized deformations ($\phi^0(T,X) = T$).

The Hooke's law (obtained by the equating zero of surface variation of deformation history ϕ^i) takes the form

$$\frac{\partial \mathcal{L}_e}{\partial \phi^m_{,I}} = P^I_m, \quad I, m = 0, 1, 2, 3. \tag{11}$$

Here

$$P^I_m = -\frac{\partial P^I}{\partial \phi^m}$$

is the first Piola-Kirchoff tensor, with P^I being the components of the traction surface density ($\dot{W} d^3\Sigma = P^I d\Sigma_I$). Using Hooke's law and assuming the absence of body forces ($\nabla F = 0$) one can rewrite the elasticity Equations in the well known form

$$\frac{\partial \mathcal{L}_e}{\partial \phi^m} - \frac{\partial}{\partial X^I} P^I_m = 0, \ m = 1, 2, 3. \tag{12}$$

If $\mathcal{L}_e$ is traslationally invariant in space, the first term in the left side vanishes.

Aging Equations

Variation of the action with respect to the metric G give us the equations of the material metric G evolution i.e. the aging equations (10) where

$$\frac{1}{2}\sqrt{-|G|}\, T_{IJ} = \frac{\delta(\mathcal{L}_e)}{\delta G^{IJ}}$$

defines the "canonical" Energy-Momentum tensor. This tensor is symmetric and has a close relation with the Eshelby Energy-Momentum tensor b_{IJ} ([8],[9],[7]). Indeed (see Appendix D) components of these tensors in a case of a block-diagonal metric G are related as follows

$$\sqrt{-|G|}\ T_{IJ} = b_{(IJ)} + \mathcal{L}_e G_{IJ}(1 - \delta^0_I \delta^0_J). \tag{13}$$

Notice also that the spacial part of the tensor T coincide with the symmetrized second Piola-Kirchoff tensor S:

$$\sqrt{-|G|}T_{IJ} = S_{(IJ)},\ \ I.J = 1,2,3.$$

Equations (9-10) together with the expression (2) for the reference density form the closed system of equations for dynamical variables (G_{IJ}, E^{el}). They complemented with the initial and boundary conditions, provides one with a closed non-linear boundary value problem for deformation and material properties evolution.

In general system (9-10) seems rather complex especially if the L_e dependence $Ric(g_t)$ or $\mathcal{K}$ is included. Yet some problems can be readily analysed.

Block-diagonal metric G, sinchronized ϕ

In this case

$$(K_{IJ}) = \begin{pmatrix} 0 & 0 \\ 0 & \frac{1}{\sqrt{-G_{00}}} G_{IJ,0} \end{pmatrix}.$$

From this it follows that only derivatives in $X^I,\ I = 1,2,3$ that appears in

$$L_m = F(G) + Q(G)Tr(\mathcal{K}) + p_2(\mathcal{K}) + \tau R(g)$$

(p_2 is a homogeneous function of invariants of tensor $\mathcal{K}$ of degree 2) are those in $R(g_t)$ and that g is equal to the restriction of G to B_t for each t. No derivatives in G_{00} appears anywhere in $\mathcal{L}$. In particular, (00)-equation is not a dynamical equation but rather the condition, similar to the "energy condition" in the gravity, see [10].

This equation has the form

$$G_{00}(\sqrt{g_t}(\gamma + \tau R(g_t)) + f(E^{el})) + \sqrt{g_t} p_2(g^{IA}\dot{g}_{AJ}) = 0, \tag{14}$$

where $\sqrt{g_t}$ is the volume element of the 3D metric g, p_2 is the quadratic part of L_m and f is the strain energy.

This equation can be used to exclude G_{00} from the other six equations (10). Alternatively, it can be used as the additional equation to select convinient variables (see Sec.VI below).

Spacial part of equation (3.6) takes the form

$$-\frac{\sqrt{g}}{2\sqrt{-G_{00}}}\left(\alpha g_{IJ}g_{AB}+\beta g_{IA}g_{JB}\right)\dot{g}^{AB}+q_{IJ}(g,\dot{g},G_{00},\dot{G}_{00})+\xi\tilde{\mathcal{E}}_{IJ}(g_t)=S_{(IJ)}. \qquad (15)$$

Here $\tilde{\mathcal{E}}_{IJ}(g)$ is the analog of the Einstein tensor of the 3D-metric g_t. The difference with the usual Einstein tensor is due to the presence of the factor $\sqrt{-G_{00}}$ in the term $\sqrt{-|G|}R_3(g)$ of the Lagrangian density ($\sqrt{-|G|}=\sqrt{-G_{00}}\sqrt{g_t}$).

Term q on the left side depends on the metric coefficients and their first derivatives in time.

Right side of this equation contains no derivatives of metric coefficients. Third term in the right side contains only derivatives of G_{IJ}, $I,J=1,2,3$ by X^I, $I=1,2,3$ but does not contain time derivatives. The first two terms in the left side on the contrary, contain only derivatives in time but no space derivatives. This equation is of the second order in time. In the case where the term with the constant α dominate one with the constant β (for example, if $\beta=0$) this equation can be easily transformed to the normal form

$$\frac{\partial^2 G_{IJ}}{\partial t^2}+F(G,\frac{\partial G}{\partial t},\frac{\partial G}{\partial X},\frac{\partial^2 G}{\partial X^2},\nabla\phi)=0.$$

Notice 3 special cases.

1) Homogeneous media

In a case of a homogeneous media tensor $\mathcal{E}_{IJ}(g)$ is identically zero. As a result, (15) becomes a system of quasilinear **ordinary** differential equations of the second order for G_{IJ}. Cauchy problem for this system is correct if $\alpha >> \beta$.

In a case, where $Ric(g_t)\approx 0$, a good approximation of the general system (9-10) can be proposed. If the total deformation ϕ is approximated by the ground deformation $\bar{\phi}$ in evaluation of EMT T_{IJ} in the right side of (10), the latter becomes decoupled from equilibrium equation (9). This allows to study aging equations separately and, after obtaining solution G of these equations, substitute them into elastic equilibrium equation (9) and solve it as the usual elasticity equation **with variable elastic moduli.**

2) Static case

If G does not depend on time. $\mathcal{K} = 0$, $p(\mathcal{K}) = 0$ and (14) reduces to the "energy balance equation" (with scalar curvature $R_3(g)$ plaing the role of metric energy) while (15) becomes the second equilibrium equation describing the stress produced by the curvature of the metric g and "frozen" into the media.

3) homogeneous rod (1-D case).

In a case of a 1D media (rod) the curvature of g is identically zero. Then the equations (3.6) reduces to a nonlinear dynamical system for G_{00} and G_{11}. In Sec.6 (and in Appendix C) an evolution of a homogeneous rod is further discussed.

4. Balance equations.

As it is usual for a Lagrangian field theory, action of any one-parameter group of transformations of the space $P \times M$ commuting with the projector to the first factor leads to the corresponding balance law (see [21]). In particularly, translations in the "laboratory space-time" M lead to the equations of motion (9) (including zeroth one that is trivially valid here), rotations in the "laboratory space" lead to the angular momentum balance law (conservation law in isotropic case). Respectivelly, translations in the "material space-time" P lead to the **energy balance law** (translations along T axis) and to the **material momentum balance law** (called also "pseudomomentum" [12],[26],[23]), rotations in the material space B lead to the "material angular momentum" balance law.

In the table below we present basic balance laws together with the transformations generating them. It is instructive to compare the space and material balance laws.

Symmetry	Laboratory space-time (Material independent)	Material space-time (Space independent)
Homogeneity of 3D-space	Linear momentum balance law (equilibrium equations) $\mathrm{div}(\sigma)=f_{ext}$	Material momentum (pseudomomentum) balance law $\mathrm{div}(b)=f_{mat}$
Time homogeneity	Intrinsic time evolution equation: $\delta L_t / \delta \varphi^0 = 0$	Energy balance law: $\partial_t (\mathscr{E}^{tot} = \mathscr{E}^{el} + \mathscr{E}^{m} + \mathscr{E}^{dis}) =$ $\mathrm{div}(P^{tot} = P^{el} + P^{m} + P^{dis})$
Isotropy of 3D-space	Angular momentum balance law ≡ h-symmetry of Cauchy stress-tensor σ $I:\sigma = \sigma:I$	Material angular momentum balance law ≡ C-symmetry of Eshelby stress tensor b $b : C = C : b$

Relations between the space and material balance (conservation) laws are given by the deformation gradient:

$$\begin{pmatrix} \eta_0 \\ \dots \\ \eta_4 \end{pmatrix} = \begin{pmatrix} 1 & \phi^1_{,0} & \dots & \phi^3_{,0} \\ 0 & \phi^1_{,1} & \dots & \phi^1_{,3} \\ \dots & \dots & \dots & \\ 0 & \dots & \dots & \phi^3_3 \end{pmatrix} \begin{pmatrix} \nu_0 \\ \dots \\ \nu_4 \end{pmatrix}. \tag{16}$$

Similar to the relativistic elasticity ([15,],[16]) system of material momentum balance laws $\eta_I = 0, I = 1,2,3$ is equivalent to the elasticity equations $\nu_m = 0$ while energy balance law $\eta_0 = 0$ (which is the material law) follows from any of these two systems: $\eta_0 = \sum_{i=1}^{i=3} V^i \nu_i$. This reflects the fact that the deformations we consider are not really 4-dimensional, and that we restrict the class of deformations to sinchronized ones.

In terms of the 4D Eshelby tensor $b = -\mathcal{L}_e \delta^I_J + \frac{\partial \mathcal{L}_e}{\partial \phi^i_{,I}} \phi^i_{,J}$, material energy-momentum conservation law has the form (see Appendix D)

$$div_4 b = b^I_{J,I} = \frac{\partial}{\partial X^I} \left(\mathcal{L}_m \delta^I_J - \frac{\partial \mathcal{L}_m}{\partial G^{AB}_{,I}} G^{AB}_{,J} - \frac{\partial \mathcal{L}_e}{\partial G^{AB}_{,I}} G^{AB}_{,J} \right). \tag{17}$$

Energy balance law plays special role in our considerations. In the table above $\mathcal{E}^{tot}$ is the total inner energy density. That equation has the standard form "rate of change of inner energy equals to the 3D flow of energy". The total inner energy $\mathcal{E}^{tot}$ is composed of the usual elastic strain energy

$$\mathcal{E}^{el} = -\mathcal{L}_e + \frac{\partial \mathcal{L}_e}{\partial G^{AB}_{,0}} G^{AB}_{,0},$$

the "metric energy" term

$$\mathcal{E}^m = -\mathcal{L}_m + \frac{\partial \mathcal{L}_m}{\partial G^{AB}_{,0}} G^{AB}_{,0}$$

is a "cohesive" energy i.e. a part of the total energy density associated with the integrity of the media. Reduction of the cohesive energy due to the aging can be related

to an increase of brittleness. This relation is a subject of different article. Third part is the "dissipation term"

$$\mathcal{E}^t = -\mathcal{L}_t + \frac{\partial \mathcal{L}_t}{\partial G^{AB}_{,0}} G^{AB}_{,0},$$

related to the slowing or enfastering of the processes due to the aging phenomena. Correspondingly we have, in the right side of this balance law the flows, where

$$\mathcal{P}^{el} = P^I_i \phi^i_{,0}$$

is the usual traction force power, second term

$$\mathcal{P}^m = \frac{\partial \mathcal{L}_m}{\partial G^{AB}_{,I}} G^{AB}_{,0}$$

is a "material forces power" (comp. [8],[12],[13]), and the third term wil be interpreted as the dissipation flow (due to the heat transfer and other thermodynamical processes). More detailed analysis of this balance law and its relation to the entropy production balance as well as with the dissipation inequality will be published elsewhere.

For the external "observer" all three terms represent the total energy while from the point of view of "internal observer" this total interior energy comprises three terms corresponding to the different processes going in the media.

If the elastic Lagrangian $L_e = L_e(E^{el})$ depends only on the strain tensor E^{el} and if L_m is function of $|G|$ and $\mathcal{K}$ only while $L_t = 0$ (for example, in a sinchronized case), energy balance law takes the following form (see Apendix D)

$$\frac{\partial}{\partial T}\left(\mathcal{E}^{tot} = -\mathcal{L}_e - \mathcal{L}_m + \frac{\partial \mathcal{L}_m}{\partial G^{AB}_{,0}} G^{AB}_{,0}\right) = -\sum_{I=1}^{I=3} \frac{\partial}{\partial X^I}\left(P^I_i \phi^i_{,0}\right). \tag{18}$$

In the section 5 this balance will be presented in the more specific terms in the case of an aging rod.

In the case of the conventional elasticity intrinsic metric G does not depend on time and the energy balance takes its classical form.

5. Examples: Aging Rod.

In that section we consider two examples of an elasticity deformation in a homogeneous **rod** (with the coordinate X, $0 < X < L$ and the time variable T) with the intrinsic metric G evolving in time. Since we assume the homogeneity of deformation, metric G and the elastic strain tensor E^{el} are functions of time only.

The rod is subjected to the load F applied to its right end $X = L$ while its left end $X = 0$ is fixed. For $F = 0$ rod undergone the natural free aging that is described by the metric G. If $F \neq 0$, then elastic deformation is also present. Total deformation ϕ^{tot} that is seen in experiment consists in two parts. Below we specify both of them. Inelastic, irreversible part of deformation is described by the metric G whose evolution depends on the load F. Elastic part that manifests itself in the difference between the total and pure inelastic ("ground") deformation, goes with the variable Young module $E(t)$ that is also specified by the metric G. In an experiment it is the Young module $E(t)$ (or density $\rho(T)$) and the total deformation ϵ^{tot} (or, more exactly, deformation rate $\dot{\epsilon}^{tot}$) that is seen and measured. Aging equations define evolution of the metric G and, therefore, evolution of the Young module and the rate of deformation.

Equilibrium equations are trivially satisfied and stress tensor σ or deformation ϕ can be defined from the boundary conditions (see below). Aging equations (10) are now **ordinary differential equations** for the metric $G(T)$ and the energy-momentum tensor T is calculated through G and the boundary conditions for deformation or stress.

We restrict to the case of a block-diagonal metric $G = \begin{pmatrix} G_{00} & 0 \\ 0 & G_{11} \end{pmatrix}$. Metric Lagrangian is taken in the form

$$\mathcal{L}_m = \sqrt{-|G|}\left(F(G_{00}, |g_t|) + Q(G_{00}, |g_t|)Tr\mathcal{K} + \alpha_0 Tr(\mathcal{K}^2)\right), \tag{19}$$

where functions F, Q of variables $G_{00}, |g_t|$ and the constant α_0 will be specified later on.

Elastic Lagrangian has the form

$$\mathcal{L}_e = \sqrt{-G_{00}}\frac{\mu}{2}Tr(E^{el})^2 = \sqrt{-G_{00}}\frac{\mu}{2}E^{el}{}_1^1{}^2, \tag{20}$$

since $\bar{\rho}_0 = \sqrt{\frac{-G_{00}}{|G|}}$. Elastic deformation $E^{el} = \frac{1}{2}ln(G^{11}\phi_1^1{}^2)$.

Hook's law has the form

$$\sigma_{11} = \frac{\sqrt{-G_{00}}\mu}{2}\frac{E^{el}}{\phi^1_{,1}}, \tag{21}$$

For the second Piola-Kirchoff tensor S we have

$$S_{11} = G^2_{11}\psi^1_{,1}\sigma_{11} = G^2_{11}(\phi^1_{,1})^{-1}\sigma_{11} = \frac{\sqrt{-G_{00}}f'}{G^{11\ 2}\phi^{1\ 2}_1}. \tag{22}$$

In the ground state (GS) approximation where we put $\phi^1 \approx \sqrt{G_{11}}X$, that is assume that the **elastic deformation is small in compare to the inelastic one,**

$$S_{11} \approx G^{\frac{3}{2}}_{11}\sigma_{11}. \tag{23}$$

We also have

$$\sigma_{11} = [\frac{\sqrt{-G_{00}}\mu}{2\phi^1_{,1}}]\epsilon^{el}_{11} \approx [\frac{\sqrt{-G_{00}}\mu}{2\sqrt{G_{11}}}]\epsilon^{el}_{11}, \tag{24}$$

second formula being true in the GS-approximation (see above).

Calculating variations of $\mathcal{L}_e$ by G^{00}, G^{11} we find (for an arbitrary strain energy f) the Energy-momentum tensor density

$$\frac{\sqrt{|G|}}{2}\mathcal{T} = \begin{pmatrix} -\frac{G_{00}}{2}\mathcal{L}_e & 0 \\ 0 & -\frac{1}{2}(G^{11}\phi^{1\ 2}_1)S_{11} = -\frac{\sigma_{11}}{2}G_{11}\phi^1_1 \end{pmatrix}. \tag{25}$$

As a result, aging equations (9-10) has the form

$$\begin{cases} \dfrac{\delta\mathcal{L}_m}{\delta G^{00}} = -\dfrac{G_{00}}{2}\mathcal{L}_e, \\ \dfrac{\delta\mathcal{L}_m}{\delta G^{11}} = -\dfrac{1}{2}(G^{11}\phi^{1\ 2}_1)S_{11}. \end{cases} \tag{26}$$

To calculate variations of the metric Lagrangian and to preform the analysis of the aging equations we employ the following notations: $x = -G_{00}$, $y = G_{11}$ and get

$$\mathcal{L}_m = f(x,y) + q(x,y)\dot{y} + \alpha(x,y)\dot{y}^2, \tag{27}$$

where

$$f = \sqrt{xy}F(x,y),\ q = \frac{Q(x,y)}{\sqrt{y}},\ \alpha = \alpha_0 x^{-1/2} y^{-3/2}.$$

As a result, aging equation has the form

$$\begin{cases} x^2(f_x + q_x\dot{y} + \alpha_x\dot{y}^2) = \dfrac{x}{2}\mathcal{L}_e \\ -y^2(f_y - q_x\dot{x} + \alpha_y\dot{y}^2 - 2(\alpha\dot{y})\cdot) = -\dfrac{\sigma_{11}}{2}(y\phi_1^1) \end{cases} \tag{28}$$

Now we turn to the discussion of the two situations mentioned above.

1. Free aging.

Consider the situation where the rod of a material is not subjected to any load or volume forces, its left end being fixed. There is no any elastic deformation in this case ($E^{el} = 0, \sigma = 0$) but there may be an inelastic defomation $\phi^1(T,X) \neq X$. This deformation is defined from the equation $E^{el} = \frac{1}{2}ln(g_3^{-1}C(\phi)) = 0$, or $C(\phi) = g_t$ (g_t is flat). Then, clearly, ϕ is defined up to an arbitrary time-dependent rigid rotation. If we fix a point in the body and a frame in this point and require ϕ to preserve it during the deformation, ϕ is defined uniquelly: $\phi_1^{1^2} = G_{11}$,

$$\phi^1(X,T) = \sqrt{G_{11}(T)}X.$$

Aging equations are

$$\begin{cases} \dot{x} = \dfrac{f_y - \alpha_y\lambda^2 - 2\alpha\lambda\lambda_y}{q_x + 2\alpha_x\lambda + 2\alpha\lambda_x}, \\ \dot{y} = \lambda(x,y) = \dfrac{2f_x}{q_x \pm \sqrt{q_x^2 - 4\alpha_x f_x}}, \end{cases} \tag{29}$$

where function λ is defined by the second equation.

We take

$$\begin{gathered} f(x,y) = ay + c(x-1)^k, a < 0 \\ q = q_0(x-1)^m,\ m < 1. \end{gathered} \tag{30}$$

Graphs of typical solutions of this system with $G_{00}(T=0), G_{11}(T=0) > 1$ are presented in the Appendix C. One sees as the inelastic deformation $E^{ir} = \sqrt{G_{..}}$ leads to the shrinking of the rod and as the Young module $E(t) = E(0)\sqrt{\frac{-G_{00}}{G_{11}}}$ diminishes.

2. Rod with the fixed boundary.

In this case we assume that the rod is fixed on the boundary and (due to a homogeneity assumption) total deformation is zero: $\phi^1(T,X) = X$,$C(\phi) = h, E^{el} = \frac{1}{2}ln(G^{11})$. That does not mean that there are now stresses in the rod: expansion deformation due to the fixed boundary is compensated by the shrinking due to the aging process. As a result, intrinsic stresses are developed in the body.

We have Energy-momentum tensor has, in this case, the form

$$\begin{pmatrix} \frac{x}{2}\sqrt{x}f(-\frac{1}{2}ln(y)) & 0 \\ 0 & -\frac{y}{2}\sqrt{x}f'(-\frac{1}{2}ln(y)). \end{pmatrix}$$

For $f(E^{el}) = \frac{\mu}{2}E^{el\ 2}$ we get aging equations in the form

$$\begin{cases} \dot{x} = \dfrac{f_y - \frac{\mu\sqrt{x}ln(y)}{4y^2} - \alpha_y\lambda^2 - 2\alpha\lambda\lambda_y}{q_x + 2\alpha_x\lambda + 2\alpha\lambda_x}, \\ \dot{y} = \lambda(x,y) = \dfrac{2(f_x - \frac{\mu x\sqrt{x}}{8}(ln(y))^2)}{q_x \pm \sqrt{q_x^2 - 4\alpha_x(f_x - \frac{\mu x\sqrt{x}}{8}(ln(y))^2)}}, \end{cases} \tag{31}$$

Graphs of typical solutions of this system with $G_{00}(T=0), G_{11}(T=0) > 1$ are presented in the Appendix C. One sees as the inelastic deformation $E^{ir} = \sqrt{G_{11}}$ leads to the shrinking of the rod and as the Young module $E(t) = E(0)\sqrt{\frac{-G_{00}}{G_{11}}}$ diminishes.

Comparision of these graphs shaws that during the aging of the rod with the fixed boundary, both inelastic deformation and the decrease of the Young module happens more slowly and their limit value is closer to the pure elastic case (in the absence of aging).

6. Conclusion.

A variational approach is proposed to formulate constitutive equations for aging media. The approach is based on the assumption that the metric tensor of the inner (material) space-time geometry together with an elastic strain tensor constitute a complete set of parameters of state. This assumption combined with classical Hamilton's principle provides a framework for derivation the constitutive and balance equations modeling material behaviour. Selection of a particular form of the Lagrangian, as it is usual in a variational formulation, leads to a particular constitutive equations. Thus, for one of the simplest linearized case the approach leads to a model of well studied creep behavior of a material with fading memory. Analysis of various forms of Lagrangian, the resulting models of material behavior, comparison with the experimental data as well as with conventional thermodynamic restrictions is the subject of our next work.

Appendix A. Historical background.

Development of Elasticity Theory in the end of the last and in the beginning of this century was one of several principal factors that ensured the formation of Differential Geometry as independent and powerful branch of mathematics. Classical works of Levi-Chivita, Ricci on Tensor Analysis and Absolute Calculus are examplery works that support strength of the influence of Elasticity Theory. Yet it seemed that later development of Continuum Mechanics as well as that of the Material Science influenced predominantly development of analytical domains of mathematics rather then that of geometrical domaines.

During the last twenty years development of the Classical Field Theory that was triggered by the studies in Gauge Field Theories and Hamiltonian Mechanics resulted in the development of new powerful mathematical methods of analysis and geometry, and, simultaniously, revived interest in studying of geometrical structures that appeares in continuum mechanics, astrophysics and solid state physics.

At the same time there appeared works in Continuum Mechanics where inner, material properties of media are presented by geometrical structures effectivelly reflecting the specific properties of solids and liquid media.

In a series of works A.G.Hermann ([14],[26]), A. Golebowska-Hermann ([12],[13]) and their collaborators have studied and clarified the relation between the "laboratory" and "material" conservation laws (balance equations) of Elasticity and Thermoelasticity.

Developments of the structural theory of continuous media pioneered in the works by Eshelby ([8,9]), Kondo ([17]) and developed in works by E.Kroner, C.-C.Wang ([32]), W.Noll ([25]), G.Mougen, M.Epstein, and others ([22],[7],[23],[1]) demonstrated importance of studying of "material connections" that reflects the inhomogeneity of the properties of media and the elegance of the "dual" space-material picture in Elasticity Theory.

Works of B.Carter and H.Quintana (see [2],[3]), G.Maugin on the Relativistic Elasticity Theory make a great use of specific geometrical structures and relations between such structures in 4D-Lorentz space-time of General Relativity and that of 3D-Riemannian space of the body (of a star). Further works in this direction made by J.Kijowski and G.Magli ([15],[16]) support the opinion that relations between the inner geometry of media and its dynamics deserves further investigation.

On the other hand in the works by J.Marsden, J.Simo, T.Hughes and P. Krishnaprasad ([20],[27],[21],[28]) there was introduced and successfully exploated the notion of "material metric" G inner to the media. These authors reformulated the classical non-linear Elasticity

Theory as the Lagrangian Theory where the Lagrangian is the functional of two metrics on the body - inner metric G and $\phi^* h$ induced by a deformation ϕ from the Eucledian metric of the "laboratory "space. They have developed the covariant approach to the balance equations of the Elasticity Theory ([21]) and have studied the relations between the "space" and "material" energy-momentum tensors ([27]).

Our approach is a kind of development of this last point of view together with the scheme of Relativistic Elasticity Theory. We are studying the Elasticity Theory for media (body B) whose properties are changing with time, but in difference to the usual theories of media with memory this dependence manifestates through the "material" metric in 4D-"material space-time" $P = \{R\} \times B$ where the first factor stays for inner time parameter T. Deformation is presented by an embedding ϕ of P to the 4D-"laboratory space-time" M of Newton. The last term means that $M = R^4$ is endowed by a degenerate (3D) metric along the space slices ([24]).

Appendix B. Measure of Strain and Elasticity Modulus.

We fix coordinates $t, x^i, i = 1, 2, 3$ in the laboratory space-time $M = R^4$ and endow it with the 3D Eucledian metric $h = \sum_i dx^{i\ 2}$ which is considered as the covariant 2-tensor in M (degenerate metric).

In the 4D material space-time $P = R \times B$ we consider the coordinates $(T = X^0, X^I, I = 1, 2, 3)$ (that is body B is covered by one coordiante system, for example defined by initial coordinates of material points in R^3). Denote by B_T the slicing of P by the surfaces $T = const$. P is endowed by the metric G of the signature $(-, +, +, +)$. Denote by u the vector field in P of the time-directed unit $(< u, u >= -1)$ vectors orthogonal to the slices B_T. Then, in coordinates (T, X^I) we have $u_I = (a, 0, 0, 0); u^I = aG^{I0}, I = 0, 1, 2, 3$ where $a = (-G^{00})^{-1/2}$.

Deformation $\phi : P \longrightarrow M$ defines the slicing $B_{\phi,t} = \phi^{0\ -1}(t)$ of the cylinder P. We assume that 3D-surfaces of this slicing are space-like. Denote by u_ϕ the vector field composed of future directed unit vectors $(< u_\phi, u_\phi >= -1)$ orthogonal to the slices.

In the sinchronized case $(\phi^0 = T)$ slicing $B_{\phi,t}$ coincide with the slicing B_T defined above and $u_\phi = u$.

Orthonormal projector to the slices $B_{\phi,t}$ is generated by the covariant 2-tensor ([2],24])

$$\gamma = G + u_\phi \otimes u_\phi. \tag{B.1}$$

Tensor $\Pi = G^{-1}\gamma = I + u^{\cdot}_{\phi} \otimes u_{\cdot\ \phi}$ is the projector to the tangent spaces to the slices $B_{\phi,t}$. Denote by g_t the 3D metric on the slice $B_{\phi,t}$ induced by the tensor γ ([2],[24]).

Deformation history $\phi : P \longrightarrow M$ defines the 4D Cauchy-Green tensor

$$C_4(\phi) = \phi^* h = \begin{pmatrix} \|v\|^2 & v^i \phi^i_{,L} \\ v^i \phi^i_{,K} & C(\phi) = \phi^i_{,K} \phi^i_{,L} \end{pmatrix}, \tag{B.2}$$

where we assume summation by $i = 1, 2, 3$ and use standard notations $v^i = \phi^i_{,0}$ for the vector of 4-velocity. Here $C(\phi)$ is the conventional 3D Cauchy-Green tensor.

Define the (1,1) tensor K as

$$K^{\cdot}_{\cdot} = G^{-1} C_4(\phi) - u^{\cdot}_{\phi} \otimes u_{\cdot,\phi},$$

see [15],[7], and the elastic strain tensor as follows

$$E^{el}_{\cdot}{}^{\cdot} = \frac{1}{2}\Pi ln(K)\Pi. \tag{B.3}$$

E^{el} is the tensor in P such that $E^{el}u_\phi = 0 = E^{el}{}^*u_\phi$. We will denote by the same letter the restriction of this tensor to the slices $B_{\phi,t}$. Notice that for a case of a Minkowski metric G and of the small sinchronized deformation ϕ this reduces to the usual definition

$$E^{\cdot}_{\cdot} = \frac{1}{2}(C(\phi) - h).$$

For a sinchronized deformations ϕ and a block-diagonal metric $G = \begin{pmatrix} G_{00} & 0 \\ 0 & g_t \end{pmatrix}$ we have

$$\gamma = \begin{pmatrix} 0 & 0 \\ 0 & g_t \end{pmatrix}, \quad \Pi = \begin{pmatrix} 0 & 0 \\ 0 & I_3 \end{pmatrix}, \quad G^{-1}\phi^* h = \begin{pmatrix} G_{00}^{-1}\|V\|^2 & G_{00}^{-1}V^i F^i_L \\ g_t^{-1}V^i F^i_K & g_t^{-1}C_3, \end{pmatrix}$$

and, finally,

$$E^{el}_{\cdot}{}^{\cdot} = \begin{pmatrix} 0 & 0 \\ 0 & \frac{1}{2}ln(g_t^{-1}C) \end{pmatrix} \tag{B.4}$$

i.e. E^{el} coincide with the usual classical expression for the (nonlinear) strain tensor in the case of Eucledian metric g_t.

Consider now the sinchronized deformations ϕ (so, $T = t$). If the curvature tensor $R(g_t) = 0$ then the 3D-metric $g_t = \gamma|_{B_t}$ induced by γ on the slices B_t is a flat metric and, therefore, for all $T = t$ there exists (local, or, in the case of a body B of simple structure, global) embedding (deformation) $\bar{\phi}(T, \ ) : B_T \longrightarrow R^3$ such that $g(T) = \bar{\phi}^* h|_{B_T} = C(\bar{\phi})$. We will call this deformation **ground state (GS)**. This GS-deformation is unique modulo the time-dependent eucledian motion in R^3. If we put an extra codition for a body to have, at any moment T, zero total linear momentum and total angular momentum then **the ground state** is unique up to the constant rigid motion. Notice that for the ground state (and only for it) $E^{el}(\bar{\phi}) = 0$. In components (in sincronized case) we have

$$C_{IJ} = h_{ij}\bar{\phi}^i_{,I}\bar{\phi}^j_{,J} = G_{IJ} - \frac{G_{I0}G_{0J}}{G_{00}},\ I,J = 1,2,3. \tag{B.5}$$

In the case where $G = \eta$ (Minkowski metric), $\gamma = h$ ground deformation $\bar{\phi}$ - is just the undeformed state of the Classical Elasticity.

Denote by h 3D- Eucledian metric pullbacked to all the slices B_T by the projection $P \longrightarrow B$ parallel to the T-axes. Then we define at each moment T

Total deformation $E^{tot}(\phi) = ln(h^{-1}C(\phi))$,
Elastic deformation $E^{el} = ln(g^{-1}C(\phi))$,
Inelastic deformation $E^{ir} = ln(h^{-1}g)$.

These quantities are related by

$$E^{tot} = ln(e^{E^{el}}e^{E^{ir}}),$$

which in the simpliest cases (diagonal tensors, 1D case) takes the usual form

$$E^{tot} = E^{el} + E^{ir}. \tag{B.6}$$

To get the "space" form of the strain tensors we apply the transformation induced by the deformation ϕ at any moment of time T. That is we have $\phi_* C(\phi) = h$, $\phi_* h = \psi^* h$, $q \equiv \phi_* g$ $(= \psi^*\bar{\phi}^* h$ for a zero curvature case) for 3D-metric involved and

Total deformation $\epsilon^{tot} = ln((\psi^* h)^{-1}h)$,
Elastic deformation $\epsilon^{el} = ln(q^{-1}h)$,
Inelastic deformation $\epsilon^{ir} = ln((\psi^* h)^{-1}q)$,

and we have, as for material strain tensors,

$$\epsilon^{tot} = ln(e^{\epsilon^{el}}e^{\epsilon^{ir}}),$$

which in the simpliest cases (diagonal tensors, 1D case) takes the usual form

$$\epsilon^{tot} = \epsilon^{el} + \epsilon^{ir}. \tag{B.7}$$

We take the elastic part of Lagrangian density $\mathcal{L}_e$ to be a scalar expression of the strain tensor E^{el} of order less or equal to two with the coefficients that may depend on the curvature tensor $R(g_t)$ of the 3D metric g_t and on the tensor $\mathcal{K}$ of the extrinsic curvature of the slicing B_t. As a result

$$\mathcal{L}_e = \sqrt{-|G|}\rho_0(Tr(e_1(|G|, \mathcal{K}, R(g_t))E^{el}) + Tr(e_2(|G|, \mathcal{K}, R(g_t))E^{el}E^{el}), \qquad \text{(B.8)}$$

where $e_i(|G|, \mathcal{K}, R(g_t))$, $i = 1, 2$ are elasticity tensors (moduli), depending on the intrinsic metric G. Notice also that the volume element and the reference density ρ_0 are also functions of G. As a result, elsticity moduli depend on the metric G even in the simpliest case of constant isotropic homogeneous coefficients e_i: $e^{ik}_{jl} = \frac{\mu}{2}\delta^i_l\delta^k_j + \frac{\lambda}{4}\delta^i_j\delta^k_l$. In the examples presented in this paper we restrict to the case of such elsticity tensor. More general situation will be discussed elsewhere.

Appendix C. Aging Rod.

In that section we consider three examples of an elasticity deformation in a homogeneous **rod** (with the coordinate X, $0 < X < L$ and the time variable T) with the intrinsic metric G evolving in time. Since we assume the homogeneity of deformation, metric G and the elastic strain tensor E^{el} are functions of time only.

The rod is subjected to the load F applied to its right end $X = L$ while its left end $X = 0$ is fixed. For $F = 0$ rod undergone the natural free aging that is described by the metric G. If $F \neq 0$, then elastic deformation is also present. Total deformation ϕ^{tot} that is seen in experiment consists in two parts. Below we specify both of them. Inelastic, irreversible part of deformation is described by the metric G whose evolution depends on the load F. Elastic part that manifests itself in the difference between the total and pure inelastic ("ground") deformation, goes with the variable Young module $E(t)$ that is also specified by the metric G (see below). In an experiment it is the Young module $E(t)$ (or density $\rho(T)$) and the total deformation ϵ^{tot} (or, more exactly, deformation rate $\dot{\epsilon}^{tot}$) that is seen and measured. Aging equations define evolution of the metric G and, therefore, evolution of the Young module and the rate of deformation.

Equilibrium equations are trivially satisfied and stress tensor σ or deformation ϕ can be defined from the boundary conditions (see below). Aging equations (3.7) are now **ordinary differential equations** for the metric $G(T)$ and the energy-momentum tensor T is calculated through G and the boundary conditions for deformation or stress.

We restrict to the case of a block-diagonal metric $G = \begin{pmatrix} G_{00} & 0 \\ 0 & G_{11} \end{pmatrix}$. Metric Lagrangian is taken in the form

$$\mathcal{L}_m = \sqrt{-|G|}\left(F(G_{00}, |g_t|) + Q(G_{00}, |g_t|)Tr\mathcal{K} + \alpha_0 Tr(\mathcal{K}^2)\right), \tag{C.1}$$

where functions F, Q of variables $G_{00}, |g_t|$ and the constant α_0 will be specified later on.

Elastic Lagrangian has the form

$$\mathcal{L}_e = \sqrt{|G|}\bar{\rho}_0 f(E^{el}) = \sqrt{-G_{00}} f(E^{el}), \tag{C.2}$$

since $\bar{\rho}_0 = \sqrt{\frac{-G_{00}}{|G|}}$. Here $E^{el} = \frac{1}{2} ln(G^{11}\phi_1^{1\ 2})$.

Elasticity equation (for an arbitrary $f(E^{el})$) has the form

$$\frac{\delta \mathcal{L}}{\delta \phi^1} = \frac{\partial}{\partial X}\left(\sqrt{-G_{00}} f'(E^{el}) \cdot \frac{1}{\phi^1_1}\right) = 0 \tag{C.3}$$

and in our (homogeneous) case is trivially satisfied.
We will take

$$f(E^{el}) = \frac{\mu}{2} Tr(E^{el})^2 = \frac{\mu}{2} {E^{el}}^1_1{}^2$$

and get,

$$\mathcal{L}_e = \frac{\sqrt{-G_{00}}\mu}{8} [ln(G^{11}{\phi^1_1}^2)]^2. \tag{C.4}$$

The only component of the first Piola-Kirchoff Tensor is

$$P^1_1 = \frac{\partial \mathcal{L}_e}{\partial \phi^1_{,1}} = \frac{\sqrt{-G_{00}}}{\phi^1_1} f'(E^{el}) = \frac{\sqrt{-G_{00}}\mu}{2} \frac{E^{el}}{\phi^1_{,1}}, \tag{C.5}$$

the last expression being true for the strain energy (C.4).
Since in general $\sigma_{ij} = J(\phi)^{-1} h_{js} \phi^s_{,I} P^I_i$, we have in our case

$$\sigma_{11} = (\phi^1_{,1})^{-1} \phi^1_{,1} P^1_1 = P^1_1 \tag{C.6}$$

we get Hook's law in the form

$$\sigma_{11} = \frac{\sqrt{-G_{00}}}{\phi^1_1} f'(E^{el}) = \frac{\sqrt{-G_{00}}\mu}{2} \frac{E^{el}}{\phi^1_{,1}}, \tag{C.7}$$

the last expression being true for the strain energy (C.4).
For the second Piola-Kirchoff tensor S we have $S^{IJ} = P^{kI}\psi^J_{,k}$ and

$$S_{AB} = G_{AI} G_{BJ} S^{IJ} = G_{AI} G_{BJ} P^{kI} \psi^J_{,k}. \tag{C.8}$$

Calculating the only component of S_{IJ} we get (since $\sigma_{11} = P_1^1$)

$$S_{11} = G_{11}^2 \psi_{,1}^1 \sigma_{11} = G_{11}^2 (\phi_{,1}^1)^{-1} \sigma_{11} = \frac{\sqrt{-G_{00}} f'}{G^{11\ 2} \phi_1^{1\ 2}}. \tag{C.9}$$

In the ground state (GS) approximation where we put

$$\phi^1 \approx \sqrt{G_{11}} X$$

, that is assume that the **elastic deformation is small in compare to the inelastic one**,

$$S_{11} \approx G_{11}^{\frac{3}{2}} \sigma_{11}. \tag{C.10}$$

Relation between the material and laboratory strain tensors is taken to be

$$\epsilon_j^{el\ i} = E_J^{el\ I} F_I^i F_j^{-1\ J}. \tag{C.12}$$

In 2D-case this reduces to

$$\epsilon_1^{el\ 1} = E_1^{el\ 1}, \tag{C.13}$$

and, combining that formula with C.1? we get (in the case of Lagrangian C.4)

$$\sigma_{11} = [\frac{\sqrt{-G_{00}}\mu}{2\phi_{,1}^1}]\epsilon_{11}^{el} \approx [\frac{\sqrt{-G_{00}}\mu}{2\sqrt{G_{11}}}]\epsilon_{11}^{el}, \tag{C.14}$$

second formula being true in the GS-approximation (see above).

Calculating variations of $\mathcal{L}_e$ by G^{00}, G^{11} we find (for an arbitrary strain energy f) the Energy-momentum tensor density

$$\frac{\sqrt{|G|}}{2} \mathcal{T} = \begin{pmatrix} -\frac{G_{00}}{2}\mathcal{L}_e & 0 \\ 0 & -\frac{1}{2}(G^{11}\phi_1^{1\ 2})S_{11} = -\frac{\sigma_{11}}{2} G_{11} \phi_1^1 \end{pmatrix}. \tag{C.15}$$

As a result, aging equations (3.5-6) has the form

$$\begin{cases} \dfrac{\delta \mathcal{L}_m}{\delta G^{00}} = -\dfrac{G_{00}}{2}\mathcal{L}_e, \\ \dfrac{\delta \mathcal{L}_m}{\delta G^{11}} = -\dfrac{1}{2}(G^{11}\phi_1^{1\ 2})S_{11}. \end{cases} \tag{C.16}$$

To calculate variations of the metric Lagrangian and to preform the analysis of the aging equations we employ the following notations: $x = -G_{00}$, $y = G_{11}$.

Using the fact that $\mathcal{K}_1^1 = \frac{(ln\dot{(}y))}{\sqrt{x}}$, we rewrite C.1 in the form

$$\mathcal{L}_m = \sqrt{xy}\left(F(x,y) + Q(x,y)\frac{(ln\dot{(}y))}{\sqrt{x}} + \alpha_0(\frac{(ln\dot{(}y))}{\sqrt{x}})^2\right) =$$

$$= f(x,y) + q(x,y)\dot{y} + \alpha(x,y)\dot{y}^2, \tag{C.17}$$

where second equality serve as the definition of functions

$$f = \sqrt{xy}F(x,y),\ q = \frac{Q(x,y)}{\sqrt{y}},\ \alpha = \alpha_0 x^{-1/2}y^{-3/2}.$$

Now we calculate

$$\frac{\delta \mathcal{L}_m}{\delta G^{00}} = \frac{\partial \mathcal{L}_m}{\partial G^{00}} = G_{00}^2\frac{\partial \mathcal{L}_m}{\partial x} = x^2(f_x + q_x\dot{y} + \alpha_x\dot{y}^2). \tag{C.18'}$$

Similarly, we get

$$\frac{\delta \mathcal{L}_m}{\delta G^{11}} = -y^2(f_y - q_x\dot{x} + \alpha_y\dot{y}^2 - 2(\alpha\dot{y})\cdot). \tag{C.18"}$$

As a result, aging equation has the form

$$\begin{cases} x^2(f_x + q_x\dot{y} + \alpha_x\dot{y}^2) = \dfrac{x}{2}\mathcal{L}_e \\ -y^2(f_y - q_x\dot{x} + \alpha_y\dot{y}^2 - 2(\alpha\dot{y})\cdot) = -\dfrac{\sigma_{11}}{2}(y\phi_1^1) \end{cases} \tag{C.19}$$

Now we turn to the discussion of the three situations mentioned above.

1. Free aging

Consider the situation where the rod of a material is not subjected to any load or volume forces, its left end being fixed. There is no any elastic deformation in this case ($E^{el} = 0, \sigma = 0$) but there may be an inelastic defomation $\phi^1(T, X) \neq X$. This deformation is defined from the equation

$$E^{el} = \frac{1}{2} ln(g_3^{-1} C(\phi)) = 0,$$

or $C(\phi) = g_t$ (g_t is flat). Then, clearly, ϕ is defined up to an arbitrary time-dependent rigid rotation. If we fix a point in the body and a frame in this point and require ϕ to preserve it during the deformation, ϕ is defined uniquelly:

$$\phi_1^{1^2} = G_{11}, \ \phi^1(X, T) = \sqrt{G_{11}(T)} X.$$

Energy-momentum tensor T is zero and using notations $x = -G_{00}$, $y = G_{11}$ we get for G the system of ODE:

$$\begin{cases} (f_x + q_x \dot{y} + \alpha_x \dot{y}^2) = 0 \\ (f_y - q_x \dot{x} + \alpha_y \dot{y}^2 - 2(\alpha \dot{y})^{\cdot}) = 0 \end{cases} \tag{C.20}$$

Solving the first equation for $\dot{y}$ and using it in the second equation we can rewrite this system in the form

$$\begin{cases} \dot{x} = \dfrac{f_y - \alpha_y \lambda^2 - 2\alpha\lambda\lambda_y}{q_x + 2\alpha_x \lambda + 2\alpha\lambda_x}, \\ \dot{y} = \lambda(x, y) = \dfrac{2f_x}{q_x \pm \sqrt{q_x^2 - 4\alpha_x f_x}}, \end{cases} \tag{C.21}$$

where function λ is defined by the second equation.

We take

$$\begin{aligned} f(x, y) &= ay + c(x-1)^k, a < 0 \\ q &= q_0 (x-1)^m, \ m < 1. \end{aligned} \tag{C.22}$$

Graphs of typical solutions of this system with $G_{00}(T=0), G_{11}(T=0) > 1$ looks as follows

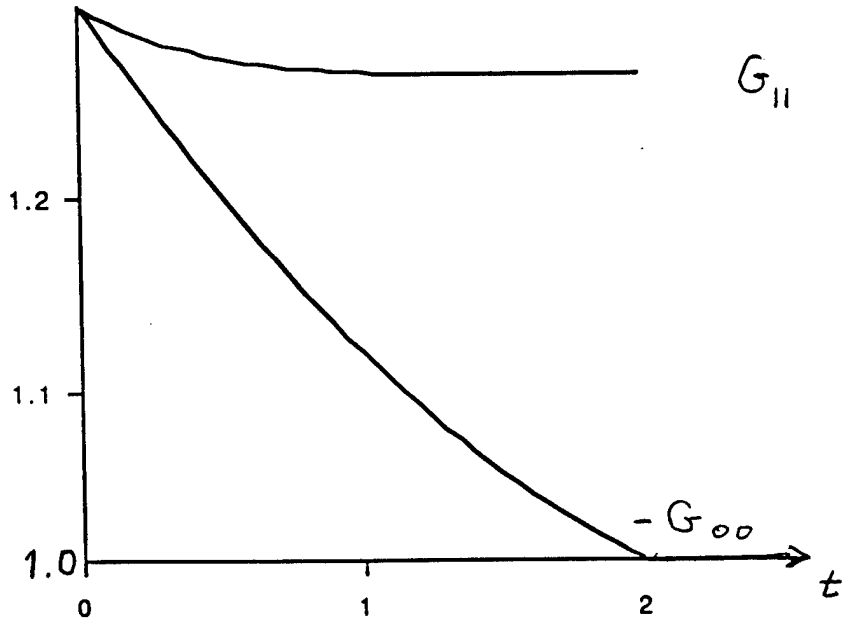

2. Rod with the fixed boundary

In this case we assume that the rod is fixed on the boundary and (due to a homogeneity assumption) total deformation is zero: $\phi^1(T,X) = X$,$C(\phi) = h, E^{el} = \frac{1}{2}ln(G^{11})$. That does not mean that there are now stresses in the rod: expansion deformation due to the fixed boundary is compensated by the shrinking due to the aging process. As a result, intrinsic stresses are developed in the body.

We have $\mathcal{L}_e = \sqrt{-G_{00}}f(E^{el})$. From this we get

$$\sigma_{11} = P_1^1 = \sqrt{-G_{00}}f'(E^{el}),\ S_{11} = \frac{\sqrt{-G_{00}}}{G^{11\ 2}}f'(E^{el})$$

and the energy-momentum tensor has the form

$$\begin{pmatrix} \frac{x}{2}\sqrt{x}f(-\frac{1}{2}ln(y)) & 0 \\ 0 & -\frac{y}{2}\sqrt{x}f'(-\frac{1}{2}ln(y)). \end{pmatrix}$$

For $f(E^{el}) = \frac{\mu}{2}E^{el\ 2}$ we get (substituting into (C.19)),

$$\begin{cases} \dot{x} = \dfrac{f_y - \frac{\mu\sqrt{x}ln(y)}{4y^2} - \alpha_y\lambda^2 - 2\alpha\lambda\lambda_y}{q_x + 2\alpha_x\lambda + 2\alpha\lambda_x}, \\ \dot{y} = \lambda(x,y) = \dfrac{2(f_x - \frac{\mu x\sqrt{x}}{8}(ln(y))^2)}{q_x \pm \sqrt{q_x^2 - 4\alpha_x(f_x - \frac{\mu x\sqrt{x}}{8}(ln(y))^2)}}, \end{cases} \tag{C.23}$$

Graphs of typical solutions of this system with $G_{00}(T=0), G_{11}(T=0) > 1$ looks as follows

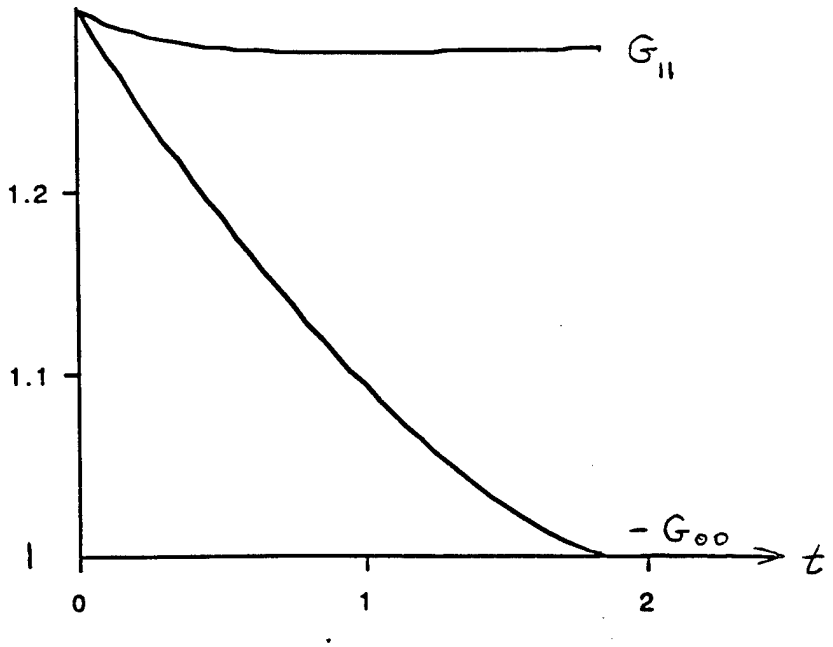

Comparision of these graphs shaws that during the aging of the rod with the fixed boundary, both inelastic deformation and the decrease of the Young module happens more slowly and their limit value is closer to the pure elastic case (in the absence of aging).

Appendix D. Energy-momentum conservation law and the relation between the Canonical Energy-Momentum and the Eshelby tensor.

Energy-momentum conservation law.

Local material translations $X^J \to X^J + \delta X^J$ generate variations of components ϕ^i of deformations and their derivatives. Calculating variation of Lagrangian we get material balance equations. Our calculations are similar to the arguments of J.Eshelby (see [8]) or [12]). We use the fact that the Lagrangian density has the form $\mathcal{L} = \sqrt{-G}(L_m(G) + L_e(G,E))$, where dependence of metrical and elastic parts of Lagrangian on G and $\mathcal{K}$ is not specified so that all dependence on X^I goes through ϕ and its gradient and through G and its derivatives. We get

$$\frac{\delta \mathcal{L}}{\delta X^J} = \frac{\partial \mathcal{L}}{\partial \phi^i}\frac{\partial \phi^i}{\partial X^J} + \frac{\partial \mathcal{L}}{\partial \phi^i_{,I}}\frac{\partial \phi^i_{,I}}{\partial X^J} + \frac{\partial \mathcal{L}}{\partial G^{AB}}\frac{\partial G^{AB}}{\partial X^J} + \frac{\partial \mathcal{L}}{\partial G^{AB}_{,I}}\frac{\partial G^{AB}_{,I}}{\partial X^J} =$$

$$= \frac{\delta \mathcal{L}}{\delta \phi^i}\phi^i_{,J} + \frac{\partial}{\partial X^I}\left(\frac{\partial \mathcal{L}}{\partial \phi^i_{,I}}\phi^i_{,J}\right) + \frac{\delta \mathcal{L}}{\delta G^{AB}}G^{AB}_{,J} + \frac{\partial}{\partial X^I}\left(\frac{\partial \mathcal{L}}{\partial G^{AB}_{,I}}G^{AB}_{,J}\right). \qquad \text{(D.1)}$$

where

$$\frac{\delta \mathcal{L}}{\delta \phi^i} = \frac{\partial \mathcal{L}}{\partial \phi^i} - \frac{\partial}{\partial X^I}\left(\frac{\partial \mathcal{L}}{\partial \phi^i_I}\right)$$

and where variational derivative $\frac{\delta \mathcal{L}}{\delta G}$ has the corresponding form. When the equation of motion (3.5-3.6) are satisfied we get the following conservation law ($J = 0, 1, 2, 3$)

$$\frac{\partial}{\partial X^I}\left(\mathcal{L}\delta^I_J - \frac{\partial \mathcal{L}}{\partial \phi^i_{,I}}\phi^i_{,J} - \frac{\partial \mathcal{L}}{\partial G^{AB}_{,I}}G^{AB}_{,J}\right) = 0. \qquad \text{(D.2)}$$

For $J = 0$ we get the energy conservation law in the form

$$\frac{\partial \mathcal{E}^{tot}}{\partial T} = \frac{\partial}{\partial T}\left(-\mathcal{L} + \frac{\partial \mathcal{L}}{\partial G^{AB}_{,0}}G^{AB}_{,0}\right) = -\sum_{I=1}^{3}\left(\frac{\partial \mathcal{L}}{\partial \phi^i_{,I}}\phi^i_{,0} + \frac{\partial \mathcal{L}}{\partial G^{AB}_{,I}}G^{AB}_{,0}\right)_{,I}. \qquad \text{(D.2')}$$

Notice that in our, quasistatical case, Lagrangian does not depend on $\phi_{,0}$. Expression

$$\mathcal{E}^{tot} = -\mathcal{L} + \frac{\partial \mathcal{L}}{\partial G^{AB}_{,0}} G^{AB}_{,0}$$

is the total inner energy density which includes elastic energy and the "metric energy" which we consider as reflecting the irreversible processes that goes in the system. In the right side we have the total flow density $\mathcal{F}$. Notice that from the print of view of outside observer there is no division of $\mathcal{L}$ in the elastic and non-elastic part and, as a result, conservation laws has their usual form $\frac{\partial(\mathrm{Energy})}{\partial T} = \mathit{Flow}$. On the other hand, from the point of view of inside observer energy splits and different terms in the balance of energy will have special meaning (see below).

Introduce the **material energy-momentum tensor**

$$b^I_J = -\mathcal{L}_e \delta^I_J + \frac{\partial \mathcal{L}_e}{\partial \phi^i_{,I}} \phi^i_{,J}. \tag{D.3}$$

Tensor b is the 4D-dynamical energy-momentum tensor P^*_{lj} of J.Eshelby (introduced in [9]), known mainly in its 3D-version (see [8], [23],[7] and [22]). It unifies in itself the 3D-Eshelby tensor b, the 1-form of *quasi-momentum (pseudomomentum)* $\mathcal{P}$ (see [26],[23]), energy and the energy flow vector. In the (quasistatical) case studied here we do not have the kinetic energy term and, as a result, $\mathcal{L}_e$ does not depend on $\phi_{,0}$. It follows that $b^0_J = 0$ for $J = 1, 2, 3$ while $b^0_0 = \mathcal{E}$ is the energy density. In the case of a block-diagonal metric G we have $b_{0B} = 0$ for all B=1,2,3 and $b_{00} = -\mathcal{L}_e$. Tensor b_{IJ} is not symmetric in general.

Splitting $\mathcal{L}$ in the first and the last term in the right side at (D.2) and regrouping terms we get

$$div_4 b = b^I_{J,I} = \frac{\partial}{\partial X^I}\left(\mathcal{L}_m \delta^I_J - \frac{\partial \mathcal{L}_m}{\partial G^{AB}_{,I}} G^{AB}_{,J}\right) - \frac{\partial}{\partial X^I}\left(\frac{\partial \mathcal{L}_e}{\partial G^{AB}_{,I}} G^{AB}_{,J}\right). \tag{D.4}$$

Notice that in this formula second term on the right is related with the inhomogeneities and the evolution of elastic moduli of the media (these moduli depends on the metric G through the volume element and the reference density and, maybe, also through tensors $\mathcal{K}$ and $Ric(g_t)$. At the same time first term is defined by the metrical part of Lagrangian density and is related to the changes of the intrinsic metric (comp. with [7]).

For $J-0$ we get the energy conservation law (using T instead of X^0)

$$\frac{\partial}{\partial T}\left(-\mathcal{L}_e+\frac{\partial \mathcal{L}_e}{\partial \phi^i_{,0}}\phi^i_{,0}-\mathcal{L}_m+\frac{\partial \mathcal{L}_m}{\partial G^{AB}_{,0}}G^{AB}_{,0}+\frac{\partial \mathcal{L}_e}{\partial G^{AB}_{,0}}G^{AB}_{,0}\right)=$$

$$=-\sum_{I=1}^{I=3}\frac{\partial}{\partial X^I}\left(P^I_i\phi^i_{,0}+\frac{\partial \mathcal{L}_m}{\partial G^{AB}_{,I}}G^{AB}_{,0}+\frac{\partial \mathcal{L}_e}{\partial G^{AB}_{,I}}G^{AB}_{,0}\right) \qquad \text{(D.5)}$$

Here P^I_i is the first Piola-Kirchoff tensor. In the left side of this equation we have the time derivative of the total energy $\mathcal{E}^{tot}$ of the system. We see that this total energy splits into the usual part: elastic energy plus kinetic energy (first two terms), metric energy that is defined by L_m (next two terms) and the last term that is related to the time dependence of the elastic moduli and can be called the "kinetic energy of elastic moduli". The sum in the right side represents the flows present in the scheme - the flow of the Piola-Kirchoff stress tensor

$$\sum_{I=1}^{I=3}(\frac{\partial \mathcal{L}_e}{\partial \phi^i_{,I}}\phi^i_{,0})_{,I}$$

and the flows related to the change of the inner metric G.

If the metric G does not depend on time and, therefore, $\mathcal{K}=0$ and if $Ric(g_t)=0$, we get the usual energy conservation law of Elasticity Theory (see [HM], Chapter 5,Sec.5):

$$\frac{\partial e}{\partial T}=-\sum_{I=1}^{I=3}\frac{\partial}{\partial X^I}(P^I_i\phi^i_{,0}).$$

If the metric G does not depend on time and, therefore, $\mathcal{K}=0$ but $Ric(g)\neq 0$, the energy conservation law will contain a term representing "energy of **frozen** defects".

Notice that energy conservation law appears here as the "material" and not as the "space" law.

In the case of a block diagonal metric G and homogeneous media we have the extrinsic curvature in the form

$$(K_{IJ})=\begin{pmatrix}0 & 0\\ 0 & \frac{1}{u_0}G_{IJ,0}\end{pmatrix}$$

and, as a result no flow terms except usual Piola-Kirchoff flow appear in the right side in (D.5):

$$\frac{\partial}{\partial T}\left(\mathcal{E}^{el}-\mathcal{L}_m+\frac{\partial \mathcal{L}_m}{\partial G^{AB}_{,0}}G^{AB}_{,0}+\frac{\partial \mathcal{L}_e}{\partial G^{AB}_{,0}}G^{AB}_{,0}\right)=-\sum_{I=1}^{I=3}(P^I_i\phi^i_{,0})_{,I}. \tag{D.6}$$

Now we would like to specialize the energy conservation law in the case of the most simple elastic Lagrangian function $L_e = L_e(E)$). In this case last term in the left side vanishes and if, in addition, we take

$$L_m = F(G) + Q(G)Tr\mathcal{K} + \alpha Tr(\mathcal{K}^2) + \beta(Tr\mathcal{K})^2$$

we get

$$\frac{\partial}{\partial T}\left(\mathcal{E}^{el}-[F(G)-\alpha Tr(\mathcal{K}^2)-\beta(Tr\mathcal{K})^2]\sqrt{-G}\right)=-\sum_{I=1}^{I=3}(P^I_i\phi^i_{,0})_{,I} \tag{D.7}$$

Consider an example of the 2D-metric

$$G_1=\begin{pmatrix} G_{00} & 0 \\ 0 & G_{11}\end{pmatrix}.$$

Here $u_0=\sqrt{-G_{00}}$, $\mathcal{K}^1_1=\frac{(ln(G_{11}),_0}{\sqrt{-G_{00}}}$. We also put $\beta=0$ and denote $\epsilon^{ir}=\sqrt{G_{11}}$, $\tilde{E}=\sqrt{\frac{-G_{00}}{G_{11}}}$ (See Appendix B). We have

$$\frac{\partial\left(\mathcal{E}^{el}-\sqrt{-G}(F(G)+\frac{\alpha}{G_{00}}((ln(G_{11}),_0)^2)\right)}{\partial T}=-\frac{\partial}{\partial X}(P^1_1\phi^1_{,0}). \tag{D.8}$$

Expression of the metric part of energy can be rewritten as follows

$$\sqrt{-G}(F(G)+\frac{\alpha}{G_{00}}((ln(G_{11}),_0)^2)=e_0\sqrt{-G}-\frac{\alpha}{\sqrt{\frac{-G_{00}}{G_{11}}}}((ln(G_{11}),_0)^2=e_0\sqrt{-G}-\frac{4\alpha}{\tilde{E}}(\epsilon^{ir})^2,$$

so that finally energy balance law takes the form

$$\frac{\partial\left(\mathcal{E}^{el}-e_0\sqrt{-G}+\frac{4\alpha}{E}(\dot{\epsilon}^{ir})^2\right)}{\partial T}=-\frac{\partial}{\partial X}(P_1^1\phi_{,0}^1). \tag{D.9}$$

Notice that it is natural to have $e_0<0$ (see above or Appendix B, where the condition was put, notice also that $\alpha>0$). As a result the first term in the expression for the metric energy, corresponding to the ground energy reserve, shows that as $\sqrt{-G}$ grows, energy $\mathcal{E}$ decreases. Second term contains derivative $\dot{E}$ so (as it is natural) that when $E(t)$ grows, (elastic) energy grows too and vice versa. This term describes change of elastic energy due to the change of elastic properties of material. Finally we interpret the last term (containing second time derivative of ϵ^{ir}) as the energy exchange due to the irreversible deformation.

Canonical Energy-Momentum Tensor, Piola-Kirchoff Tensor and Eshelby tensor

Now we would like to discuss the relation between the Eshelby Stress-Energy-Momentum Tensor b that appears in the energy-momentum balance law (D.4) and the canonical Energy-Momentum tensor defined by the relation $T\frac{\sqrt{-G}}{2}=\frac{\delta\mathcal{L}_e}{\delta G}$ of Lagrangian field theory with the 4D-metric G. Tensor T is symmetrical by definition and, in the case of a block-diagonal metric G, has the form

$$\begin{pmatrix} T_{00} & 0 \\ 0 & T_{IJ}, I, J=1,2,3 \end{pmatrix}.$$

On the other hand tensor b is not symmetrical and its $I0$ terms are non-zero even for a block-diagonal metric. Below we will get comparision of 00 and IJ, $I,J=1,2,3$ terms of these tensors.

Here we consider the Lagrangian of the form

$$\mathcal{L}_e=L_e\sqrt{-G}=\rho_0 f(E^{el},\mathcal{K})\sqrt{-G}=\sqrt{-G_{00}}f(E^{el},\mathcal{K}) \tag{D.10}$$

where

$$E_J^{el\ I}=\frac{1}{2}\Pi_K^I ln(Q)_L^K\Pi_J^L,\ Q_J^I=G^{IA}C(\phi)_{AJ}+u^I u_J$$

(see Appendix B). We present the strain energy function as the function of 3D-tensor $Q_3 = \Pi Q \Pi$ instead of E^{el}: $f(E^{el}, \mathcal{K}) = h(Q_3, \mathcal{K})$ and we will calculate derivatives and variations using this representation. Explicit dependence of elastic lagrangian on G goes through the dependence of the factor $\sqrt{-G_{00}}$ and through possible dependence of h (or f) on $\mathcal{K}$.

Calculations below are done for the BD-metrics only. In this case

$$Q_3{}^I_J = \frac{1}{2} G^{IA} C_{AJ} A, I, J = 1, 2, 3$$

As the first step we recall the calculation of the first and the second Piola-Kirchoff tensors. We have

$$P_i^I = \frac{\partial \mathcal{L}_e}{\partial F_I^i} = \frac{1}{2} \frac{\partial \mathcal{L}}{\partial Q_B^A} G^{AK} (h_{ij} F_B^j \delta_K^I + h_{ji} F_K^j \delta_B^I) = \frac{\partial \mathcal{L}_e}{\partial Q_{BK}} (h_{ij} F_B^j \delta_K^I + h_{ji} F_K^j \delta_B^I), \quad \text{(D.11)}$$

since

$$Q_{CD} = Q_D^I G_{IC}$$

and

$$\frac{\partial \mathcal{L}_e}{\delta Q_B^A} = \frac{\delta \mathcal{L}_e}{\partial Q_{CD}} \cdot (\delta_D^B G_{AC}) = \frac{\partial \mathcal{L}_e}{\partial Q_{CB}} G_{AC}.$$

From this it follows that

$$\frac{\partial \mathcal{L}_e}{\partial Q_B^A} G^{AK} = \frac{\partial \mathcal{L}_e}{\partial Q_{BK}}.$$

Recall the definition of S_{AB} as

$$S_J^I = P_m^I F_J^m = \frac{\partial \mathcal{L}_c}{\partial F_I^m} F_J^m = \frac{\partial \mathcal{L}_c}{\partial Q_B^A} \cdot G^{AK} (\delta_K^I h_{nm} F_B^n + \delta_B^I h_{mn} F_K^n) F_J^m =$$

$$= \frac{\partial \mathcal{L}_c}{\partial Q_B^A} \cdot G^{AK} (\delta_K^I C_{BJ} + \delta_B^I C_{KJ}) = \frac{\partial \mathcal{L}_c}{\partial Q_I^A} \cdot G^{AK} C_{KJ} + \frac{\partial \mathcal{L}_c}{\partial Q_B^A} \cdot G^{AI} C_{BJ},$$

from which it follows that

$$S_{IJ} = \frac{\partial \mathcal{L}_c}{\partial Q^A_B} \cdot G^{AK} C_{KJ} G_{BI} + \frac{\partial \mathcal{L}_c}{\partial Q^I_B} \cdot C_{BJ}. \tag{D.12}$$

Now using the the fact that $Q_{IJ} = C(\phi)_{IJ}$ is symmetric and that

$$\frac{\partial L_e}{\partial Q^I_J} = \frac{\partial L_e}{\partial Q_{AJ}} G_{AI}.$$

As a result we rewrite the first term in the right side of the last formula as

$$\frac{\partial \mathcal{L}_c}{\partial Q_{CB}} G_{CA} \cdot G^{AK} C_{KJ} G_{BI} = \frac{\partial \mathcal{L}_c}{\partial Q_{KB}} G_{BI} C_{KJ} = \frac{\partial \mathcal{L}_c}{\partial Q_{BK}} G_{BI} C_{KJ} = \frac{\partial \mathcal{L}_c}{\partial Q^I_K} C_{KJ},$$

and, as a result two terms in the expression for S_{IJ} coincide and we have

$$S_{IJ} = 2 \frac{\partial \mathcal{L}_c}{\partial Q^I_K} C_{KJ}. \tag{D.13}$$

Now we calculate the Eshelby tensor b:

$$b^I_J = -\mathcal{L}_e \delta^I_J + P^I_i F^i_J = -\mathcal{L}_e \delta^I_J + S^I_J$$

Covariant tensor b is

$$b_{IJ} = G_{IS} b^S_J = -\mathcal{L}_e G_{IJ} + S_{IJ} \tag{D.14}$$

Taking symmetrical part of all tensors here we get

$$b_{(IJ)} = -\mathcal{L}_e G_{IJ} + S_{(IJ)}, \tag{D.15}$$

where we denoted by $A_{(IJ)} = \frac{1}{2}(A_{IJ} + A_{JI})$ the symmetric part of a covariant tensor A.

Canonical Energy-Momentum tensor for the Lagrangian (D.10) is $(I, J = 1, 2, 3)$

$$\frac{\sqrt{-G}}{2} T_{IJ} = \frac{\delta \mathcal{L}_e}{\delta G^{IJ}} = \frac{\delta \mathcal{L}_e}{\delta G^{IJ}}_{exp} + \frac{\delta \mathcal{L}_e}{\delta Q^A_B} \frac{\delta Q^A_B}{\delta G^{IJ}} =$$

$$\frac{\delta \mathcal{L}_e}{\delta G^{IJ}}_{exp} + \frac{\delta \mathcal{L}_e}{\delta Q^A_B} (\delta^A_I C_{JB} + \delta^A_J C_{IB}). \tag{D.16}$$

Comparing (D.13) and (D.16) we get $(I, J = 1, 2, 3)$:

$$\frac{\sqrt{-G}}{2} T_{IJ} = \frac{\delta \mathcal{L}_e}{\delta G^{IJ}}_{exp} + \frac{1}{2} S_{(IJ)} = \frac{\delta \mathcal{L}_e}{\delta G^{IJ}}_{exp} + \frac{1}{2} b_{(IJ)} + \frac{1}{2} \mathcal{L}_e G_{IJ}. \tag{D.17}$$

Consider the case where L_e does not depend on $\mathcal{K}$ and all the explicit dependence on G is through G_{00}. Calculate the term

$$k_{IJ} = \frac{\delta \mathcal{L}_e}{\delta G^{IJ}}_{exp}$$

of the CEM-tensor. We have

$$\mathcal{L}_e = \rho_0 \sqrt{-G} f(E^{el}) = \sqrt{-G_{00}} f(E^{el}).$$

Using

$$\delta G_{AB} = -\delta G^{IJ} \cdot G_{IA} G_{JB}$$

we get

$$\frac{\delta \sqrt{-G_{00}}}{\delta G^{IJ}} = -\frac{1}{2} (-G_{00})^{-\frac{1}{2}} \frac{\delta G_{00}}{\delta G^{IJ}} = -\frac{1}{2} \sqrt{-G_{00}} \frac{G_{I0} G_{J0}}{G_{00}},$$

and the input into the tensor k_{IJ} from the term $S(X)\sqrt{-G_{00}} L_e$ is $\mathcal{L}_e Z_{IJ}$, $Z_{IJ} = -\frac{1}{2} \frac{G_{I0} G_{J0}}{G_{00}}$.

For a case of a block-diagonal metric G where $G_{0I} = 0, I = 1, 2, 3$, tensor Z^A_J has only 00 non-zero term. As a result k has the form $\begin{pmatrix} -\frac{G_{00}}{2} \mathcal{L}_e & 0 \\ 0 & 0. \end{pmatrix}$.

As a result (D.17) takes (in the BD case without dependence of $\mathcal{K}$) the form ($I, J = 1, 2, 3$):

$$\sqrt{-G}\, T_{IJ} = b_{(IJ)} + \mathcal{L}_e G_{IJ}(1 - \delta^0_I \delta^0_J). \tag{D.18}$$

This gives a relation between the Eshelby tensor and the Canonical Energy-Momentum tensor (CEM-tensor).

We see that symmetrical part of the Eshelby tensor ($I, J = 1, 2, 3$) is that (non-volume) part of energy-momentum tensor where dependence on the metric G goes through the **elastic moduli** (those are hidden in the definition of strain tensor E). The term k is "flow term" in that it depends on the "space-time" (mixed) part of the metric G and has only 00-component for the block-diagonal metric G (Robertson-Walker, for example).

If L_e depends on G also through $\mathcal{K}$, then the expression for tensor k becomes more complex.

Bibliography.

[1] Bloom, F *Modern Differential Geometrical Techniques in the Theory of Continuous distributions of Dislocations*, Lect. Notes in math., vol. 733, Springer, Berlin, 1979.

[2] B. Carter, H. Quintana., Foundations of general relativistic high-pressure elasticity theory., Proc. R. Soc. Lond., A.331, pp.57-83 (1972).

[3] B. Carter, Elastic Perturbation Theory in General Relativity and a Variation Principle for a Rotating Solid Star, Comm. Math. Physics, 30, pp.261-286 (1973).

[4] A.Chudnovsky, S. Preston, Geometrical modeling of material aging, Extracta Matematicae, Congreso de Segovia, 1-15, 1995.

[5] R.M.Christensen, *Theory of viscoelasticity*, Acad. Press., N.Y., 1971.

[6] S.de Groot, P.Masur, *Non-equilibrium Thermodynamics*, Dover, N.Y.,1964

[7] M. Epstein, G. Maugin, The Energy-Momentum tensor and material uniformity in finite elasticity, Acta Mechanica 83, pp.127-133, 1990.

[8] J.D.Eshelby, The elastic energy-momentum tensor, J.of Elasticity, Vol.5, Nos. 3-4,1975, pp.321-335.

[9] J.D.Eshelby, Energy relations and the energy-momentum tensor in continuum mechanics, in *Inelastic behaviour of solids*, ed. M.Kannien, W.Adler, A.Rosenfeld, R.Jaffe, McGraw-Hill, N.Y.,1970, pp.77-113.

[10] A.Fisher, J.Marsden, The Einstein Equations of Evolution - a Geometrical Approach, J.Math. Phys., Vol.13, No.4, 1972, pp.546-568.

[11] A.M. Freudenthel, *The inelastic behavior of engineering materials and structures*, N.Y., 1950.

[12] A. Golebowska Hermann, On conservation laws of continuum mechanics, Int. J. Solid Structure, v.17, pp.1-9, 1981.

[13] G.Francfort,A.Golebowska Hermann, Conservation Laws and Material Momentum in Thermoelasticity, Transactions of ASME, Vol.49, pp. 710-714, 1982.

[14] A.G. Hermann, On physical and material conservation laws, Proc.IUTAM Symp. on Finite Elasticity, pp.201-209, Martinus Nijhof, Hague, Boston, 1981.

[15] J. Kijowski, *Elasticita finita e relativistica*, Quad. dell'Unione math. Italiana, 37, Pithagora Editrice, Bologna, 1991.

[16] J. Kijowski, G. Magli, Relativistic elastomechanics as a lagrangian field theory, J.Geom. Phys. 9, 1992, no.3, pp.207-233.

[17] K.Kondo, Non-Riemannian geometry of Imperfect Crystals from a Macroscopic Viewpoint, Memoirs of the Unifying study of the Basic Problems in Engineering Sciences by means of Geometry, Vol.1, Division D, Tokyo, Gakujutsu Benken Fukuy-Kai, 1955.

[18] L. Landau, E. Lifshitz, *The Classical Theory of Fields*, 1971, Addison-Wesley, Reading, MA.

[19] L. Landau, E. Lifshitz,*Elasticity Theory*,(2nd ed.), N.Y. Pergamon Press Inc.,Elmsford, 1970.

[20] J. Marsden, "Stress and Riemannian Metrics in Nonlinear Elasticity",

[21] J. Marsden, T. Hughes, *Mathematical Foundations of Elasticity*, Prentice-Hall, 1983.

[22] G. Maugin, M.Epstein, C.Trimarco, "Pseudomomentum and material forces in inhomogeneous materials", Int. J. Solid Structures, V.29, No.14/15, pp.1899-1900, 1992.

[23] G. Maugin, C.Trimarco, Pseudomomentum and material forces in nonlinear elasticity: variational formulations and application to brittle fracture, Acta Mechanica 94, 1-28, 1992.

[24] C. Misner, K.Thorne, J.Wheeler, *Gravitation*, 1973, Freeman, N.Y.

[25] W. Noll, Materially Uniform Simple Bodies with Inhomogeneities, Arch. fur Rational Mech. anal., Vol.27, pp.1-32, 1967.

[26] Y.Pak, G.Hermann, Conservation laws and the material momentum tensor for the elastic dielectric, Int. J.Engnr. Sci.,v.24, 8, pp.1365-1374,1986.

[27] J.Simo, J.Marsden, On the Rotated Stress Tensor and the Material version of the

Doyle-Ericksen Formula, pp.213-231, Arch. Rational Mech. Analysis 86, 1984.

[28] J. Simo, J. Marsden,P.S.Krishnaprasad, The Hamiltonian Structure of Nonlinear Elasticity: The Material and Convective Representation of Solids,Rods and Plates., Arch. Rat. Mech. Analysis, 104,n.2, 125-183, 1988.

[29] J.Simo, M.Ortiz, A unified approach to finite deformation elastoplastic analysis based on the use of hyperelastic constitutive equations, Comp. Methods in Applied Math. and Engineering, 49(1985), pp.221-245.

[30] H.Stephani, *General Relativity*, CUB, Cambridge, 1982.

[31] A.Taub, Space-times with distribution valued curvature tensors, J.Math. Phys.,21(6),1980 1431.

[32] C.-C.Wang, On the geometrical structure of simple bodies, a mathematical foundation for the theory of continuous distribution of dislocations, Arch.Rational Mech. Anal., 27, 1967, pp.33-94.